T. Hikmet Karakoc · Raj Das ·
Ismail Ekmekci · Alper Dalkiran ·
Ali Haydar Ercan   *Editors*

Green Approaches in Sustainable Aviation

Proceedings of International Symposium on Sustainable Aviation 2022

SARES
INTERNATIONAL SUSTAINABLE AVIATION
AND ENERGY RESEARCH SOCIETY

Springer

Sustainable Aviation

Series Editors

T. Hikmet Karakoc ⓘD, Eskisehir Technical University, Eskisehir, Türkiye;
Information Technology Research and Application Center, Istanbul Ticaret
University, Istanbul, Türkiye

C Ozgur Colpan ⓘD, Department of Mechanical Engineering, Dokuz Eylül
University, Buca, Izmir, Türkiye

Alper Dalkiran ⓘD, School of Aviation, Süleyman Demirel University, Isparta,
Türkiye

The Sustainable Aviation book series focuses on sustainability in aviation, considering all aspects of the field. The books are developed in partnership with the International Sustainable Aviation Research Society (SARES). They include contributed volumes comprising select contributions to international symposiums and conferences, monographs, and professional books focused on all aspects of sustainable aviation. The series aims at publishing state-of-the-art research and development in areas including, but not limited to:

- Green and renewable energy resources and aviation technologies
- Aircraft engine, control systems, production, storage, efficiency, and planning
- Exploring the potential of integrating renewables within airports
- Sustainable infrastructure development under a changing climate
- Training and awareness facilities with aviation sector and social levels
- Teaching and professional development in renewable energy technologies and sustainability

* * *

T. Hikmet Karakoc • Raj Das • Ismail Ekmekci
Alper Dalkiran • Ali Haydar Ercan
Editors

Green Approaches in Sustainable Aviation

Proceedings of International Symposium on Sustainable Aviation 2022

Editors
T. Hikmet Karakoc 🆔
Faculty of Aeronautics and Astronautics
Eskişehir Technical University
Eskişehir, Türkiye

Information Technology Research
and Application Center
Istanbul Ticaret University
Istanbul, Türkiye

Ismail Ekmekci 🆔
Faculty of Engineering
Istanbul Commerce University
Istanbul, Türkiye

Ali Haydar Ercan 🆔
Porsuk Vocational School
Eskişehir Technical University
Eskişehir, Türkiye

Raj Das 🆔
School of Engineering
RMIT University
Melbourne, Australia

Alper Dalkiran 🆔
School of Aviation
Süleyman Demirel University
Keciborlu, Isparta, Türkiye

Paper in this product is recyclable.

Preface

Global warming is a global fact that causes many consequences to our habitat and must be resolved by governmental actions and industries worldwide. The aviation industry contributes approximately 2% of total carbon emissions, and air transportation growth is increasing rapidly. Carbon emission reduction in the aviation industry is essential to combat global warming. Alternative jet fuel can achieve a further 50–80% reduction in carbon emissions and is the most efficient way to achieve carbon-neutral aviation operation. Demands from regulatory agencies for compliance with international carbon emission standards have increased, and domestic interest in bio-jet fuel-powered planes have also been rising. Nevertheless, sustainable aviation is not only for the environment but is currently the most essential common global understanding.

The carbon emission standards drive the growth of bio-jet fuel markets for international flights, which require airlines to purchase carbon offsets to compensate for the growth in emissions. Stakeholders have initiated several activities in the past 10 years, including the newly approved American Society for Testing and Materials (ASTM) bio-jet standards, bio-jet fuel development community formation, fuel certification test flights, and off-take fuel agreements between airline companies and early-stage bio-jet fuel suppliers. The US jet fuel market represents 20 billion gallons annually, but no precise, sustainable jet fuel technology exists. Biojet technologies have made progress in dealing with diverse biomass substrates, but more effort is needed to improve conversion efficiencies and reduce the cost of production. This proceedings book involves several chapters on overviews of current opportunities for developing bio-jet fuels, taxation action of green aviation, air passengers' green purchase intentions, and other highlights on Sustainable Aviation.

International Symposium on Sustainable Aviation (ISSA) is an international and multi-disciplinary symposium held online between 3–5 August 2022 in Melbourne, Australia, to address and discuss Sustainable Aviation issues. This symposium has focused on the Green Approaches in the Aviation industry. The symposium management kindly invited the academics, scientists, engineers, practitioners,

policymakers, and students to attend ISSA '22 to share knowledge, demonstrate green technologies and breakthroughs, and debate the future of sustainable aviation by defining the direction, unveiling the strategies and setting the goals in aviation sustainability. This conference has featured keynote presentations by invited speakers and general papers in oral and live video sessions.

We want to thank Springer's editorial team for their support toward the preparation of this book and the chapter authors and reviewers for their outstanding efforts.

On the other hand, we would like to give special thanks to the SARES Editorial office members for their efforts in the long run for symposium author communications, following the standards, are necessary to creating a proceedings book. Dilara Kılıç, Sinem Patatur, and Kemal Keleş have played a significant role in sharing the load and managing the gathering of the chapters.

Eskişehir, Türkiye	T. Hikmet Karakoc
Melbourne, Australia	Raj Das
Istanbul, Türkiye	Ismail Ekmekci
Keciborlu, Türkiye	Alper Dalkiran
Eskişehir, Türkiye	Ali Haydar Ercan

Contents

About the Editors

T. Hikmet Karakoc, Ph.D., graduated from the Department of Mechanical Engineering, Anadolu University. He received his M.Sc. degree in Mechanical Engineering from the Yildiz Technical University and his Ph.D. from Anadolu University, where he started his full-time teaching and received his Full Professorship. He is currently researching at the Eskisehir Technical University. He has a wide range of research interests, including Sustainable Aviation, Aircraft Propulsion Systems, Insulation, Heating, Ventilating, and Air Conditioning, Indoor Air Quality, Gas Turbines, Cogeneration Systems, Renewable Energy, Energy Economics, Fuels, and Combustion. He has participated in numerous industrial projects on these topics as a researcher, consultant, and project manager for over 30 projects and corporations. He also started a contest on special insulation applications among university students. He served as an editor-in-chief, guest editor, and editorial board member for international scientific journals. He has published national and international papers in over 300 journals and 40 books. Prof. Karakoc actively follows membership positions for the Chamber of Mechanical Engineers and many sectorial associations, international scientific organizations, and societies. He is an active Board of Directors member of the International Association for Green Energy. He is currently holding the presidency of the SARES organization, which is actively supporting scientists and students in the area of Sustainable Aviation. He also organizes four symposiums on aviation subject areas as a Founding Chair.

Raj Das, Ph.D., is a Full Professor of Applied Mechanics and leads the Simulation of Advanced Materials and Structures (SAMS) research group at the Sir Lawrence Wackett Research Centre of RMIT University, Australia. He is the Program Director in the Aerospace Engineering and Aviation discipline of the School of Engineering. He is also an honorary academic at the University of Auckland, New Zealand, and the University of Quebec, Canada. Prof. Das has nearly 20 years of experience designing, analyzing, and optimizing engineering materials and structures, focusing on computational mechanics, structural optimization, composite structures, failure analysis, and damage tolerance design. He has published more than 300 papers in

international journals and conferences in collaboration with several universities, institutes, and industries. Professor Das has a Ph.D. in Applied Mechanics from Monash University, Australia, and has previously worked at the University of Auckland, the Commonwealth Scientific and Industrial Research Organisation, and the University of Manchester. He is associated with various scientific and technical societies broadly related to theoretical and applied mechanics. He is the President of the International Congress on Mechanical Behaviour of Materials (ICM) and represents Australia as a Director on the Executive Committee of the International Congress on Fracture (ICF). Within Australia, Prof. Das is Chair of the National Committee on Applied Mechanics of Engineers Australia. He has chaired/co-chaired several well-known conferences, including ICM-13, ACAM-8, ACCM-3, and ICCM-6.

İsmail Ekmeki, Ph.D., graduated from the Department of Mechanical Engineering, Yildiz Technical University in 1980. He completed an M.Sc. degree in Mechanical Engineering at the School of Science, Yildiz Technical University in 1982 and an M. Sc. degree in Industrial Engineering from İstanbul Technical University in 1983. He received a Ph.D. from Yildiz Technical University in 1995 in Mechanical Engineering. He studied as an academic staff member at Yildız Technical University, Sakarya University, and Marmara University and continues his academic career at Istanbul Ticaret University. He has worked as a researcher, executive, and manager in academic positions with various industrial projects. His research interests cover energy, optimization, decision-making, safety, OHS, and HVAC-related topics.

Alper Dalkıran, Ph.D., received his bachelor's degree from the Avionics Department, Faculty of Aeronautics and Astronautics, Eskisehir Technical University (formerly known as Anadolu University). He completed his M.Sc. degree in Aviation Maintenance at the School of Science, Anadolu University in 2004. He earned his Ph.D. degree in 2017 in Environmental Sustainability on Airports from the School of Science, Anadolu University, by developing a model of energy-based calculations of an aerodrome. He has studied aircraft engines, sustainability, airports, and exergy. He has 17 years of professional experience in Airports in Information Technology, Automation, and Integration. He has managed teams on system design, projects, tests, commissioning, operational readiness, and operations. He has been working in the School of Aviation at Suleyman Demirel University since 2019 and lecturing in Flight Theory, Airline Management, and Airport Design subjects.

Ali Haydar Ercan, Ph.D., is currently a Lecturer at the Electronics and Automation Department, Porsuk Vocational School, Eskisehir Technical University. He received his bachelor's degree in Mechanical Engineering from the Faculty of Engineering, University of Cumhuriyet, Sivas; his M.Sc. degree in Mechanical Engineering from the University of Gazi, Ankara; and his Ph.D. from the Department of

Aerodynamics, University of Liverpool, where he worked on boundary layer theory on flat plate surfaces and developed empiric formulas for transition development distance. He also earned a postgraduate degree in software technologies from the University of Liverpool. Dr. Ercan has a wide range of managerial experience with international commercial private companies.

Short Review on Taxation Action in the Sustainability of Green Airports

Filiz Ekici ⬡**, Öner Gümüş, Alper Dalkiran** ⬡**, and T. Hikmet Karakoc** ⬡

Nomenclature

IPCC	Intergovernmental Panel on Climate Change
ICAO	International Civil Aviation Organization
IATA	International Air Transport Association
ACI	Airport Council International
SHGM	Civil Aviation General Directorate of Turkey

1 Introduction

Today, climate change and global warming are common problems of all mankind and are problems that, by their very nature, require collective action in solving (Uysal, 2022). Emissions arise due to flight operations (Yu et al., 2019), and it has

F. Ekici (✉)
Department of Finance, Banking and Insurance, Igdır Vocational School, Igdır University, Igdır, Türkiye

Ö. Gümüş
Department of Accounting and Tax, Tavşanlı Vocational School, Kütahya Dumlupınar University, Kütahya, Türkiye

A. Dalkiran
School of Aviation, Suleyman Demirel University, Keciborlu, Isparta, Türkiye
e-mail: alperdalkiran@sdu.edu.tr

T. H. Karakoc
Faculty of Aeronautics and Astronautics, Eskişehir Technical University, Eskişehir, Türkiye

Information Technology Research and Application Center, Istanbul Ticaret University, Istanbul, Türkiye

been proven by many studies that the aviation sector also has an undeniable impact on these problems (Ekici, 2020; Kayaalp et al., 2021; Timko et al., 2010; Wey et al., 2007). All aviation activities both affect and are affected by the environment (Öndeş, 2022). At this point, in addition to flight operations, airport's heating services, logistics, lighting needs, as well as the construction process are issues that need to be addressed in terms of sustainability (Ballini & Bozzo, 2015).

The concept of sustainability has been established at every stage of production over time and has gained a place in the aviation sector as well. At this point, the concept of "green airport" has become a prominent element in the aviation sector in terms of ensuring sustainability (Winter et al., 2021). Sustainable airport development brings positive external effects such as reduction of energy consumption, reduction of negative impacts on water and air quality, minimization of waste, and reduction of negative environmental impacts of airport construction (Boca Santa et al., 2020). These contributions become more valuable considering the negative effects of the sector on the environment.

According to the data announced at the Intergovernmental Panel on Climate Change (IPCC), 13% of greenhouse gas emissions, which have contributed significantly to global warming in the past half century, were announced to be caused by the aviation sector. These and similar published reports have shown again that green airports are the most logical choice for sustainable development (Xiong et al., 2022).

2   Green Airport Taxation

Under all these negative effects, the air transportation sector should act decisively to establish and maintain a balance between economic development, social progress, and environmental responsibility (three pillars of sustainability) by placing itself on a sustainable footing. Considering these reasons, instead of acting with the aim of uncontrolled capacity expansion, road maps that are sustainable and meet current needs without reducing the resources of future generations become a necessity, not a choice, when making plans for airports (SHGM, 2010). At this point, more and more airports have started to pay attention to the issue by placing the issue of sustainability at the focus point. Especially with the efficient use of resources, increasing the importance given to recycling and reducing waste, awareness has been established to protect the environment and ensure sustainability. The demand and support by consumers are other factors that force aviation businesses to be more sensitive (Korul, 2003) and aviation sector has become a part of this change with all its actors. Of the major organizations in the sector, Airports Council International (ACI) and the International Civil Aviation Organization (ICAO) work on common projects about green airports to create infrastructures that target the ecological planning in airports, to distribute land use plans based on this issue, and to form an appropriate system for airport managements. Currently, there are 400 airports around the world that are under construction or are making radical changes and infrastructure works to adapt to the green airport concept (Silva & Henkes, 2021). This change is more

Table 1 Environmentally sensitive management versus traditional management

	Traditional approach	Environmentally sensitive management
Aims	Economic growth, profit, increasing the wealth of share holders	Sustainability and quality of life, stakeholder welfare
Values	Human-centered	Bio-centered
Products	Products designed for function, style, and price	Environmentally friendly products
Production system	Energy-intensive production	Low energy and resource usage
Environment	Establishing dominance over the environment, accepting waste as output	Compliance with the environment, waste management

Adapted from Shrivastava (1995)

clearly deciphered in Table 1, which shows the difference between today's environmentally sensitive management approach and traditional management approach. While in traditional management, there is a profit-oriented, human-centered, and environmentally oriented understanding, with the integration of the concept of sustainability into all areas of life over time, the environmentally friendly production management approach with an environmentally friendly, bio-centered structure has become a standard.

Today, green building applications are increasing at bio-center-oriented green airports operating with an environmentally sensitive management approach. Green building practices are contributing to the ecosystem by improving water quality, increasing biodiversity, conserving natural resources, and minimizing environmental effects such as alleviating negative consequences of global warming, reduction of operation and maintenance costs as well as economic performance, management approach, depending on today's environmentally conscious, eco-friendly service delivery, such as the realization of the economic and social impact in terms of sustainability is a topic that is supported by the authorities (Nilashi et al., 2015; Boca Santa et al., 2020).

Important environmental problems and the lack of natural resources have led humanity to an environmentally responsible consumption approach. Nowadays, more and more institutions have started to produce environmentally friendly products, and consumers have also increased the level of willingness to pay to purchase these products (Joshi & Rahman, 2015). There is a similar economic situation for green airports. However, in some cases, lack of environmental awareness pushes consumers to buy anti-environmental products. In such a situation, using financial instruments as an element of coercion emerges as an effective way to ensure the sustainability of green airports.

Decisively, the willingness to pay is a significant factor in the relationship between climate change and the goal of action (Winter et al., 2021). For this reason,

an effect that will create a change in willingness to pay can be achieved by taxation action.

In the case of imperfect competition between polluters, an optimal emission tax may be more costly than increasing environmental awareness (Abdul Baki & Marrouch, 2022). Therefore, tax is not the only way to ensure the sustainability of green airports. The main important point is to increase the awareness of individuals.

The Ramsey rule can be applied for long-haul flights at non-congested airports (Saremi et al., 2021). In this context, it is possible to suggest that the elasticity of demand for long-haul flights is low. If a higher tax is levied on long-haul flights for environmental sustainability at non-congested airports and a lower tax is levied on short-haul flights, both CO_2 emissions will be less, and tax revenue will be generated. The tax revenues collected can be used to maintain the effectiveness of green airports.

Specific and indirect taxes on tourism can internalize costs and provide improvements in terms of revenue without hindering the economy. However, indirect taxes are more applicable, fair, and impartial in the revenues that can be collected from tourism activities than specific taxes (Gago et al., 2009). Especially if it is considered in terms of charter flights applied by travel agencies, it is possible to suggest that indirect taxes can be applied at green airports and thus consumers' willingness to pay can be increased.

Carbon taxes are a very popular tax in reducing externalities. However, this type of taxes limits the willingness to pay. An air passenger tax that will be levied on first-class and long-haul flights instead of the carbon tax will further increase the willingness of passengers to pay (Seetaram et al., 2018). In this context, the collection of air passenger tax from first-class passengers of long-haul flights to green airports will be effective in maintaining the financing of green airports. Fig. 1 demonstrates green airports and taxation in a three logical dimensions.

The bonus/malus tax also has the potential to be effective in maintaining green airports. The bonus/malus tax has three types of effects (Hilton et al., 2014):

- In bonus/malus tax, rewarding one side creates a feeling of support, while punishing the other side can create a feeling of absence.
- Another effect that will arise in the implementation of the bonus/malus tax is as follows: While some behaviors are desired by society, some behaviors may not be desired by society.
- If the bonus/malus tax is perceived as an interventionist tax, crowding out effect may occur.

The application of a bonus/malus tax in the financing of green airports may limit the willingness to pay for certain parts of society. The person who is penalized in this system feels psychologically excluded from the services offered by green airports. The reason for this situation is since the services are supplied by private sector.

Environmental awareness is also important in the sustainability of green airports. If the environmental sensitivity of the society is high, the application of the bonus/malus system may be considered appropriate by the society. However, it is not possible to state that societies that have not yet been able to meet their basic needs
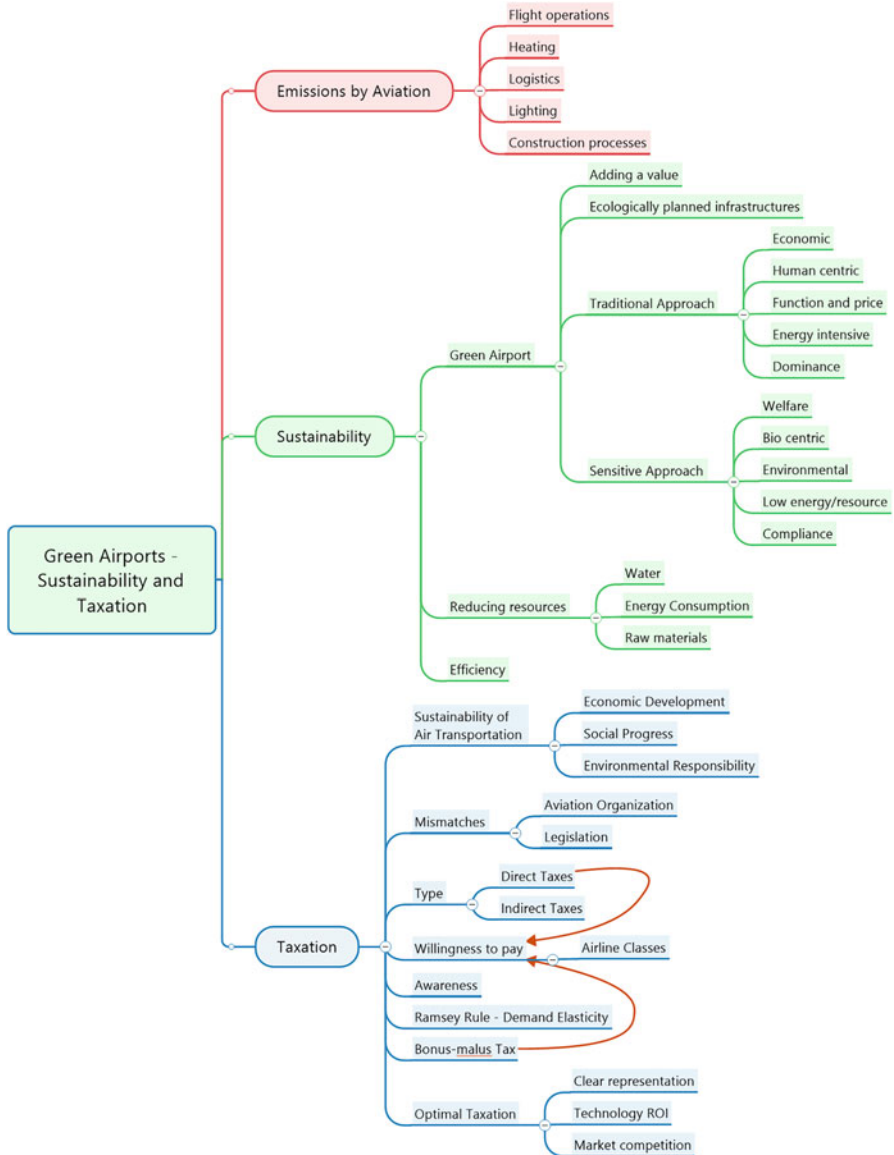
Fig. 1 Green airports, sustainability, and taxation

will reasonably meet the implementation of such a system. Therefore, it is possible to encounter a tax refusal.

There may be an exclusion of the private sector from the market in bonus/malus tax. In the application of bonus/malus tax, which will be used as a financing tool to ensure the sustainability of green airports, the penalty increases the investment costs

of the private sector. In such a situation, the private sector stops investing, and the presence of the state becomes more felt in the market.

The effects of certain taxes on emissions may differ from each other due to the legislation of countries (Dube & Nhamo, 2019; Hájek et al., 2021). In determining the criteria related to green airports, these legislative differences may create uncertainty in whether the effects that will arise in the presence of an emission tax will be positive or negative. For instance, because of flights between the green airports of the two countries where the emission tax is applied, it is possible that the problem of double taxation may arise. In this context, the harmonization of the legislations can eliminate the problem of double taxation and thus increase the willingness of consumers to pay. With the increase in willingness to pay, pricing and financing will also increase in ensuring the sustainability of green airports.

Traditional measures aimed at excessive tax burden do not seriously address the real loss of effectiveness of taxation (Driffill & Rosen, 1983). For this reason, an optimal taxation is necessary to maintain the effectiveness of green airports.

3   Conclusions

Three elements are important in optimal taxation. The first of these is the clear representation of individual preferences, technology with a fixed return on scale, and a market where there is full competition. The second is related to the fact that the government should increase revenues by a fixed amount with a limited number of tax tools managed in a cost-free manner. The third is related to the existence of a criterion function that ranks the results. In this way, the best (optimal) tax system is selected in a limited set of tax tools. The focus is primarily on minimizing the loss of efficiency in the resulting optimal taxation preference. Then, it is discussed how the selected tax system affects the welfare distribution and how the efficiency loss should be balanced because of this distribution (Slemrod, 1990). In this context, it can be suggested that the following considerations should be taken while taking taxation action to ensure the sustainability of green airports:

- First, a taxation that will increase the willingness to pay should be carried out.
- The goods and services to be offered at green airports should be realized in accordance with consumer preferences. In this way, the revenue potential will be created, which will form a justification for taxation.
- All income-generating elements that will operate at green airports should be produced as much as possible under the conditions of a free market economy.
- It is necessary to adjust the use of technology at green airports in such a way as to provide at least according to constant returns to scale.
- Taxation is levied by the states. For this reason, the tax tools to be used by the states for sustainability in green airports should be both limited and generate revenue.

- The tax revenues generated in this way can be used by the states to finance green airports.
- Because taxes are collected from individuals and households, social welfare is affected by the act of taxation. Therefore, a balance should be achieved between the tax system to be chosen and social welfare.
- The loss of efficiency in the tax system to be selected for the financing of green airports should be minimal.
- It should not be enough just to choose a tax system. In addition, public awareness should be increased about the importance of green airports.
- In the tax system to be selected, the tax rates for long-haul flights should be high. To minimize the loss of activity, designing flight schedules that will create congestion at green airports should be avoided.
- A tax system with indirect taxes should be preferred for flights for tourism purposes because in this way, financial anesthesia will arise, and tax revenue can be collected. This will facilitate the financing of green airports.
- In a tax system where there are popular taxes such as the carbon tax, efficiency cannot be achieved on first-class and long-haul flights. Instead, resorting to traditional taxes can eliminate tax refusal.
- Taxpayers who fulfil their obligations in the tax system to be selected should not be penalized. However, taxpayers who fulfil their obligations should be rewarded. This logic will increase the tax zeal of taxpayers who do not fulfil their obligations.
- The tax system to be chosen should not create crowding-out effect. Otherwise, the idea of a perfect competitive market may disappear.

A tax system, the characteristics of which are mentioned above, will ensure the financing of green airports and, consequently, their sustainability. Therefore, it will be possible to contribute to the sustainability of the green economy in the field of civil aviation through a fiscal instrument such as an optimal taxation.

References

Abdul Baki, G., & Marrouch, W. (2022). Environmental taxation in the Bertrand differentiated duopoly: New insights. *Resource and Energy Economics, 70*, 101329. https://doi.org/10.1016/j.reseneeco.2022.101329

Ballini, F., & Bozzo, R. (2015). Air pollution from ships in ports: The socio-economic benefit of cold-ironing technology. *Research in Transportation Business & Management, 17*, 92–98. https://doi.org/10.1016/j.rtbm.2015.10.007

Boca Santa, S. L., Ribeiro, J. M. P., Mazon, G., Schneider, J., Barcelos, R. L., & de Guerra, J. B. S. O. A. (2020). A green airport model: Proposition based on social and environmental management systems. *Sustainable Cities and Society, 59*, 102160. https://doi.org/10.1016/j.scs.2020.102160

Driffill, E. J., & Rosen, H. S. (1983). Taxation and excess burden: A life cycle perspective. *International Economic Review, 24*(3), 671. https://doi.org/10.2307/2648793

Dube, K., & Nhamo, G. (2019). Climate change and the aviation sector: A focus on the Victoria Falls tourism route. *Environmental Development, 29*, 5–15. https://doi.org/10.1016/j.envdev.2018.12.006

Ekici, S. (2020). Thermodynamic mapping of A321-200 in terms of performance parameters, sustainability indicators and thermo-ecological performance at various flight phases. *Energy, 202*, 117692. https://doi.org/10.1016/j.energy.2020.117692

Gago, A., Labandeira, X., Picos, F., & Rodríguez, M. (2009). Specific and general taxation of tourism activities. Evidence from Spain. *Tourism Management, 30*(3), 381–392. https://doi.org/10.1016/j.tourman.2008.08.004

Hájek, M., Zimmermannová, J., & Helman, K. (2021). Environmental efficiency of economic instruments in transport in EU countries. *Transportation Research Part D: Transport and Environment, 100*, 103054. https://doi.org/10.1016/j.trd.2021.103054

Hilton, D., Charalambides, L., Demarque, C., Waroquier, L., & Raux, C. (2014). A tax can nudge: The impact of an environmentally motivated bonus/malus fiscal system on transport preferences. *Journal of Economic Psychology, 42*, 17–27. https://doi.org/10.1016/j.joep.2014.02.007

Joshi, Y., & Rahman, Z. (2015). Factors affecting green purchase behaviour and future research directions. *International Strategic Management Review, 3*(1–2), 128–143. https://doi.org/10.1016/j.ism.2015.04.001

Kayaalp, K., Metlek, S., Ekici, S., & Şöhret, Y. (2021). Developing a model for prediction of the combustion performance and emissions of a turboprop engine using the long short-term memory method. *Fuel, 302*, 121202. https://doi.org/10.1016/j.fuel.2021.121202

Korul, V. (2003). *Havaalanı Çevre Yönetim Sistemi, 3*(1), 99–120. Checked on 12/12/2022.

Nilashi, M., Zakaria, R., Ibrahim, O., Majid, M. Z. A., Mohamad Zin, R., Chugtai, M. W., et al. (2015). A knowledge-based expert system for assessing the performance level of green buildings. *Knowledge-Based Systems, 86*, 194–209. https://doi.org/10.1016/j.knosys.2015.06.009

Öndeş, E. B. (2022). *Pilotlarda Aşırı Yorgunluk Kavramı Üzerine Nicel Bir Çalışma: Türkiye*. Master's dissertation. Anadolu Üniversitesi, Eskişehir. Sosyal Bilimler Enstitüsü, checked on 12/15/2022.

Saremi, M., Fallahi, F., Pels, E., Salmani, B., & Covich, M. P. (2021). Ramsey pricing of aircraft landing fees: A case study of Iranian airports. *Research in Transportation Economics, 90*, 100922. https://doi.org/10.1016/j.retrec.2020.100922

Seetaram, N., Song, H., Ye, S., & Page, S. (2018). Estimating willingness to pay air passenger duty. *Annals of Tourism Research, 72*, 85–97. https://doi.org/10.1016/j.annals.2018.07.001

SHGM. (2010). *Havaalanlarında Çevresel Etkiler*. With assistance of Sivil Havacılık Genel Müdürlüğü, checked on 12/12/2022.

Shrivastava, P. (1995). Ecocentric management for a risk society. *The Academy of Management Review, 20*(1), 118. https://doi.org/10.2307/258889

Silva, E. S., & Henkes, J. A. (2021). Uma Analise Sobre As Exigências, Medidas E Procedimentos Para Obter A Qualificação. *Green Airport, 1*(2), 142–163. Available online at https://rbac.cia.emnuvens.com.br/revista/article/view/28, checked on 12/12/2022

Slemrod, J. (1990). Optimal taxation and optimal tax systems. *Journal of Economic Perspectives, 4*(1), 157–179. Available online at https://www.jstor.org/stable/1942838#metadata_info_tab_contents, checked on 12/15/2022

Timko, M. T., Onasch, T. B., Northway, M. J., Jayne, J. T., Canagaratna, M. R., Herndon, S. C., et al. (2010). Gas turbine engine emissions—Part II: Chemical properties of particulate matter. *Journal of Engineering for Gas Turbines and Power, 132*(6), Article 061505. https://doi.org/10.1115/1.4000132

Uysal, Y. (2022). İklim Değişikliği ve Küresel Isınma ile Mücadelede Yerel Yönetimlerin Rolü: Tespitler ve Öneriler. *kesit, 30*(30), 324–354. https://doi.org/10.29228/kesit.57382

Wey, C. C., Anderson, B. E., Wey, C., Miake-Lye, R. C., Whitefield, P., & Howard, R. (2007). Overview on the aircraft particle emissions experiment (APEX). *Journal of Propulsion and Power, 23*(5), 898–905. https://doi.org/10.2514/1.26406

Winter, S. R., Crouse, S. R., & Rice, S. (2021). The development of 'green' airports: Which factors influence willingness to pay for sustainability and intention to act? A structural and mediation model analysis. *Technology in Society, 65*, 101576. https://doi.org/10.1016/j.techsoc.2021. 101576

Xiong, S.-H., Chen, Z.-S., Chiclana, F., Chin, K.-S., & Skibniewski, M. J. (2022). Proportional hesitant 2-tuple linguistic distance measurements and extended VIKOR method: Case study of evaluation and selection of green airport plans. *International Journal of Intelligent Systems, 37*(7), 4113–4162. https://doi.org/10.1002/int.22714

Yu, Z., Timko, M. T., Herndon, S. C., Miake-Lye, R. C., Beyersdorf, A. J., Ziemba, L. D., et al. (2019). Mode-specific, semi-volatile chemical composition of particulate matter emissions from a commercial gas turbine aircraft engine. *Atmospheric Environment, 218*, 116974. https://doi. org/10.1016/j.atmosenv.2019.116974

A Covariance Matching-Based Adaptive EKF for Nanosatellite Attitude Estimation

Hasan Kinatas and Chingiz Hajiyev

Nomenclature

ADCS   Attitude determination and control subsystem
COTS   Commercial off the shelf
EKF   Extended Kalman filter
FFs   Fading factors
MSFs   Multiple scaling factors
SSF   Single scaling factor

1 Introduction

The small satellite industry is developing at a faster pace day by day and is conducive to more people and companies to conduct work in the field of space technologies. Although they attract a lot of attention due to their low cost and short development time, small satellites also bring some engineering challenges with them. Cheap and commercial off the shelf (COTS) components used to reduce the cost increase the risk of a system malfunction, and attitude determination and control subsystem (ADCS) is one of subsystems that suffers most from this risk (Tafazoli, 2008). Any fault in attitude-related sensors can reduce the accuracy of the attitude estimation algorithm and, as a result, may cause incorrect control actions to be taken, which can lead to fatal consequences. Therefore, this study specifically addresses the problem of inaccurate attitude estimation in case of sensor faults. This problem

H. Kinatas (✉) · C. Hajiyev
Istanbul Technical University, Istanbul, Türkiye
e-mail: kinatas16@itu.edu.tr; cingiz@itu.edu.tr

becomes more important especially for nanosatellites, because being strictly constrained in size and mass makes conventional solutions, such as hardware redundancy impractical.

Attitude estimation methods for a nanosatellite can be divided into two main categories: single-frame and filtering algorithms (Hajiyev & Soken, 2021). Single-frame algorithms use vectors measured by attitude sensors (sun sensors, magnetometers, etc.) in the body frame and corresponding reference vectors in the reference frame (sun direction, magnetic field, etc.). The goal is finding the transformation (attitude) matrix between these two frames. Many different single-frame algorithms have been developed to date (TRIAD, q-method, QUEST, SVD, etc.), and extensive studies explaining and comparing these methods can be found in the literature (Cilden & Hajiyev, 2014). On the other hand, filtering methods use satellite's mathematical model in addition to measurements. Thus, even if there is no measurement available, attitude still can be estimated. Filtering algorithms, especially Kalman filtering, have been used in satellite attitude estimation for many years and it is possible to find many studies in the literature on this subject (Lefferts et al., 1982). However, since satellite's mathematical model and some attitude sensor measurement models (e.g. magnetometer) are nonlinear, the attitude estimation process requires nonlinear filtering which inherently increases the computational load. This is particularly undesirable for nanosatellites. In order to cope with this problem, filtering algorithms can be integrated with single-frame algorithms (Hajiyev & Bahar, 2003). These integrated algorithms make the measurement model for the filter linear and, thus, reduce the computational load. Integrated algorithms also give better estimations than the estimations given by the individual algorithms.

Kalman filters can give poor estimations in case of uncertainties and malfunctions. These possibilities should be considered in the design process and the designed filter should be robust against the changing conditions and compensate for the faults. In the literature, these type of Kalman filters are known as adaptive Kalman filters, and there are different techniques to make a Kalman filter adaptive such as multiple model adaptive estimation, join state and covariance estimation, autocorrelation, and covariance matching techniques (Hajiyev & Soken, 2021). Covariance matching techniques are one of the most widely used techniques where the main idea is scaling the Q- or R-noise covariance matrix depending on the source of the fault using a single scaling factor (SSF) or multiple scaling factors (MSFs).

In this study, an integrated adaptive TRIAD/R-adaptive extended Kalman filter (EKF) attitude estimation algorithm is presented where a single-frame algorithm (TRIAD) and a filtering algorithm (EKF) are integrated in order to take advantage of the good aspects of both. In the first step of the algorithm, TRIAD produces an initial attitude estimation. In the second step, this estimation is given to the EKF as input, and after the filtering process, final estimation is obtained. The proposed integrated algorithm is made adaptive via two different covariance matching techniques, using SSF and MSFs, and they are compared with a simulation.

2   Adaptive Kalman Filter via Covariance Matching

The TRIAD (Shuster & Oh, 1981) and conventional EKF algorithms (Lefferts et al., 1982) are well explained in other studies and will not be repeated here for the sake of brevity. However, adaptive EKF algorithms via covariance matching techniques differ from the traditional EKF at several points. Following subsections explain the R-adaptive EKF routines using SSF and MSFs.

2.1   R-Adaptive EKF with a Single Scaling Factor

The R-adaptive EKF with an SSF scales the measurement noise covariance matrix, R, in case of faults using a calculated SSF. SSF is calculated by comparing the real and theoretical innovation covariance matrices. The trace of these covariance matrices is matched such that (Hajiyev, 2007)

$$tr\left[e(k)e^T(k)\right] = tr\left[H(k)P(k|k-1)H^T(k) + \text{SSF}(k-1)R(k)\right] \tag{1}$$

where $e(k)$ is the EKF innovation sequence, $\text{SSF}(k-1)$ is the introduced SSF, and tr [·] is the trace of the related matrix. P, H, and R matrices are the classical Kalman filter matrices and known as estimation error covariance matrix, observation matrix, and measurement noise covariance matrix, respectively. Solving the Eq. (1) for the $\text{SSF}(k-1)$, the following is obtained:

$$\text{SSF}(k-1) = \frac{e^T(k)e(k) - tr[H(k)P(k|k-1)H^T(k)]}{tr[R(k)]} \tag{2}$$

Then, using the calculated SSF, the diagonal R matrix element corresponding to the faulty measurement channel is adjusted as

$$R_{\text{adjusted}_{j,j}}(k) = \text{SSF}(k-1)R_{j,j}(k) \tag{3}$$

2.2   R-Adaptive EKF with Multiple Scaling Factors

For the case of R-adaptive EKF with MSFs, the real and theoretical innovation covariance matrices are matched such that (Hajiyev & Soken, 2021)

$$\frac{1}{\xi}\sum_{k=m-\xi+1}^{m} \boldsymbol{e}(k)\boldsymbol{e}^T(k) = H(k)P(k|k-1)H^T(k) + \text{MSFs}(k-1)R(k) \quad (4)$$

where ξ is the window size, namely the number of measurements that will be considered, and *MSFs*$(k-1)$ is the scaling matrix that contains scaling factors for each measurement channel. Solving Eq. (4) for the MSFs$(k-1)$ gives

$$\text{MSFs}(k-1) = \left\{ \frac{1}{\xi}\sum_{k=m-\xi+1}^{m} e(k)e^T(k) - H(k)P(k|k-1)H^T(k) \right\} R^{-1}(k) \quad (5)$$

After calculating the scaling factor matrix, Kalman gain now can be adjusted as

$$K(k) = \frac{P(k|k-1)H^T(k)}{H(k)P(k|k-1)H^T(k) + MSFs(k-1)R(k)} \quad (6)$$

In the literature, it is possible to find slightly different algorithms to find the scaling factor matrix. In Kim et al. (2015), authors present an R-adaptive EKF for various types of global navigation satellite system (GNSS) faults using what they call fading factors (FFs). Although the fundamental idea is the same, in their study they calculate the scaling matrix in a slightly different way as

$$\text{FFs}(k-1) = \begin{bmatrix} FF(1) \\ FF(2) \\ \vdots \\ FF(N) \end{bmatrix} = \max\left(1, \frac{\text{diag}\left(\widehat{C_k}\right)}{\text{diag}(C_k)} \right) \quad (7)$$

where $\max(\cdot)$ function gives the higher value inside of it and *diag*$(\cdot)$ gives the diagonal elements of the related matrix. The term $\widehat{C_k}$ is the real innovation covariance and given as

$$\widehat{C_k} = \frac{1}{\xi-1}\sum_{k=m-\xi+1}^{m} \boldsymbol{e}(k)\boldsymbol{e}^T(k) \quad (8)$$

Note that, in this version, the term $\xi - 1$ is used instead of ξ. The term C_k is the theoretical innovation covariance and similar to Eq. (4), it is given as

$$C_k = H(k)P(k|k-1)H^T(k) + R(k) \quad (9)$$

After the scaling matrix FFs is calculated, Kalman gain is now updated as

$$K(k) = \frac{P(k|k-1)H^T(k)}{FFs(k-1)[H(k)P(k|k-1)H^T(k) + R(k)]} \quad (10)$$

Note that, in this version, the whole denominator of the Kalman gain is scaled using the scaling matrix rather than scaling only the R matrix.

3 Simulation Results and Discussion

In order to compare the performance of the R-adaptive EKF with SSF, MSFs, and FFs, a simulation is performed where the measurement noise of the x-axis magnetometer is increased 100 times at the 3500th second of the simulation and this effect is maintained for 100 s. Figure 1 shows the performance of the conventional EKF, R-adaptive EKF with SSF, MSFs, and FFs. As can be seen from Fig. 1, with the introduction of the noise increment, the tracking performance of the conventional EKF reduces significantly and it starts to give unreliable attitude estimations. On the other hand, R-adaptive EKFs continue to follow the ground truth. Since the results of the MSFs and FFs are very similar, they overlap with each other and MSFs results are not visible.

Apart from Fig. 1, Table 1 shows the root mean square error (RMSE) values of the conventional EKF, R-adaptive EKF with SSF, MSFs, and FFs. The performance
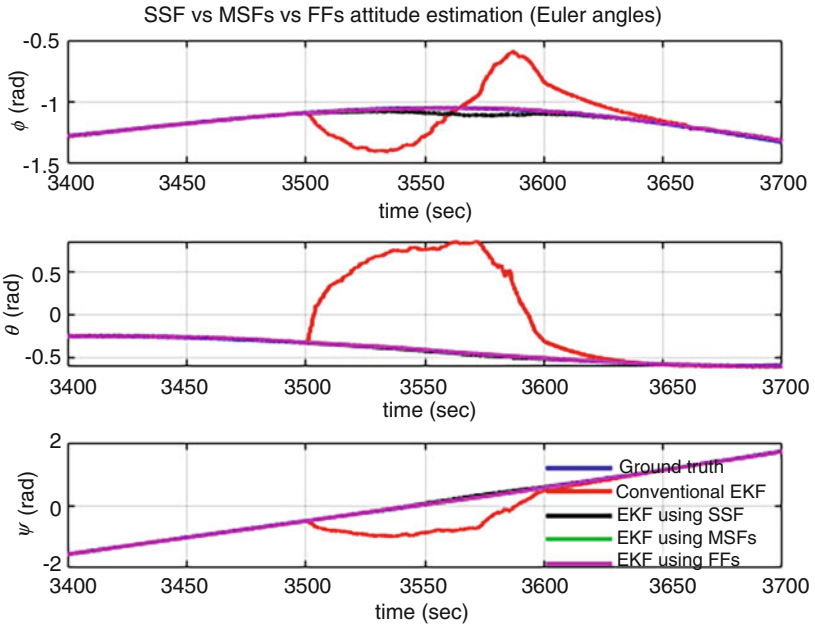
Fig. 1 Attitude estimation results in case of noise increment in the x-axis magnetometer

Table 1 RMSE values of standard and R-adaptive EKF with SSF, MSFs, and FFs during magnetometer noise increment

Euler angle (rad)	Standard EKF	SSF	MSFs	FFs
φ (roll)	0.274645	0.035006	0.002552	0.002567
θ (pitch)	0.997492	0.006021	0.005015	0.004972
ψ (yaw)	0.712692	0.026243	0.005962	0.005931

of each algorithm can be seen more clearly in Table 1. Regardless of the method, R-adaptive EKFs improve the results significantly. In addition, the superiority of the MSFs and FFs algorithms over the SSF algorithm is obvious. However, although the MSFs and FFs algorithms are slightly different, no visible difference is observed between these two algorithms.

4   Conclusion

In this study, three different integrated TRIAD/R-adaptive EKF algorithms are presented. TRIAD algorithm is used as the first-phase attitude estimation algorithm and obtained estimation is given to the R-adaptive EKF as input. As the adaptive method, covariance matching technique is chosen with single scaling and multiple scaling factors. Also, two different algorithms are presented for the multiple scaling approach. In order to verify the performance of the proposed algorithms, one simulation is performed where the x-axis magnetometer noise is increased 100 times. Simulation result shows that while the tracking performance of the conventional EKF algorithm decreases significantly, proposed R-adaptive EKF algorithms maintain their tracking performance and continue to give reliable attitude estimations. In addition, while it is observed that MSF and FF approaches give better results than the SSF approach, no significant difference is observed between the MSFs and FFs algorithms.

References

Cilden, D., & Hajiyev, C. (2014). Small satellite attitude determination methods with vector observations. *Journal of Astronautical Sciences, 7*(2), 35–43.

Hajiyev, C. (2007). Adaptive filtration algorithm with the filter gain correction applied to integrated INS/radar altimeter. *Proceedings of IMechE Part G: Journal of Aerospace Engineering, 221*, 847–855. https://doi.org/10.1243/09544100JAERO173

Hajiyev, C., & Bahar, M. (2003). Attitude determination and control system design of the ITU-UUBF LEO1 satellite. *Acta Astronautica, 52*, 493–499. https://doi.org/10.1016/S0094-5765(02)00192-3

Hajiyev, C., & Soken, H. E. (2021). *Fault tolerant attitude estimation for small satellites*. CRC Press/Taylor & Francis Group.

Kim, S. Y., Kang, C. H., & Park, C. G. (2015). A fault detection algorithm using an adaptive fading Kalman filter for various types of GNSS fault. In *2015 6th international conference on intelligent systems, modelling and simulation* (pp. 113–117). https://doi.org/10.1109/ISMS.2015.18

Lefferts, E. J., Markley, F. L., & Shuster, M. D. (1982). Kalman filtering for spacecraft attitude estimation. *Journal of Guidance, Control, and Dynamics, 5*(5), 417–429. https://doi.org/10.2514/3.56190

Shuster, M. D., & Oh, S. D. (1981). Three-axis attitude determination from vector observations. *Journal of Guidance and Control, 4*(1), 70–77. https://doi.org/10.2514/3.19717

Tafazoli, M. (2008). A study of on-orbit spacecraft failures. *Acta Astronautica, 64*, 195–205. https://doi.org/10.1016/j.actaastro.2008.07.019

Internal Heat Gain in Airport Buildings via Occupants

Okan Kon and **İsmail Caner**

Nomenclature

T	Temperature (°C, K)
ε	Clothes emissivity
σ	Stefan-Boltzmann constant
Q	Heat gain (W)
Re	Reynold number
Nu	Nusselt number
Pr	Prandtl number
Gr	Grashof number
Ra	Rayleigh number
g	Gravitational acceleration (m/s^2)
β	Coefficient of volume expansion (1/K)
l	Lenght (m)
υ	Kinematic viscosity (m^2/s)
v	Air velocity (m/s)
h	Heat convective coefficient ($W/m^2.K$)
λ	Air heat conduction coefficient (W/m.K)
A	People surface area (m^2)

O. Kon · İ. Caner (✉)
Department of Mechanical Engineering, Balikesir University, Balikesir, Türkiye
e-mail: okan@balikesir.edu.tr

© The Author(s), under exclusive license to Springer Nature Switzerland AG 2024
T. H. Karakoc et al. (eds.), *Green Approaches in Sustainable Aviation*, Sustainable
Aviation, https://doi.org/10.1007/978-3-031-33118-3_3

Subscripts

cov.   Convection
rad.   Radiation
in-rad.   Indoor air radiation

1   Introduction

Some parameters are considered heat loss, such as respiration, convection, radiation heat transfer and evaporation, and these parameters can also be considered as heat gains produced by people while calculating the energy consumption calculations of buildings in terms of thermal comfort. In the energy consumption calculations of the buildings, the gains from the people are considered as the heat gains from the internal environments of the buildings.

When calculating metabolic heat gains from occupants in buildings, heat gains are taken into account first by respiration, secondly by convection and radiation from the clothes surface, and thirdly by evaporation from the skin surface. The heat gain used here is the amount of heat produced by humans. In the literature, air velocity and temperature values in airport interiors vary from floor to ceiling. This situation varies depending on floor or ceiling heating and air blowing speed and method (Liu et al., 2018; Zhao et al., 2020; Weng et al., 2017; Liu et al., 2019).

The aim of this study is to find the sum of the heat transfer amounts that occur with convection and radiation from people in the airport buildings. Then, the aim is to calculate the indoor heat gains depending on the number of passengers. 0.2, 0.5, 1.0, 3.0, and 5.0 m/s air velocity and 20 °C indoor temperatures are accepted for convection heat transfer. The study will contribute to the literature in terms of finding the human-induced heat gains of airport buildings for different indoor conditions.

2   Material and Method

2.1   Convective Heat Transfer Calculation

Reynold number (Çengel, 2011):

$$\mathrm{Re} = \frac{V_{in}.l}{\upsilon} \tag{1}$$

The forced convective heat transfer for circular (cylindrical) surfaces (de Dear et al., 1997; Çengel, 2011):

$$4,000 < \text{Re} < 40,000 \; Nu_{\text{Forced}} = 0.193 \; Re^{0.618} \; Pr^{1/3} \tag{2}$$

$$40,000 < \text{Re} < 400,000 \; Nu_{\text{Forced}} = 0.27 \; Re^{0.805} \; Pr^{1/3} \tag{3}$$

Grashof number:

$$\text{Gr} = \frac{g.\beta.(T_{\text{cloth.}} - T_{\text{in}}).l^3}{v^2} \tag{4}$$

Rayleigh number:

$$\text{Ra} = \text{Gr.Pr} \tag{5}$$

Here, g is the gravitational acceleration, β ($1/T_m$) is the coefficient of volume expansion, T_m is the clothes and indoor temperature average, T_{clothes} is the clothes surface temperature (taken as 30 °C), T_{in} is the indoor air temperature of airport building (taken as 20 °C), l is the length of human (taken as 1.7 m), v is the kinematic viscosity, v_{in} is the air velocity in airport, Nu is the Nusselt and Pr is the Prandtl number (Çengel, 2011; TS 825, 2013; Lewandowski & Lewandowska-Iwaniak, 2014).

The free convective heat for circular (cylindrical) surfaces:

$$104 < \text{Ra} < 109 \; Nu_{\text{Free}} = 0.59 \; Ra^{1/4} \tag{6}$$

$$1010 < \text{Ra} < 1013 \; Nu_{\text{Free}} = 0.1 \; Ra^{1/3} \tag{7}$$

Free and forced heat transfer için combine Nusselt number:

$$Nu_{\text{comb.}} = \left((Nu_{\text{Forced}})^3 + (Nu_{\text{Free}})^3 \right)^{1/3} \tag{8}$$

Total convective heat transfer coefficient:

$$h_{\text{cov.}} = \frac{Nu.\lambda}{l} \tag{9}$$

Here, λ is the heat conduction coefficient of indoor air of airport building. People clothes external surface total convective heat gain between people clothes surface and people environment (indoor air environment temperature) can be calculated from below equation (Evangelisti et al., 2017; Najjaran et al., 2012; Çengel, 2011):

$$Q_{\text{cov}} = h_{\text{cov}}.A_{\text{peopl.}}.(\text{T}_{\text{cloth.}} - \text{T}_{in}) \tag{10}$$

2.2 Radiation Heat Transfer Calculation

The radiation temperature of airport building (Hannouch et al., 2020):

$$T_{\text{in} - \text{rad.}} = 0.724\,(T_{\text{in}} - 31.93) + 29 \tag{11}$$

Here, T_{in} is the indoor environment temperature of airport. Human's clothes external surface radiative heat gains' between a clothes surface and interior radiation of airport can be calculated from below equation:

$$\text{Q}_{\text{rad}} = \sigma.\varepsilon_{\text{surf}}.A_{peopl.}\left(T^4_{\text{cloth.}} - T^4_{\text{in} - \text{rad.}}\right) \tag{12}$$

Here, σ is Stefan-Boltzmann constant, $\varepsilon_{\text{surf}}$ is the surface emissivity of clothes (taken as 0.9), T_{clothes} is the external surface temperature of clothes, $A_{\text{peopl.}}$ is the surface area of clothes (taken as 1.7 m^2). The heat gain equation with the total convection and radiation heat transfer from the occupants at the airport is given below (Lewandowski & Lewandowska-Iwaniak, 2014; Çengel, 2011):

$$Q_{\text{Total}} = Q_{\text{conv.}} + Q_{\text{rad.}} \tag{13}$$

3 Results and Discussion

In the study, based on 0.2, 0.5, 1.0, 3.0, and 5.0 m/s indoor air velocity and 20 °C and 30 °C clothes surface temperatures; Nusselt numbers were calculated between 170.518 and 518.100. The Nusselt number and convection heat transfer coefficient based on these air velocities are given in Fig. 1. The amount of convection heat transfer and radiation heat caused by people due to different indoor air velocities and their total amount are shown in Fig. 2. Total heat transfer values for indoor air velocity depending on the number of passengers of airport buildings are given in Fig. 3.

Important parameters for convection heat transfer are indoor air velocity and temperature and clothes surface temperature. For radiation heat transfer, the parameters are clothes surface emissivity and indoor temperature and clothes surface temperature. In this study, the clothes surface temperature in the airport buildings was assumed to be unchanged and was taken as constant (30 °C). The clothes surface emissivity value is taken as a constant (0.9) in dark color. As
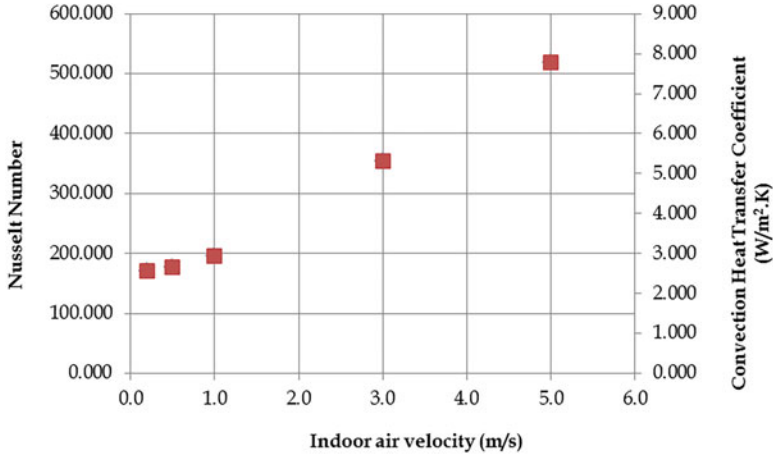
Fig. 1 Nusselt number and Convection heat transfer coefficient dependent on different indoor air velocity
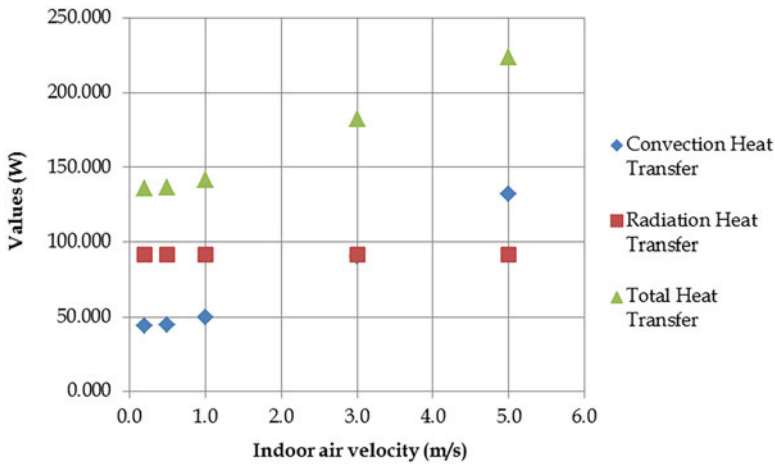
Fig. 2 Convection, radiation and total heat transfer values based on the different air velocity

the indoor air velocity value changes, the convection heat transfer value changes. Convection heat transfer amount has been calculated to vary between 44,183 and 132,175 W. However, since the indoor temperature, clothes surface temperature, and emissivity values are constant, the amount of radiation heat transfer is constant. The radiation heat transfer amount is calculated as 91,536 W.
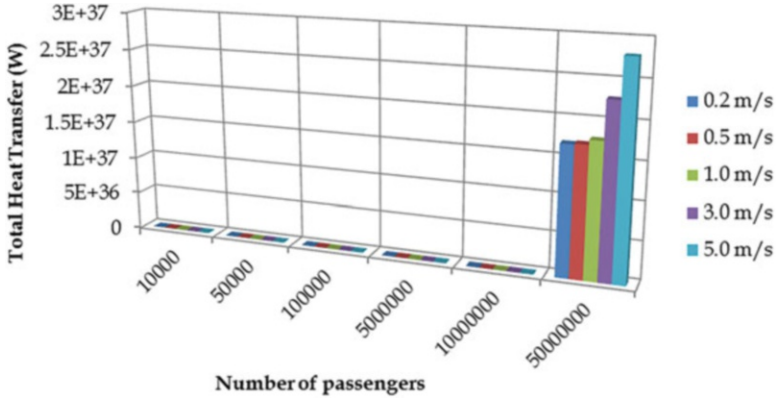
Fig. 3 Total heat transfer values for different indoor air velocity depending on the number of passengers at the airport

4   Conclusion

The results of the calculations and examinations made in the study can be summarized as follows. As the indoor air velocity increases, the amount of convection heat transfer increases. Due to this, the amount of heat transfer gain caused by human increases.

As the number of passengers (the number of people) in the airport buildings increases, the internal heat gains due to the indoor conditions increases. This is an important parameter that needs to be taken into account in the calculations of the total heating energy needs of airport buildings. The sum of the amount of convection and radiation heat transfer interior heat gain for a passenger is calculated between 136 and 224 W, depending on the indoor air velocity.

Depending on the indoor air velocity between 0.2 and 5.0 m/s in airport buildings, internal heat gain from people between 1.357,190 and 2.79639E+37 W was determined for 10,000 to 50,000,000 passengers.

Future studies will focus on all metabolic heat gains through human convection and radiation, respiration, and evaporation from the skin surface.

References

Çengel, Y. A. (2011). *Isı ve kütle transferi pratik bir yaklaşım*. Izmir.
de Dear, R. J., Arens, E., Hui, Z., & Oguro, M. (1997). Convective and radiative heat transfer coefficients for individual human body segments. *International Journal of Biometeorology, 40*, 141–156.
Evangelisti, L., Guattari, C., Gori, P., & Bianchi, F. (2017). Heat transfer study of external convective and radiative coefficients for building applications. *Energy and Buildings, 151*, 429–438.

Hannouch, A., Habchi, C., Lemenand, T., & Khoury, K. (2020). Numerical evaluation of the convective and radiative heat transfer coefficients for preterm neonate body segments inside an incubator. *Building and Environment, 183*, 107085.

Lewandowski, W. M., & Lewandowska-Iwaniak, W. (2014). The external walls of a passive building: A classification and description of their thermal and optical properties. *Energy and Buildings, 69*, 93–102.

Liu, X., Lin, L., Liu, X., Zhang, T., Rong, X., Yang, L., & Xiong, D. (2018). Evaluation of air infiltration in a hub airport terminal: On-site measurement and numerical simulation. *Building and Environment, 143*, 163–177.

Liu, X., Liu, X., Zhang, T., & Guan, B. (2019). On-site measurement of winter indoor environment and air infiltration in an airport terminal. *Indoor and Built Environment, 28*(4), 564–578.

Najjaran, A., Tahavvor, A. R., Najjaran, A., & Ahmadfard, M. A. (2012). Determination of radiation heat transfer coefficient of standing human body model by numerical approach. *Frontiers in Heat and Mass Transfer (FHMT), 3*, 033007.

Turkish Building Insulation Standard (TS 825). (2013, December). Thermal insulation requirements for buildings.

Weng, J., Zhao, K., & Ge, J. (2017). Field measurement and numerical simulation of air infiltration from entrances in an airport in winter. *Procedia Engineering, 205*, 2655–2661.

Zhao, K., Weng, J., & Ge, J. (2020). On-site measured indoor thermal environment in large spaces of airports during winter. *Building and Environment, 167*, 106463.

Cold Flow Properties of Biojet Fuels in Aviation

Mustafa Acaroğlu and **Fatma Düzenli**

1 Introduction

The fact that the fuels used for transportation in the world are of fossil origin leads to both more pollution of the environment and the gradual depletion of reserves. To protect the environment and reduce dependence on fossil fuels, alternative solutions to existing non-renewable resources are needed. The use of alternative fuels contributes to the reduction of emissions from fossil-derived fuels and to the economy of countries by reducing foreign dependence (Acaroğlu, 2013; Bouriazos et al., 2014; Köse, 2018; Ozcanli et al., 2013).

In this study, it is easy to grow, low cost and has no food value for humans and animals due to its thorny structure, causing crop losses in agricultural lands. This study aimed to produce an alternative biojet fuel by obtaining biofuel from the *Onopordum* plant and mixing it with certain amounts of aviation fuel. The new fuel obtained will both reduce the impact of emissions from conventional jet fuel on the environment and contribute to the economy of the country. In addition, some additives will be added to the biojet fuel obtained to improve the cold flow properties, which are of great importance in aviation fuels.

Jet fuels from renewable raw materials can reduce the aviation industry's dependence on a single energy source, prevent oil price fluctuations, and reduce greenhouse gas emissions (ATAG, 2011; ICAO, 2013). Therefore, the use of cleaner alternative fuels in the aviation industry will significantly improve the environment. Biomass-sourced jet (biojet) fuel has become an important element in the aviation industry's strategy to reduce operating costs and environmental impacts (Sgouridis, 2014). Biomass-based jet fuel has lower environmental impacts than petroleum-derived fuels and aviation industry and military petroleum fuels and may provide a

M. Acaroğlu (✉) · F. Düzenli
Mechanical Engineering Department, Selçuk University, Konya, Türkiye
e-mail: acaroglu@selcuk.edu.tr

Table 1 Properties of JP-8 and *Onopordum* biodiesel fuel

Properties	Unit	JP-8 (NATO F-34)	*Onopordum* biodiesel
Density	kg/l	0.775–0.840	0.883
Kinematic viscosity	mm^2/s	8 ($-20°$ C)	3.5 ($40°$ C)
CP	°C	–	-2.5
FP	°C	-47.0	-5.0
Flash point	°C	38	180
Ho	MJ/kg	42.8	40.0

good long-term solution (Asiedu et al., 2019; Dangol et al., 2017; Wang & Tao, 2016). In this study, JP-8 military aviation fuel was used as the experimental fuel. The characteristics of JP-8 fuel are shown in Table 1.

One of the most important problems of biodiesel is its cold flow properties such as cloud point, pour point, freezing point, and cold filter clogging point, which are worse than aviation fuels. Biojet fuel to be used as a fuel in the aviation industry, it must be within the limits given in aviation fuel standards. In this study, pure blank and PMA additives were added to regulate the cold flow properties of the new biojet fuel, which is obtained by mixing biodiesel fuel with JP-8 fuel in various proportions, as an aviation fuel. After the fuel properties were determined, the results were examined and the compliance of the obtained fuels with the JP-8 fuel standard was checked.

2 Material and Method

The experiment carried out in this study consists of two stages. The first stage of the experiment is to produce biodiesel from the oil of *Onopordum* plants. Biodiesel was produced from the obtained crude oil by transesterification method accompanied by alcohol and catalyst. The biodiesel used for the experiment is manufactured in accordance with EN 14214 standard. The second stage of the experiment is to obtain a biojet fuel that can be an alternative to aviation fuels. For this purpose, certain proportions of JP-8 fuel used in the aviation sector (%2, %3, %5) were mixed with the biodiesel produced from *Onopordum* oil. Then, the properties of the fuel mixtures obtained by adding cold flow additives (PMA) to improve the cold flow properties of the prepared fuel mixtures were studied. Crude oil obtained from the seeds of *Onopordum* plants was used for biodiesel production. JP-8 has been accepted as a uniform fuel for military use by NATO countries in 1988. The properties of JP-8 (NATO F-34) fuel are given in Table 1. To produce biojet fuel, blends of B2, B3, and B5 with JP-8 fuel and *Onopordum* biodiesel were prepared (Table 1). To improve the fuel properties, some cold flow improver additives have been used to be added to aviation fuel and biojet fuel. PMA, TBHQ, BHT and Pentanol additives were used to test the cold flow properties (Bhale et al., 2009). In the process of biodiesel production, biodiesel reactor, precision scales, magnetic

stirrer, thermometer, stopwatch, and free fatty acid measuring device were used. In determining the properties of all fuels and their mixtures; Density, kinematic viscosity, calorimeter, cold filter plugging point, cloud and pour point measuring device were used Acaroğlu (2013).

The cold filter plugging point value of all fuels and fuel mixtures was measured with an AFP-102 Model from Tanaka (Acaroğlu et al., 2018; Dehaghani & Rahimi, 2018). The cloud point and pour point values of all fuels and fuel mixtures were measured with a device purchased from Polyscience. This device can measure in accordance with ASTM D 97 standards (Onurbaş Avcıoğlu et al., 2011). Transesterification method was used to obtain biofuel from *Onopordum* plant. After the production of biodiesel, the fuel mixtures were prepared (Monirul et al., 2017; Ozcanli et al., 2013). In this experiment, which was carried out to determine the effect of biofuel mixtures on fuel properties in aviation fuels, 2%, 3% and 5% *Onopordum* biofuel was added to JP-8 fuel, which is one of the aviation fuels, to obtain biojet fuels ((Altaie et al., 2015; Elias et al., 2016; Serrano et al., 2014; Sorate & Bhale, 2015). In addition, to determine the effect of the additives on the cold flow properties of the fuel, the fuel properties were tested by adding certain ratios of PMA additives to the fuels. Just before starting the tests, the fuel mixtures were mixed at 600 rpm for 15 min using a thermomagnetic mixer at room temperature to obtain a homogeneous mixture in the tests (Acaroğlu, 2013; Özcanli et al., 2012). AF-1, AF-3, ..., AF-27 are single digits without additives, AF-2, AF-4, ..., AF-28 are fuels with 0.005% (by weight) PMA additives.

3 Research Results and Discussion

The fuel mixtures prepared for the experiment and the additives added to the mixtures are given in Table 2.

The pure density value of JP-8 fuel was measured as 0.7897 kg/l. While the densities remained the same according to the mixing ratios of the fuel and additives, the kinematic viscosity values showed little variation. The fuel with the highest density was AF-28 fuel with a value of 0.7917 kg/l, and the fuel with the lowest density was AF-23 fuel with a value of 0.787 kg/l. The viscosity value of JP-8 fuel without additives was 1.38 mm^2/s. The fuel with the highest kinematic viscosity was AF-20 fuel with a value of 1.54 mm^2/s. The viscosity values of AF-19 and AF-21 fuels were the same as those of the JP-8 fuel used in the experiments.

According to the test results, the cold filter plugging point of the pure JP-8 fuel was −20 °C, cloud point −23.3 °C, pour point −31.13 °C, and freezing point −47 °C (Benjumea et al., 2007; Chiu et al., 2004; Ming et al., 2005; Soriano Jr et al., 2006). According to the figure, the cold filter plugging, clouding, pour and freezing point values of AF-6 fuel were, respectively, −23 °C, −26.15 °C, −34.265 °C, and − 52 °C. These values show that AF-6 fuel has the best cold flow properties. After AF-6 fuel, the fuel with the best CFPP and FP point among biodiesel blended fuels are AF-13 fuel with the best CP and PP point is AF-21. It has been observed that

Table 2 Alternative fuel blends to JP-8 Fuel

Fuels	Code	KV (40 oC mm²/s)	Ho (MJ/kg)	Density (kg/l)	CFPP	CP	PP	FP
JP8	AF-6	1.45	46.095	0.7896	−23	−26.15	−34.265	−52
B2	AF-13	1.45	45.622	0.7885	−22	−25.20	−33.22	−51
B3	AF-21	1.38	45.709	0.7894	−22	−25.50	−33.55	−50
JP8	AF-7	1.35	46.121	0.7899	−21	−24.25	−32.175	−50
B2	AF-14	1.35	45.697	0.789	−20	−23.30	−31.13	−50
JP8	AF-2	1.40	45.81	0.790	−22	−25.50	−33.55	−49
B5	AF-27	1.32	46.136	0.7909	−21	−24.50	−32.45	−49
JP8	AF-3	1.43	45.849	0.790	−21	−24.25	−32.175	−49
B3	AF-20	1.54	45.602	0.7891	−21	−24.25	−32.175	−49
B3	AF-16	1.40	45.642	0.7893	−21	−24.50	−32.45	−48
JP8	AF-4	1.35	46.459	0.7897	−21	−24.25	−32.175	−48
B2	AF-9	1.46	45.712	0.7916	−21	−24.25	−32.175	−48
JP8	AF-5	1.31	45.779	0,7896	−20	−23.50	−31.35	−48
B2	AF-10	1.36	45.561	0,7913	−20	−23.50	−31.35	−48
B5	AF-28	1.34	46.348	0,7917	−20	−23.50	−31.35	−47
JP8	AF-1	1.38	46.574	0,7897	−20	−23.30	−31.13	−47
B2	AF-11	1.45	45.593	0,7914	−20	−23.30	−31.13	−47
B2	AF-12	1.31	45.582	0,7916	−19	−22.50	−30.25	−47
B3	AF-17	1.33	45.663	0,7891	−19	−22.50	−30.25	−47

AF-6 fuel has the best cold filter plugging point value, with a value of −23 °C, which is nearest to the density of JP-8 fuel. Considering the relationship between density and CFPP, the effect of additives is clearly visible. Although the densities remained more or less the same, it is seen that the fuel values of AF-6 and AF-21 have improved.

While there was not much change in the density values according to the mixing ratios of the fuel and additives, the kinematic viscosity values showed little variation. The fuel with the best cold flow properties among the witness fuels is AF-21, whose CFPP, CP, PP, and FP values are −22 °C, −25.5 °C, −33.55 °C, and −50 °C, respectively. According to the test results, the fuel with the highest calorific value is AF-28 fuel, and the fuel with the lowest calorific value is AF-24 fuel. Although the addition of other additives has reduced the calorific value, the values found are in the range of values suitable for fuel standards. While the density values remained the same according to the mixing ratios of biodiesel and additives, the kinematic viscosity values showed little variation. The viscosity value of AF-25 fuel (B5 + PMA additive fuel) was observed to be at the nearest value to the viscosity value of JP-8 fuel used in the experiments. With the PMA additive, cold filter plugging point, cloud point, and pour point values of all non-additive fuels were reduced by approximately −3 °C, and the freezing point value was reduced by approximately −5 °C. For all values, the PMA additive gave the best effect in improving the cold flow properties when used together with the TBHQ additive, followed by PMA-pentanol and then PMA-BHT blends, respectively. The fuel with the highest heating value is AF-1 fuel, followed by AF-27 fuel with biodiesel blend after AF-4 and AF-6 fuels. It is observed that the PMA additive stabilizes the viscosity, density, and heating values.

4 Conclusions and Recommendations

4.1 Results

In this study, to obtain biojet fuel from the *Onopordum* crops, which has no nutritional value, does not need irrigation and can be grown easily, experiments have been carried out and the results have been examined and alternative fuels to JP-8 fuel have been found. B2, B3, and B5 fuel mixtures formed by mixing *Onopordum* biofuel and JP-8 fuel in certain proportions were used in the experiments, and PMA additives were added to the mixtures in certain proportions to improve the cold flow properties of these fuels. According to the test results, it has been observed that there are many fuel mixtures that can be used as alternatives to JP-8 fuel and even have more advanced fuel properties. The kinematic viscosity, density, and calorific values of all test fuels comply with JP-8 fuel standards. However, the freezing point value of some mixtures does not comply with the JP-8 fuel standard.

The search for alternative fuels has accelerated due to depletion of fossil fuels and the ever-increasing energy need worldwide. The properties of pure B2, B3, and B5 fuels remained below JP-8 standards. However, addition of additives to these fuels showed improved fuel properties, and many fuels have been brought into compliance with the standards. It was concluded that the PMA mixture among the additives had the best effect on improving the fuel properties. In addition to JP-8 fuel, B2 fuel

mixtures are shown to exhibit the best fuel properties. Addition of 0.05 (%w) PMA additives and the use of B2 fuel mixtures as an alternative to JP-8 fuel will significantly improve the cold flow properties of jet fuels. *This is the first study on Onopordum biofuel, and it is possible to test the additives added to the fuel mixtures with different ratios or to produce different alternative fuels by diversifying the types of additives used.* Future studies should focus on the analysis of engine performance values of the biojet fuels with additives and on the development of the most suitable additive mixtures based on the values obtained in this study.

References

Acaroğlu, M. (2013). *Renewable energy sources*. Nobel Akademik Yayıncılık Eğitim Danışmanlık Tic. Ltd. Şti.

Acaroğlu, M., Aydoğan, H., & Özçelik, A. E. (2018). *Yakıtlar ve Yanma*. Nobel Akademik Yayıncılık Eğitim Danışmanlık Tic. Ltd. Şti.

Altaie, M. A. H., Janius, R. B., Rashid, U., Yap, Y. H. T., Yunus, R., & Zakaria, R. (2015). Cold flow and fuel properties of methyl oleate and palm-oil methyl ester blends. *Fuel, 160*, 238–244.

Asiedu, A., Barbera, E., Naurzaliyev, R., Bertucco, A., & Kumar, S. (2019). Waste cooking oil to jet-diesel fuel range using 2-propanol via catalytic transfer hydrogenation reactions. *Biofuels, 12*(6), 723–736.

ATAG. (2011). *Beginner's guide to aviation biofuels*. Air Transport Action Group.

Benjumea, P. N., Ramiro-Agudelo, J., & Ríos, L. A. (2007). Propiedades de flujo a baja temperatura del biodiesel de aceite de palma. *Revista Facultad de Ingeniería, 42*, 94–104.

Bhale, P. V., Deshpande, N. V., & Thombre, S. B. (2009). Improving the low temperature properties of biodiesel fuel. *Renewable Energy, 34*(3), 794–800.

Bouriazos, A., Ikonomakou, E., & Papadogianakis, G. (2014). Aqueous-phase catalytic hydrogenation of methyl esters of Cynara cardunculus alternative low-cost non-edible oil: A useful concept to resolve the food, fuel and environment issue of sustainable biodiesel. *Industrial Crops and Products, 52*, 205–210.

Chiu, C.-W., Schumacher, L. G., & Suppes, G. J. (2004). Impact of cold flow improvers on soybean biodiesel blend. *Biomass and Bioenergy, 27*(5), 485–491.

Dangol, N., Shrestha, D. S., & Duffield, J. A. (2017). Life-cycle energy, GHG and cost comparison of camelina-based biodiesel and biojet fuel. *Biofuels, 11*(4), 399–407.

Dehaghani, A. H. S., & Rahimi, R. (2018). An experimental study of diesel fuel cloud and pour point reduction using different additives. *Petroleum*. https://doi.org/10.1016/j.petlm.2018.06.005

Elias, R. C., Senra, M., & Soh, L. (2016). Cold flow properties of fatty acid methyl ester blends with and without triacetin. *Energy & Fuels, 30*(9), 7400–7409.

ICAO. (2013). *ICAO environmental report 2013 aviation and climate change*. ICAO.

Köse, H. (2018). *Cynara Cardunculus'dan Biyoyakıt Üretimi Ve Üretilen Yakıtın Farklı Karışımlarının Motor Performansına Etkisinin İncelenmesi*. Doktora Tezi, Selçuk Üniversitesi Fen Bilimleri Enstitüsü, Konya.

Ming, T. C., Ramli, N., Lye, O. T., Said, M., & Kasim, Z. (2005). Strategies for decreasing the pour point and cloud point of palm oil products. *European Journal of Lipid Science and Technology, 107*(7–8), 505–512.

Monirul, I., Kalam, M., Masjuki, H., Zulkifli, N., Shahir, S., Mosarof, M., & Ruhul, A. (2017). Influence of poly (methyl acrylate) additive on cold flow properties of coconut biodiesel blends and exhaust gas emissions. *Renewable Energy, 101*, 702–712.

Onurbaş Avcıoğlu, A., Türker, U., Demirel Atasoy, Z., & Koçtürk, D. (2011). *Tarımsal Kökenli Yenilenebilir Enerjiler-Biyoyakıtlar*. Nobel Akademik Yayıncılık Eğitim Danışmanlık Tic. Ltd. Şti.

Özcanli, M., Serin, H., Saribiyik, O. Y., Aydin, K., & Serin, S. (2012). Performance and emission studies of Castor bean (Ricinus Communis) oil biodiesel and its blends with diesel fuel. *Energy Sources, Part A: Recovery, Utilization, and Environmental Effects, 34*(19), 1808–1814.

Ozcanli, M., Gungor, C., & Aydin, K. (2013). Biodiesel fuel specifications: A review. *Energy Sources, Part A: Recovery, Utilization, and Environmental Effects, 35*(7), 635–647.

Serrano, M., Oliveros, R., Sánchez, M., Moraschini, A., Martínez, M., & Aracil, J. (2014). Influence of blending vegetable oil methyl esters on biodiesel fuel properties: Oxidative stability and cold flow properties. *Energy, 65*, 109–115.

Sgouridis, S. (2014). Are we on course for a sustainable biofuel-based aviation future? *Biofuels, 3*(3), 243–246.

Sorate, K. A., & Bhale, P. V. (2015). Biodiesel properties and automotive system compatibility issues. *Renewable and Sustainable Energy Reviews, 41*, 777–798.

Soriano, N. U., Jr., Migo, V. P., & Matsumura, M. (2006). Ozonized vegetable oil as pour point depressant for neat biodiesel. *Fuel, 85*(1), 25–31.

Wang, W.-C., & Tao, L. (2016). Bio-jet fuel conversion technologies. *Renewable and Sustainable Energy Reviews, 53*, 801–822.

Innovative Process for the Purification of Green Aviation Fuel Additive "Dimethoxymethane": Pervaporation

Derya Unlu

Nomenclature

DMM Dimethoxymethane
FTIR Fourier transform infrared spectroscopy
PEI Polyetherimide
SEM Scanning electron microscopy

1 Introduction

Dimethoxymethane is a liquid, 100% miscible in diesel fuel, does not comprise C–C atomic bonds, and contains 42% oxygen by weight. The decrement of the cetane number compared to traditional diesel fuels results in a delay in the ignition time. This situation allows more air to be drawn into the fuel jet and reduce the output of particulate matter (Song & Litzinger, 2006; Marrodán et al., 2016).

Dimethoxymethane is produced by the reaction of formaldehyde or paraformaldehyde with methanol. After the synthesis reaction, dimethoxymethane is obtained as a mixture of methanol. The methylal and methanol form an azeotrope mixture with 94.06 wt% methylal. Therefore, conventional distillation methods are not appropriate for the separation of these binary and ternary mixtures. Pervaporation, reactive distillation, and extractive distillation processes have been used in the literature to separate the methylal/methanol mixtures (Dong et al., 2018; Wang

D. Unlu (✉)
Faculty of Engineering and Natural Sciences, Chemical Engineering Department,
Bursa Technical University, Bursa, Türkiye
e-mail: derya.unlu@btu.edu.tr

et al., 2012; Xia, 2012). In this study, pervaporation is used in the separation of dimethoxymethane/methanol mixtures. The optimum operation parameters were investigated.

2 Materials and Methods

2.1 Materials

PEI was acquired from Sigma Aldrich. N-methyl-2-pyrrolidone was obtained from Carlo Erba.

2.2 Membrane Preparation

Different concentrations of PEI were dissolved in N-methyl-2-pyrrolidone at 90 °C. When the polymer was completely dissolved, the resultant polymer solution was poured into glass petri dishes and dried in an oven at 120 °C for 5 h.

2.3 Membrane Characterization

The synthesized membranes were characterized by SEM, FTIR, and TGA.

The chemical bond structure of PEI membrane was analyzed using FTIR. The morphologies of the membrane was analyzed by using a scanning electron microscope. The thermal stability of PEI membranes was acquired using a Mettler Toledo thermal analyzer.

2.4 Sorption Capacity of Membrane

The sorption capacity test was performed in room temperature to investigate the interaction of methanol and dimethoxymethane with the membrane. The membranes were cut into small pieces and weighed on a precision balance to measure dry mass. The membranes were put in petri dishes containing methanol and dimethoxymethane. At certain time intervals, the membranes were dried with filter paper and reweighed in precision balance. This operation was continued until the mass of the membranes was stabilized. The sorption capacity of the membranes was calculated by determining the affinity of membrane.

2.5 Purification of Dimethoxymethane by Pervaporation

The purification of dimethoxymethane was performed in a laboratory-scale pervaporation unit. Effects of polymer concentration on membrane, feed methanol concentration, and operation temperature on separation performance were investigated. The operation temperature was controlled by using an oven. Membrane chamber was placed in an oven. While the upstream of the membrane was under atmospheric pressure, the downstream of the membrane was held below 1 mbar. The membrane area was 9.61 cm^2. Pervaporation tests were carried out for 4 h. The flux (J) and selectivity (α) were calculated to specify the purification success of the membrane.

3 Results and Discussion

3.1 FTIR Analysis of PEI Membrane

Figure 1 shows the FTIR spectrum of PEI membrane. The characteristic absorption bands of PEI membranes can be observed at 2960 and 2850 cm^{-1} (C-H), 1716 and 1650 cm^{-1} (C=O), 1364 cm^{-1} (C-N) and 1234 cm^{-1} (C-O-C), and 1050 cm^{-1} (C-O). The presence of imide groups (O=C-N-C=O) in the membrane structure can be seen in two bonds at 1716 and 1364 cm^{-1}, respectively (Manshad et al., 2016; Santos et al., 2019).
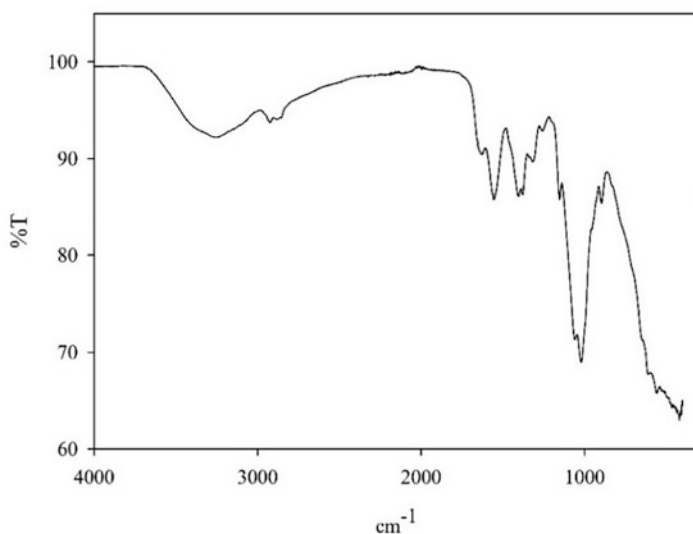
Fig. 1 FTIR spectrum of PEI membrane

Table 1 Effect of the PEI concentration on the sorption capacity of PEI membrane

	Sorption capacity of different components (%)	
Polymer concentration (wt.%)	Methanol	Dimethoxymethane
10	15	0
15	38	0
20	52	0

3.2   Sorption Capacity of PEI Membrane

Table 1 shows the effect of the PEI concentration on the sorption capacity of PEI membrane.

PEI concentration in membrane has an important effect on the sorption feature of membrane. As the PEI concentration increases, sorption capacity of membrane increases. This is related to interaction between the methanol and the functional groups of the polymer.

3.3   Pervaporation of Dimethoxymethane

Pervaporative purification performance of PEI membrane for dimethoxymethane/methanol mixture is investigated in different operation conditions. PEI membrane shows infinite selectivity. This means that PEI membrane shows an excellent separation performance.

4   Conclusion

In this research, dimethoxymethane, which is used as a fuel additive, was purified by using a PEI membrane. Dimethoxymethane/methanol mixture was separated successfully. The synthesized blend membranes were characterized by different analysis methods. The PEI membrane shows a good sorption capacity for methanol and superior separation performance in pervaporation tests. In pervaporation tests, the effects of PEI concentration, operation temperature, and feed concentration on separation performance were investigated. The results obtained are consistent with the high affinity of the membrane for methanol, so PEI membrane is appropriate for the purification of dimethoxymethane.

References

Dong, Y., Dai, C., & Lei, Z. (2018). Extractive distillation of methylal/methanol mixture using the mixture of dimethylformamide (DMF) and ionic liquid as entrainers. *Fuel, 216*, 503–512. https://doi.org/10.1016/j.fuel.2017.12.043

Manshad, S., Sazegar, M. R., Mohd. Nawawi, M. G., & Hassan, H. B. (2016). Fabrication of nanohybrid polyetherimide/graphene oxide membranes: Biofuel dehydration by pervaporation process. *RSC Advances, 6*(106), 103888–103894. https://doi.org/10.1039/C6RA22104A

Marrodán, L., Monge, F., Millera, Á., Bilbao, R., & Alzueta, M. U. (2016). Dimethoxymethane oxidation in a flow reactor. *Combustion Science and Technology, 188*(4–5), 719–729. https://doi.org/10.1080/00102202.2016.1138826

Santos, A. M., Habert, A. C., & Helen, C. F. (2019). Polyetherimide/Polyvinylpyrrolidone hollow-fiber membranes for use in hemodialysis. *Brazilian Journal of Chemical Engineering, 36*(4), 1645–1652. https://doi.org/10.1590/0104-6632.20190364s20180529

Song, K. H., & Litzinger, T. A. (2006). Effects of dimethyoxymethane blending into diesel fuel on soot in an optically accessible Di diesel engine. *Combustion Science and Technology, 178*(12), 2249–2280. https://doi.org/10.1080/00102200600637204

Wang, Q., Yu, B., & Xu, C. (2012). Design and control of distillation system for Methylal/methanol separation. Part 1: Extractive distillation using DMF as an Entrainer. *Industrial and Engineering Chemistry Research, 51*, 1281–1292. https://doi.org/10.1021/ie201946d

Xia, M. Y. (2012). Design and control of extractive dividing-wall column for separating methylal–methanol mixture. *Industrial and Engineering Chemistry Research, 51*(49), 16016–16033. https://doi.org/10.1021/ie3015395

Deceleration Behavior
of Super-Lightweight XPS Foams: Number
# of Layers Effect

Mohammad Rauf Sheikhi ⓘ**, Selim Gürgen** ⓘ**, Onder Altuntas** ⓘ**,
and Melih Cemal Kuşhan** ⓘ

Nomenclature

XPS   Extruded polystyrene
EPS   Expanded polystyrene
PD   Peak deceleration

1   Introduction

Ultralight aviation requires a lightweight design to allow for extended flying times
and reduced fuel consumption. Lightweight design entails using less material with a
lower density while maintaining or improving technical performance. Lightweight
design can improve flying performance by allowing for faster acceleration, increased
structural strength and rigidity, and improved safety, in addition to reduced emis-
sions (Zhu et al., 2018; Obradovic et al., 2012). To achieve lightweight design for
aerospace components, a common approach is to use advanced lightweight materials
in structures that can be fabricated using appropriate manufacturing methods. As a
result, the use of lightweight materials can effectively reduce weight while also
improving performance (Yancey, 2016). Although metal materials, particularly
aluminum alloys, continue to be the dominant materials in aerospace applications,
composite materials are gaining traction and competing with aluminum alloys in

M. R. Sheikhi (✉) · O. Altuntas
Faculty of Aeronautics and Astronautics, Eskişehir Technical University, Eskişehir, Türkiye
e-mail: mohammadraufsheikhi@eskisehir.edu.tr; oaltuntas@eskisehir.edu.tr

S. Gürgen · M. C. Kuşhan
Department of Aeronautical Engineering, Eskişehir Osmangazi University, Eskişehir, Türkiye
e-mail: sgurgen@ogu.edu.tr; mkushan@ogu.edu.tr

many new aircraft applications (Clyne & Hull, 2019). Composite core materials are used to complete the function of engineered structures by compensating for a specific design or performance requirement, such as weight reduction, energy absorption, impact resistance, or stiffness. It is critical to choose the right composite core material that will perform as expected and provide the properties required for advanced composites. The core materials market for composites is likely to be driven by an increase in the use of honeycomb core materials in the aerospace industry (Nunes & Silva, 2016; Stewart, 2009). The increased demand for honeycomb core materials from next-generation aircrafts is to blame for this (Pflug et al., 2003). In the last few decades, the aircraft sector has seen several advances in component manufacture. Wood and metal have been phased out of airplane component manufacturing in favor of various lightweight composites (Dhakal & Ismail, 2020). As a result of the growing use of composites in the aerospace sector, the need for core materials is expanding. Cabin linings, ceiling panels, air ducts, overhead compartments, winglets, and fins are some of the aircraft components made from core materials. Polystyrene is a synthetic aromatic hydrocarbon polymer derived from styrene as a monomer. Foamed polystyrene is a super-lightweight substance that weighs around 1% of that of earth. For insulating pavements, two forms of foamed polystyrene are commonly used: expanded polystyrene (EPS) and extruded polystyrene (XPS) (Horvath, 1994; Winterling & Sonntag, 2011). The linked spaces between the beads in EPS can allow water to pass through the insulation. XPS, on the other hand, is a closed-cell rigid foam insulating board that has no voids or moisture channels. Designers use XPS because it offers stronger strength and less water absorption than EPS.

2 Experimental Details

The material used in this study was a closed-cell extruded polystyrene (XPS) foam from Orsa Inc. XPS, with their ease of foaming, low cost, and distinct thermal insulating and mechanical qualities, play a prominent role in thermal insulation applications and core materials of composites. Design layers were created by scaling an XPS foam board into 50 mm × 50 mm × 3 mm. Fabricated XPS sheets were bonded as multi-layer using tape adhesive on the outsides. By dropping a mass on the specimens, the deceleration properties of XPS multi-layers were investigated in a drop tower impact test system. The falling head was a 15 mm diameter hemispherical rod. The falling head's mass was 1 kg, resulting in impact energy of 2.45 J for drop heights of 0.25 m. The decelerations on the multi-layer XPS foams were measured using an accelerometer bonded to the falling impactor (Fig. 1).
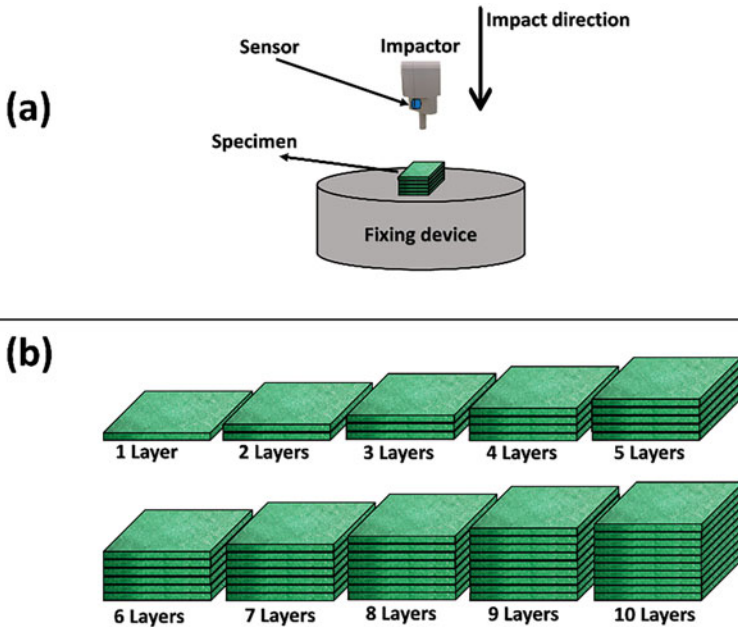
Fig. 1 (**a**) Experimental impact setup and (**b**) designed configurations for impact test

3 Results and Discussion

Peak deceleration (PD), which should be as low as feasible in safety applications, is one of the most essential aspects. Figure 2 depicts the PD amounts for several XPS multilayers. The number of XPS layers is the determining factor in PDs, as seen in Fig. 3. PD is reduced by 0.2, 2.59, and 5.2 times when comparing 1-layer specimen to 3-layer, 6-layer, and 10-layer specimens, respectively. Due to their high recoverability and buckling of cell walls after impact, foam layers display buckling of cell walls and release the absorbed energy and, thus, the spring effect mechanism becomes bigger with increasing foam layers. Figure 3 depicts the deceleration vs. time curves for a 0.25 m drop height. We may examine the role of several XPS layers in the composites by comparing configurations 1–10. There are two consecutive peaks on the 1-layer XPS curve, the first of which represents the major contact with the impactor and the second of which is connected to structural thickness. The stress shift from impactor to fixing device beneath the XPS layer causes the second peak. The deceleration rate (curve slope) is somewhat reduced when the thickness of the XPS layers is increased, and the peak base is extended over a longer period. By adding 2 layers, peak durations show almost no change compared to 1 layer. However, increasing XPS layers slightly extends the deceleration process. This effect is more pronounced in 4 layers to 6 layers. In 7 layers to 9 layers, deceleration processes exhibit further extensions while reducing curve slopes and peak points.
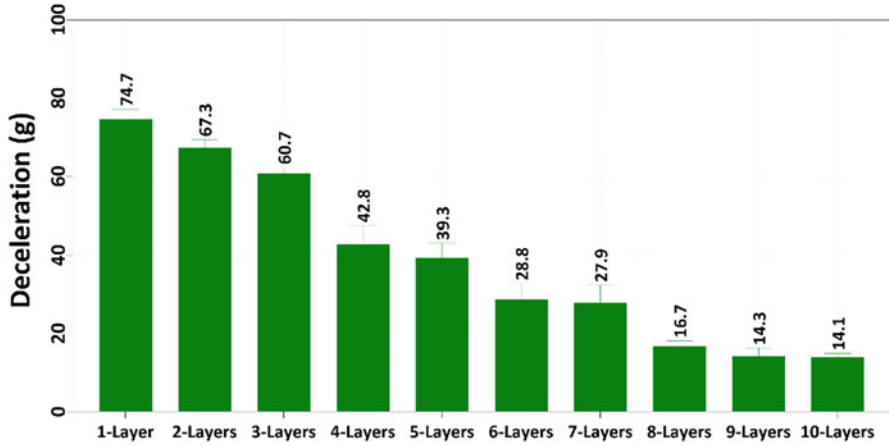
Fig. 2 Deceleration results of 1-layer to 10-layer multi-layer XPS foams
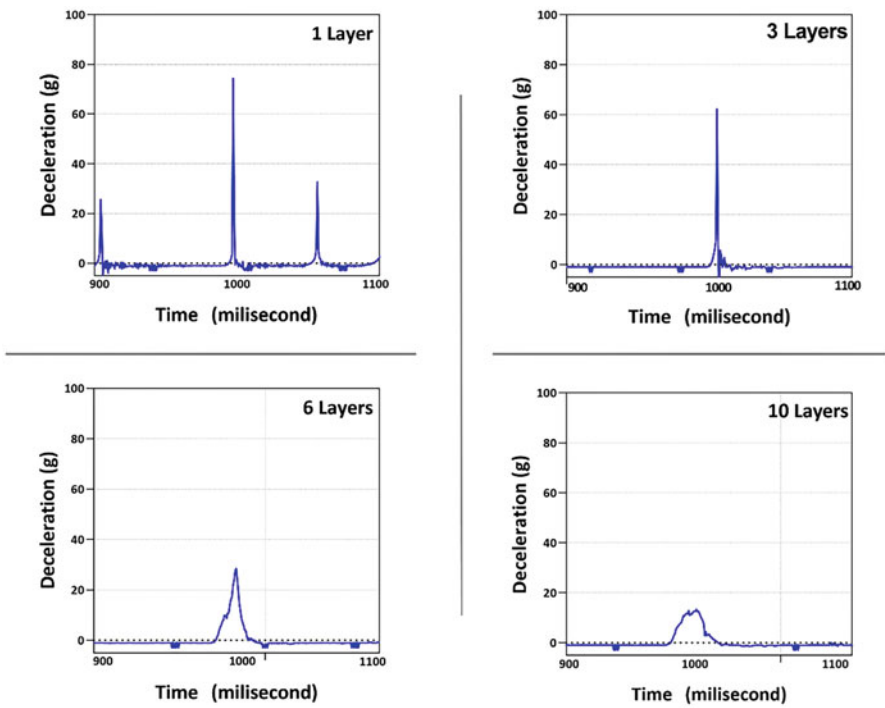
Fig. 3 Deceleration vs time curves for a drop height of 0.25 m

4   Conclusion

In this study, the deceleration properties of XPS foam multi-layers were investigated for possible applications in the core layer of the aircraft's structure to reduce its weight. Due to the super-lightness of XPS layers, the effect of the gradual increase factor of the layers on the reduction of PD was the main motivation of the study. The results showed that PD decreased five times although the weight of the 10-layer XPS sample increased only two grams. The main factor in the recovery of XPS and the high energy absorption capacity of the XPS foam structure reduced the PD value from 74.7 to 14.1 g. This reduction can be an important factor for use in the core of sandwich structures and composites as multi-thin layers more than a thick layer of the same size.

References

Clyne, T. W., & Hull, D. (2019). *An introduction to composite materials*. Cambridge University Press.

Dhakal, H. N., & Ismail, S. O. (2020). *Sustainable composites for lightweight applications*. Woodhead Publishing.

Horvath, J. (1994). Expanded polystyrene (EPS) geofoam: An introduction to material behavior. *Geotextiles and Geomembranes, 13*(4), 263–280.

Nunes, J., & Silva, J. F. (2016). Sandwiched composites in aerospace engineering. In *Advanced composite materials for aerospace engineering* (pp. 129–174). Elsevier.

Obradovic, J., Boria, S., & Belingardi, G. (2012). Lightweight design and crash analysis of composite frontal impact energy absorbing structures. *Composite Structures, 94*(2), 423–430.

Pflug, J., Vangrimde, B., Verpoest, I., Bratfisch, P., & Vandepitte, D. (2003). Honeycomb core materials: New concepts for continuous production. *Sampe Journal, 39*(6), 22–33.

Stewart, R. (2009). At the core of lightweight composites. *Reinforced Plastics, 53*(3), 30–35.

Winterling, H., & Sonntag, N. (2011). Rigid polystyrene foam (EPS, XPS). *Kunststoffe International, 101*(10), 18–21.

Yancey, R. (2016). Challenges, opportunities, and perspectives on lightweight composite structures: Aerospace versus automotive. In *Lightweight composite structures in transport* (pp. 35–52). https://doi.org/10.1016/B978-1-78242-325-6.00002-5

Zhu, L., Li, N., & Childs, P. (2018). Light-weighting in aerospace component and system design. *Propulsion and Power Research, 7*(2), 103–119.

Green Purchase Intention in the Air Travel Industry: Influence of Environmental Knowledge and Attitude

Mahmut Bakır ⓘD

Nomenclature

AVE	Average Variance Extracted
F-VIF	Full Variance Inflation Factor
GPB	Green Purchase Behavior
HTMT	Heterotrait-Monotrait Ratio of Correlations
IATA	International Air Transport Association
ICAO	International Civil Aviation Organization
PLS-SEM	Partial Least Square Structural Equation Modeling
SAF	Sustainable Aviation Fuel
VAB	Value-Attitude-Behavior

1   Introduction

The air travel industry is currently responsible for 3% of global carbon dioxide (CO_2) emissions and 11% of the total CO_2 emissions from the transport industry. Therefore, the air travel industry is one of the fastest-growing emitters of greenhouse gases (Kharina et al., 2018). Current projections indicate that demand for air travel will surpass 10 billion by 2050, resulting in roughly 21.2 gigatons of CO_2 emissions by that year (IATA, 2022).

There are numerous efforts to curb the increase in CO_2 emissions. The International Civil Aviation Organization (ICAO) focuses on two aspirational targets, including a 2% fleet-wide increase in fuel efficiency by 2050 and zero net growth

M. Bakır (✉)
Department of Aviation Management, Samsun University, Samsun, Türkiye
e-mail: mahmut.bakir@samsun.edu.tr

in aviation CO_2 emissions through the Fly Net Zero project (Kharina et al., 2018). Multiple action plans, such as sustainable aviation fuel (SAF), adoption of new technologies based on electricity and hydrogen, offsets, and carbon capture, contribute to the aim of zero net growth in CO_2 emissions (IATA, 2022). Furthermore, airlines have also implemented environmentally responsible initiatives to become more eco-friendly. For instance, Delta Air Lines has pledged $1 billion toward carbon neutrality by 2030. Similarly, JetBlue has committed to achieving its goal of being carbon neutral by 2040 and United Airlines by 2050 (Boerner, 2021).

The level of consumer sensitivity and understanding regarding the deterioration of the environment and its impact on social life is growing day by day. This circumstance has given rise to a process in which consumers evaluate their purchase decisions in light of the environment and human health (Varshneya et al., 2017). Therefore, consumers demand environmentally friendly products due to increasing environmental awareness and related concerns (Mohd Suki, 2016). For this reason, it is essential to understand the purchasing behavior of environmentally conscious consumers in the air travel industry, a significant source of CO_2 emissions.

Consumers' environmental knowledge significantly drives their propensity to purchase eco-friendly products (Li et al., 2019). On the other hand, consumers' intention to acquire green products is an indispensable manifestation of their green purchasing behavior. Understanding this aspect is critical for the development of marketing strategies by airlines (Zhuang et al., 2021). In addition, according to the value-attitude-behavior (VAB) model, the mediating role of attitude in the relationship between environmental knowledge and green purchase intention should not be overlooked. Ignoring this point may lead to an underestimation of the influence of environmental knowledge on purchase intention (Li et al., 2019). The purpose of this study is twofold: to examine the effect of environmental knowledge on green purchasing intention in the air travel industry and to examine the mediating effect of green attitude in general on the relationship between environmental knowledge and green purchase intention.

2 Literature Review

2.1 Environmental Knowledge

Environmental knowledge is an individual's comprehension and familiarity with environmental concerns (Mostafa, 2009). Individuals with a particular environmental knowledge are more likely to take pro-environmentalist actions and do not disregard the potential environmental consequences of their actions (Li et al., 2019). Kusuma and Sulhaini (2018) discovered that those with greater environmental knowledge were more likely to purchase eco-friendly products. A similar finding was also found in the meta-analysis conducted by Zhuang et al. (2021). The existing literature also suggests that environmental knowledge positively affects attitudes

toward green products (Rusyani et al., 2021). Thus, we contend, in the context of the air travel industry:

H1: Environmental knowledge positively influences green purchase intention.
H2: Environmental knowledge positively influences green attitude in general.

2.2   Green Attitude

Attitude refers to a settled style of thinking and stable psychological inclination that affects an individual's behavior (Ajzen, 1991). As an individual's favorable attitude toward a particular action grows, so does his or her propensity to engage in that conduct. Attitude is an important explanatory factor in explaining purchasing behavior toward green products (Li et al., 2019). Rusyani et al. (2021) suggested that positive green attitudes significantly predicted the eco-sustainable purchasing behavior of customers because consumers with positive green attitudes feel a part of the global community. Therefore, it would not be surprising if the green attitude affects purchase intention in airline travel. Thus, we anticipate:

H3: Green attitude in general positively influences green purchase intention.

2.3   Green Attitude as a Mediator

The value-attitude-behavior (VAB) model postulates that attitude has a mediating role in the relationship between values and behaviors (Homer & Kahle, 1988). Accordingly, attitudes potentially serve as a mediator between green buying behaviors and various stimuli. Within the Green Purchase Behavior (GPB) model, which is one of the best models for explaining the attitude-behavior relationship for green products, a meta-analysis has revealed that attitude mediates the effect of several antecedents on green purchase intention (Zaremohzzabieh et al., 2021). Thus, the following is hypothesized:

H4: The association between environmental knowledge and green purchase intention is mediated by green attitude.

3   Data and Methodology

Using a quantitative research approach, previously validated scales were used to quantify latent variables in this study. Respondents were asked to rate the items on a 5-point Likert scale ranging from 1 "Strongly Disagree" to 5 "Strongly Agree." The scales were taken from Varshneya et al. (2017) to measure green attitude in general.

The scale of environmental knowledge was borrowed from Mostafa (2009). Finally, the scale employed by Mohd Suki (2016) was used for measuring green purchase intention.

The population taken for this study is airline customers in Turkey. In 2021, Turkey hosted a total of 128,350,222 passengers, including those in transit, making it a prominent country whose civil aviation industry is seeing a significant expansion (DHMI, 2022). Therefore, the current environment is extremely beneficial for the implementation of green aviation principles and best practices. A convenience sampling approach was adopted for data collection (Varshneya et al., 2017).

A web-based questionnaire was created to collect the study data. Hulland et al. (2018) concluded in a literature review study of 202 studies that electronically based surveys are quite common in the marketing field. During the data collection process, 160 participants were surveyed. Four observations revealed a dubious response pattern known as straight-lining but no incomplete responses. After eliminating these four responses, 156 responses remained for analysis.

Kock and Hadaya (2018) recommend that the sample size for partial least squares structural equation modeling (PLS-SEM) analysis should be determined using the inverse square root or gamma exponential approaches. Since there is no expectation for a minimum path coefficient in our study model, the gamma exponential approach deems at least 146 respondents to be sufficient (Kock & Hadaya, 2018).

We used the PLS-SEM approach to analyze the data. PLS-SEM is a connoisseur of explanatory research (Hair et al., 2021) since it is devoted to maximizing the explained variance of latent variables. PLS-SEM can effectively analyze non-normal data and small sample sizes (Mohd Suki, 2016). According to Sarstedt et al. (2020), PLS-SEM can make more conservative analyses than its counterparts as it takes measurement error into account in advanced analyses such as the mediation effect. All estimations in this study were performed with ADANCO v2.3 (Henseler, 2021).

4 Results

In this study, data obtained from a total of 156 respondents were analyzed. There were 94 male respondents (60.3%) and 62 female respondents (39.7%). Regarding the age group, 87 respondents were between the ages of 18 and 25 (55.8%), while 51 respondents were between the ages of 26 and 35 (32.7%). In terms of educational background, it is also observed that the majority of respondents, namely 96 respondents (61.5%), hold a bachelor's degree. Lastly, 102 respondents (65.4%) traveled for leisure.

The PLS-SEM analysis consists of two phases: the measurement model analysis and the structural model analysis (Mohd Suki, 2016). However, in the measurement model, the risk of common method bias was initially examined using the full collinearity (F-VIF) test proposed by Kock (2017) for the PLS-SEM approach. Since the F-VIF values of the research constructs ranged from 1.362 to 1.574 (F-VIF <3.3), the data do not pose a threat of common method bias (Kock, 2017).

Table 1 Reliability and validity analysis

Construct	Items	Loading	Cronbach's alpha	Rho_A	AVE
Environmental knowledge	ENK1	0.851	0.853	0.859	0.631
	ENK2	0.820			
	ENK3	0.824			
	ENK4	0.736			
	ENK5	0.732			
Green attitude in general	ATT1	0.834	0.836	0.843	0.753
	ATT2	0.905			
	ATT3	0.863			
Green purchase intention	PUI1	0.761	0.670	0.725	0.595
	PUI2	0.850			
	PUI3	0.695			

Table 2 Discriminant assessment (HTMT-2)

Construct	ENK	ATT	PUI
ENK	–		
ATT	0.448	–	
PUI	0.652	0.624	–

In the measurement model, the three reflectively measured constructs, namely environmental knowledge, green attitude in general, and green purchase intention, were evaluated using confirmatory factor analysis. As shown in Table 1, Cronbach's α and Dijkstra-Henseler's rho (Rho_A) values of the constructs are above the recommended threshold of 0.70, except for Cronbach's α value of green purchase intention (Hair et al., 2021). However, this value is also at a tolerable level. Therefore, internal consistency was attained. According to Table 1, the average variance extracted (AVE) values of all constructs are larger than the cutoff of 0.50, and factor loadings are higher than a threshold of 0.60. Therefore, convergent validity was established in this study (Mohd Suki, 2016).

To assess discriminant validity, we applied a measure of the heterotrait-monotrait ratio of correlations (HTMT-2) that outperformed its competitors (Roemer et al., 2021). As a conservative benchmark, the HTMT-2 measure should fall below 0.85. As seen in Table 2, HTMT-2 values are much below the cutoff, proving discriminant validity.

Next, the structural model was analyzed the hypothesized relationships. This was accomplished using the percentile bootstrapping technique with 999 subsamples (Henseler, 2021). Table 3 displays the results of the structural model supporting all hypotheses (H1–H4). Accordingly, environmental knowledge positively influences green purchase intention ($\beta = 0.377$, $p < 0.01$) and green attitude in general ($\beta = 0.436$, $p < 0.01$). Hence, H1 and H2 are supported. In a similar vein, green attitude in general exerts a significant positive impact on green purchase intention ($\beta = 0.379$, $p < 0.01$), bringing evidence for H3. Finally, path estimates noted that green attitude mediates the impact of environmental knowledge on green purchase intention ($\beta = 0.165$, $p < 0.01$). Thus, H4 is also maintained. For significant path

Table 3 Hypothesis testing results

Hypothesis	β	t-value	CI (95%)	Cohen's f2	p-value	Support
ENK → PUI	0.407	7.212	[0.293; 0.514]	0.233	0.000	Yes
ENK → ATT	0.392	4.933	[0.224; 0.536]	0.181	0.000	Yes
ATT → PUI	0.349	5.188	[0.217; 0.483]	0.172	0.000	Yes
ENK → ATT → PUI	0.137	3.592	[0.068; 0.217]	NA	0.000	Yes
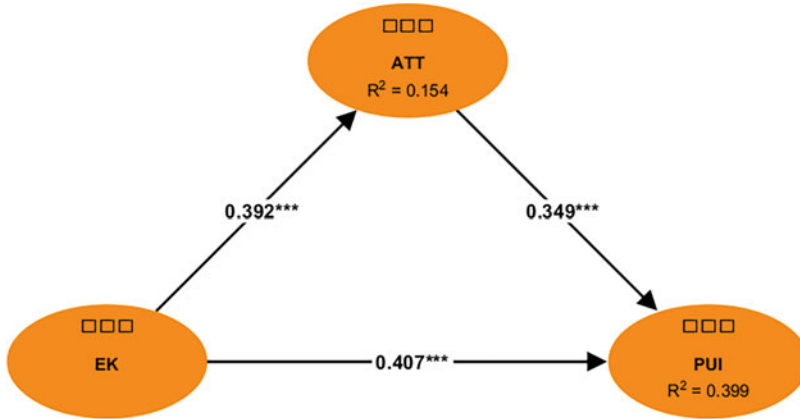
Fig. 1 Results of the structural model

coefficients, effect sizes above 0.02, 0.15, and 0.35 yield small, medium, and large effects, respectively (Hair et al., 2021). According to Table 3, H1-H3 hypotheses with a direct relationship show a medium effect.

For the structural model, we finally examined the in-sample explanatory power (R^2) of endogenous variables (see Fig. 1). Accordingly, the variances explained by green attitude in general and green purchase intention were 15.4% and 39.9%, respectively. Although the practical significance of the R^2 value varies depending on the research context, values above 0.15–0.20 are acceptable in areas such as consumer behavior (Hair et al., 2021). Thus, we may infer that the research model provides sufficient explanatory power.

5   Conclusion

As Sect. 4 delineates, our empirical results reveal significant relationships between environmental knowledge, green attitude in general, and green purchase intention. Moreover, the green attitude in general has a mediating effect in the proposed conceptual model. These findings are consistent with past research (Mohd Suki, 2016; Varshneya et al., 2017; Kusuma & Sulhaini, 2018; Chen et al., 2020; van Tonder et al., 2020). Previous research (Mohd Suki, 2016; Kusuma & Sulhaini,

2018; Li et al., 2019) has corroborated the effect of environmental knowledge on attitude and green purchase intention. In addition, the finding that attitude is also a determinant of green purchase intention is not surprising, as earlier research (Mohd Suki, 2016; Li et al., 2019; Chen et al., 2020) has demonstrated this. Moreover, similar to Li et al. (2019), this study discovered the mediating effect of green attitude on the proposed relationship.

This study has theoretical contributions. First, this study addresses the notion of green purchase intention to contribute to the body of knowledge on sustainable consumerism in the domain of civil aviation. Moreover, to the best of the author's knowledge, the association between environmental knowledge and green purchase intention has not been explored before in the context of the air travel industry. This study reveals that environmental knowledge favorably influences green purchase intention directly or through green attitude in general, thus filling the research gap.

According to the findings, an innovative airline that wants to strengthen passenger purchase intention should be able to communicate its sustainable practices to environmentally conscious customers through communication channels. Moreover, to increase green purchase intention, managers must implement marketing strategies that will reinforce consumer attitudes.

References

Ajzen, I. (1991). The theory of planned behavior. *Organizational Behavior and Human Decision Processes, 50*, 179–211. https://doi.org/10.1016/0749-5978(91)90020-T

Boerner, L. K. (2021). Airlines want to make flight more sustainable. How will they do it? *Chemical and Engineering News, 99*(32). https://cen.acs.org/environment/sustainability/Airlines-want-make-flight-sustainable/99/i32

Chen, Y. S., Chang, T. W., Li, H. X., & Chen, Y. R. (2020). The influence of green brand affect on green purchase intentions: The mediation effects of green brand associations and green brand attitude. *International Journal of Environmental Research and Public Health, 17*, 1–17. https://doi.org/10.3390/ijerph17114089

DHMI. (2022). *Statistics*. https://www.dhmi.gov.tr/Lists/Istatislikler/Attachments/244/YOLCU.pdf

Hair, J. F., Hult, G. T. M., Ringle, C. M., et al. (2021). *Partial Least Squares Structural Equation Modeling (PLS-SEM) using R: A workbook* (1st ed.). Springer.

Henseler, J. (2021). *Composite-based structural equation modeling: Analyzing latent and emergent variables* (1st ed.). Guilford Press.

Homer, P. M., & Kahle, L. R. (1988). A structural equation test of the value-attitude-behavior hierarchy. *Journal of Personality and Social Psychology, 54*, 638–646. https://doi.org/10.1037/0022-3514.54.4.638

Hulland, J., Baumgartner, H., & Smith, K. M. (2018). Marketing survey research best practices: Evidence and recommendations from a review of JAMS articles. *Journal of the Academy of Marketing Science, 46*, 92–108. https://doi.org/10.1007/s11747-017-0532-y

IATA. (2022). *Our commitment to fly net zero by 2050*. https://www.iata.org/en/programs/environment/flynetzero/

Kharina, A., MacDonald, T., & Rutherford, D. (2018). *Environmental performance of emerging supersonic transport aircraft*. https://theicct.org/wp-content/uploads/2021/06/Environmental_Supersonic_Aircraft_20180717.pdf

Kock, N. (2017). Common method bias: A full collinearity assessment method for PLS-SEM. In H. Latan & R. Noonan (Eds.), *Partial least squares path modeling* (pp. 215–257). Springer.

Kock, N., & Hadaya, P. (2018). Minimum sample size estimation in PLS-SEM: The inverse square root and gamma-exponential methods. *Information Systems Journal, 28*, 227–261. https://doi.org/10.1111/isj.12131

Kusuma, P. N. P. D., & Sulhaini, R. B. H. (2018). The effect of environmental knowledge, green advertising and environmental attitude toward green purchase intention. *Russian Journal of Agricultural and Socio-Economic Sciences, 78*, 95–105. https://doi.org/10.18551/rjoas.2018-06.10

Li, G., Li, W., Jin, Z., & Wang, Z. (2019). Influence of environmental concern and knowledge on households' willingness to purchase energy-efficient appliances: A case study in Shanxi, China. *Sustainability, 11*, 1–18. https://doi.org/10.3390/su11041073

Mohd Suki, N. (2016). Green product purchase intention: Impact of green brands, attitude, and knowledge. *British Food Journal, 118*, 2893–2910. https://doi.org/10.1108/BFJ-06-2016-0295

Mostafa, M. M. (2009). Shades of green: A psychographic segmentation of the green consumer in Kuwait using self-organizing maps. *Expert Systems with Applications, 36*, 11030–11038. https://doi.org/10.1016/j.eswa.2009.02.088

Roemer, E., Schuberth, F., & Henseler, J. (2021). HTMT2–an improved criterion for assessing discriminant validity in structural equation modeling. *Industrial Management & Data Systems*. https://doi.org/10.1108/IMDS-02-2021-0082

Rusyani, E., Lavuri, R., & Gunardi, A. (2021). Purchasing eco-sustainable products: Interrelationship between environmental knowledge, environmental concern, green attitude, and perceived behavior. *Sustainability, 13*, 1–12. https://doi.org/10.3390/su13094601

Sarstedt, M., Hair, J. F., Nitzl, C., et al. (2020). Beyond a tandem analysis of SEM and PROCESS: Use of PLS-SEM for mediation analyses! *International Journal of Market Research, 62*, 288–299. https://doi.org/10.1177/1470785320915686

van Tonder, E., Fullerton, S., & de Beer, L. T. (2020). Cognitive and emotional factors contributing to green customer citizenship behaviours: A moderated mediation model. *Journal of Consumer Marketing, 37*, 639–650. https://doi.org/10.1108/JCM-06-2019-3268

Varshneya, G., Pandey, S. K., & Das, G. (2017). Impact of social influence and green consumption values on purchase intention of organic clothing: A study on collectivist developing economy. *Global Business Review, 18*, 478–492. https://doi.org/10.1177/0972150916668620

Zaremohzzabieh, Z., Ismail, N., Ahrari, S., & Abu Samah, A. (2021). The effects of consumer attitude on green purchase intention: A meta-analytic path analysis. *Journal of Business Research, 132*, 732–743. https://doi.org/10.1016/j.jbusres.2020.10.053

Zhuang, W., Luo, X., & Riaz, M. U. (2021). On the factors influencing green purchase intention: A meta-analysis approach. *Frontiers in Psychology, 12*, 1–15. https://doi.org/10.3389/fpsyg.2021.644020

Evaluation of Air Transport Projects Development by AHP

Omar Alharasees and Utku Kale

Nomenclature

AHP	Analytical Hierarchy Process
MCDM	Multi-Criteria Decision-Making
PCM	Pairwise Comparison Matrix
CR	Consistency Ratio
ATCO	Air Traffic Controller

1 Introduction

The growth and expansion of the aeronautics and avionics systems are interdependent on each participant in the system (carriers, airports, air traffic management (ATM), airplanes producers, and so on), and this is reflected in the system's actual status (Rohács & Rohács, 2020; Kale et al., 2021). However, the literature did not highlight the duties change and roles for the aviation operators (Kale et al. 2020), which directly impacts the air transport supply quality.

Emphasizing the value of quality measurement in achieving organizational success is challenging (Aydin, 2017). In order to assess whether an organization will succeed or fail, system quality must be evaluated (Estrada & Romero, 2016; Dalkıran et al., 2022). As a result, conventional statistics use cardinal or ordinal scales to rate the quality of a system (Akdag et al., 2014).

O. Alharasees (✉) · U. Kale
Department of Aeronautics and Naval Architecture, Budapest University of Technology and Economics, Budapest, Hungary
e-mail: oalharasees@edu.bme.hu; kale.utku@kjk.bme.hu

One method for assessing supply quality involves the analytic hierarchy process (AHP), a core part of Multi-Criteria Decision-Making (MCDM) technique for several objective ranking procedures and a simplified method for handling complex decision-making (Saaty, 2008). The AHP method is used to resolve multiple difficult decision-making problems (Nakagawa & Sekitani, 2004). It is used in a variety of contexts, including business, manufacturing, medical services, and education. AHP assigns a weight to each evaluation criterion based on the decision-maker's pairwise comparisons of the criteria.

Numerous prior research papers hired AHP in aeronautics and avionics. Chou (Chao & Kao, 2015) estimated the quality service recommended by the international air transport industry which suggested that reliability and assurance are key factors for service quality qualification. Rezaei et al. (2014) examined the framework for choosing a suitable retailer for the aviation business by illustrating competing quantitative and qualitative factors in arriving at the criteria for the selection of a retailer. The core criterion illustrated by the study in picking a retailer is financial stability. Zietsman & Vanderschuren (2014) assessed and investigated the growth of a multi-airport by studying the territorial competitiveness factor in airport development rather than structure and economic activities. According to the findings, Cape Town City demands a single-airport system up until the volume of passengers increases beyond the current volume. Bruno et al. (2015) emphasized service quality, considering the customer and environmental impact in aircraft evaluation. Determining that the highly significant element in airlines is the size cabin luggage compartment.

The study aims to assess the factors affecting the supply side of the aviation industry from the perspective of aircraft operators. Based on the main criteria, the current study investigates the priorities of four expert groups: (i) air traffic controllers (ATCOs), (ii) new generation pilots, (iii) old generation pilots, (iv) aeronautical engineers & MRO operators. The analytic hierarchy process (AHP) is used to build a general hierarchical model. To generate evaluator preference loads for (i) the assessment technique, (ii) eliminating conflicts, and (iii) lacking information from other AHP functions, the utilized decision-making model is constructed on three levels. In this study, missing data was represented using matrices that could be generated using a specific method employing the Saaty-Scale for scoring.

2   Method

Thomas L. Saaty initially developed the AHP technique for organizing and analyzing difficult decisions in the 1980s. It is based on both mathematics and psychology (Saaty, 1990). AHP offers impartial mathematics for changing a person's or a group's priorities after a decision is made (Saaty, 1994).

AHP basically operates by setting standards for evaluating priorities and options. The decision hierarchy may be defined using the AHP, a method for predicting and decision-making that offers percentage distributions of options points in terms of influencing factors, which will be applied to define the decision hierarchy.

Fig. 1 AHP method steps

Building the hierarchical model

Creating the PCM-s based on the hierarchy

Quastionnaire survey

Consistency check

Aggregation by geomtric mean

Deriving weight vectors

Suggested Improvement in The current situation
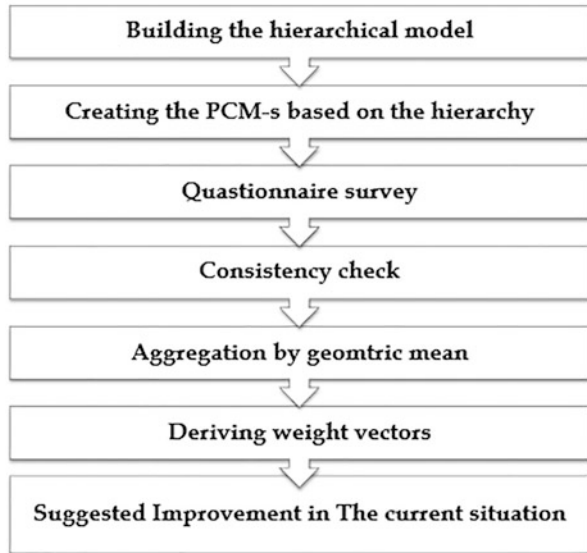
AHP is dependent on personal benchmarks of a decision ranking, implementing a predefined evaluation tool like the Saaty scale, featuring the influences that have an impact on decision-making and, if needed, the significance of the chosen decision in relation to the other elements in the model which affect the decision. So, on specific decision point, changing in importance are transformed into quantitative percentages. The steps to be taken to resolve a decision-making problem with AHP are summarized in Fig. 1.

Firstly, the current authors created a three-level hierarchy model containing the significant features and characteristics from the supply side of air transport. Figure 2 displays the model with the components of each level.

The second step after building the conceptual model is creating the pairwise matrices, Because the AHP makes use of the unique properties of pairwise comparison matrices (PCM), The intensity of the decision-makers preference between specific pairs of options (A_i versus A_j, for all $i, j = 1, 2,\ldots, n$) is represented in the matrix $A = [a_{ij}]$ illustrated in Eq. 1. They are generally chosen from a set of scales, such as the Saaty scale (Table 1). If all of the components of matrix A are positive, transitive, and reciprocal, it is said to be consistent (Saaty, 1977, 2002).
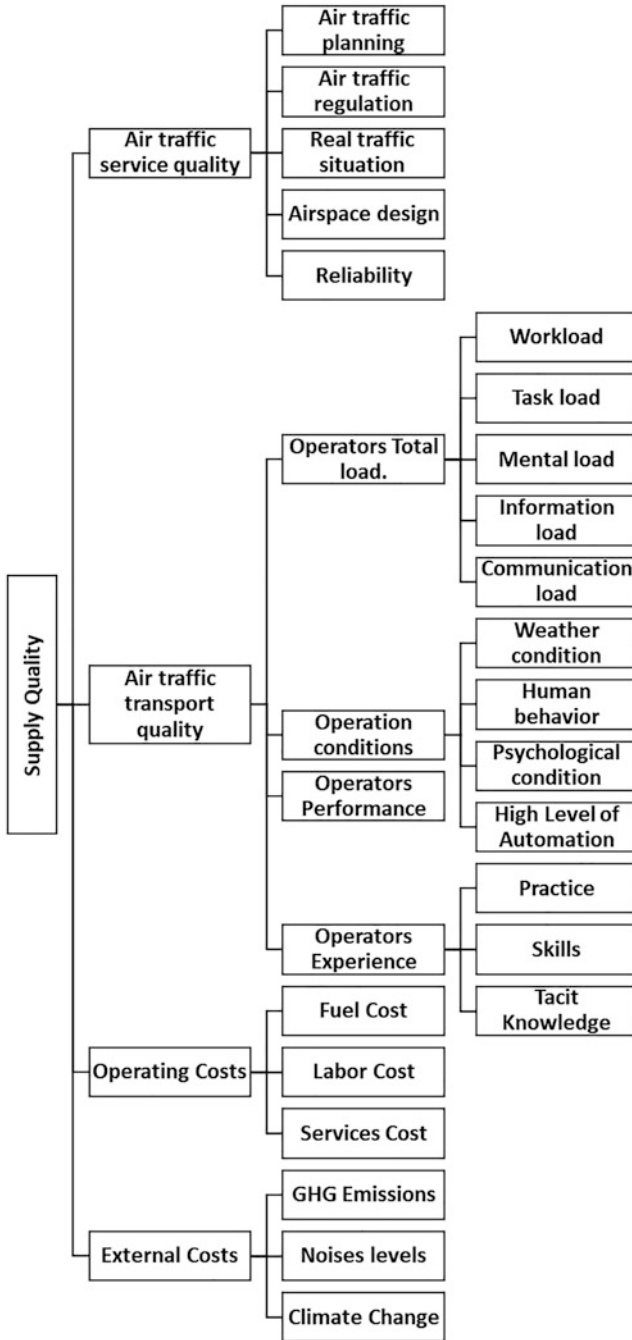
Fig. 2 The hierarchal model

Table 1 Saaty scale (Saaty, 1977)

Numerical values	Verbal scale	Explanation
1	Equal importance of both elements	Two elements contribute equally
3	Moderate importance of one element over another	Experience and judgment favor one element over another
5	Strong importance of one element over another	An element is strongly favored
7	Very strong importance of one element over another	An element is very strongly dominant
9	Extreme importance of one element over another	An element is favored by at least an order of magnitude
2,4,6,8	Intermediate values	Used to compromise between two judgments

$$
A = \begin{bmatrix} a_{ij} \end{bmatrix} = \begin{bmatrix}
1 & a_{12} & \cdots & a_{1j} & \cdots & a_{1n} \\
\dfrac{1}{a_{12}} & 1 & \cdots & a_{2j} & \cdots & a_{2n} \\
\vdots & \vdots & & \vdots & & \vdots \\
\dfrac{1}{a_{1j}} & \dfrac{1}{a_{2j}} & \cdots & a_{ij} & \cdots & a_{in} \\
\vdots & \vdots & & \vdots & & \vdots \\
\dfrac{1}{a_{1n}} & \dfrac{1}{a_{2n}} & \cdots & \dfrac{1}{a_{in}} & \cdots & 1
\end{bmatrix} \tag{1}
$$

3 Questionnaire

An AHP-based online survey was developed and implemented among 23 participants of aviation operators. The questionnaire concentrated and focused on the key elements of the supply quality for air transport system from a variety of different perspectives. Since the model highlights different overviews of the system stakeholders, depending on their knowledge and experience, the questionnaire's goal is to quantify the most crucial challenges as viewed through the viewpoint of aviation operators. The participants were arranged into four groups: (i) air traffic controllers (ATCOs) (N = 5, 40% females, M = 35 years, SD = 8.7), (ii) new generation pilots (N = 9, 44.5% females, M = 25 years, SD = 2.3), (iii) old generation pilots (N = 4, M = 36 years, SD = 6.02), and (iv) aeronautical engineers & MRO operators (N = 5, 20% females, M = 32 years, SD = 8). The matrix consistency ratio (CR) should be less than 0.1 due to the inconsistency of the majority of experience matrices. The CR for each group is calculated. Using pairwise comparison matrices, the geometric mean of each group was used to rank the importance of each model feature at each level. determining the normalization term for a weight on a connected

element so that the final sum of the weights' components is 1. The final score is then determined using the aggregated eigenvector.

4   Results and Discussions

There will be a percentage of variations between the expert groups' overviews and perspectives after processing and examining the participants' opinions on the development of the air transportation system supply quality side due to differences in experience, type and basis of the job, and understanding of the real situation and its development in more details; however, the AHP method will give more perceptions and transcendence view about air transportation development based on pairwise comparisons compared to simple methods. According to the approach, the replies were averaged using the geometric mean for each group. Tables 2, 3, 4 and 5 show the features (weights and consistency ratios) that have been computed for the first level in the air transport supply quality model characteristics from each group.

Combining the four groups' preferences would show the variations between the groups, which could raise due to the experience level and the type of the job. Comparing different groups of participants would make it easier to evaluate and

Table 2   Air traffic controllers PCMs for the first level

ATCOs – first level					
Air transport supply quality	Air traffic service quality	Air traffic transport quality	Operating costs	External costs	Weights
Air traffic service quality	1.00	1.43	1.22	1.50	31.21%
Air traffic transport quality	0.70	1.00	1.06	1.38	24.68%
Operating costs	0.82	0.94	1.00	1.58	25.84%
External costs	0.67	0.72	0.63	1.00	18.26%
CR = 0.0052	Sum =				100%

Table 3   Old generation pilots PCMs for the first level

Old generation pilots – first level					
Air transport supply quality	Air traffic service quality	Air traffic transport quality	Operating costs	External costs	Weights
Air traffic service quality	1.00	2.94	2.78	1.86	43.66%
Air traffic transport quality	0.34	1.00	1.57	0.58	17.36%
Operating costs	0.36	0.64	1.00	1.75	19.05%
External costs	0.54	1.73	0.57	1.00	19.92%
CR = 0.0858	Sum =				100%

Table 4 New generation pilots PCMs for first level

New generation pilots – first level					
Air transport supply quality	Air traffic service quality	Air traffic transport quality	Operating costs	External costs	Weights
Air traffic service quality	1.00	2.67	1.06	0.69	28.96%
Air traffic transport quality	0.38	1.00	0.82	0.61	15.98%
Operating costs	0.94	1.23	1.00	1.25	26.46%
External costs	1.45	1.64	0.80	1.00	28.59%
CR = 0.0450	Sum =				100%

Table 5 Aeronautical engineers & MRO operators PCMs for first level

Aeronautical engineers & MRO operators – first level					
Air transport supply quality	Air traffic service quality	Air traffic transport quality	Operating costs	External costs	Weights
Air traffic service quality	1.00	1.82	1.20	0.67	26.74%
Air traffic transport quality	0.55	1.00	0.58	0.77	16.32%
Operating costs	0.83	1.72	1.00	2.46	33.61%
External costs	1.50	1.29	0.41	1.00	23.33%
CR = 0.07489	Sum =				100%
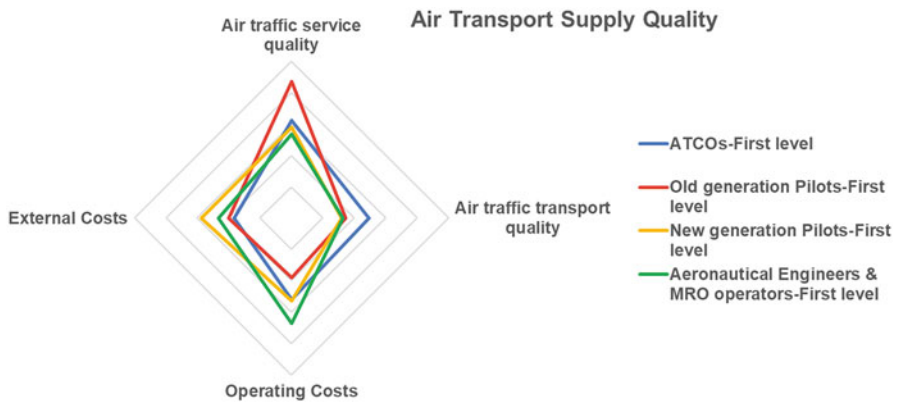
Fig. 3 Air transport supply quality first-level comparison

weigh various individual aspects of transport operators' total loads from other overviews (Fig. 3).

The findings showed that service quality strongly impacted most groups' categories opinions during the decision-making process. The real state of the air transportation system and the different categories of air transport projects that will have a

Fig. 4 Air transport service quality comparison

great influence on the system's economic growth and aims, such as efficiency, economic output, business investment, and funding, may be determined by service quality because it is the most important factor in all parties' evaluations (Fig. 4).

Although it is challenging to control the level of the criteria due to the stochastic nature of the system, looking at the second level of the model for the sub-criteria of the service quality also offers a clear overview of the particular issue from all aviation operators groups' perspectives, namely the system's reliability and the real traffic situation. The outcomes also highlighted the difference in point of view between the old generation of pilots which focused also on the air transport regulation.

5   Conclusion

The findings revealed the features of the air transport supply quality suggested model and gave a weighting percentages and scaling at each level of the hierarchy, which is an important indicator of the vital component in the current system. In order to manage different views and acquire a better understanding of the prospective environment, it was essential to use multi-criteria approaches, particularly AHP. Quantitative and qualitative criteria, as well as the traditional, classic, and streamlined and simplified analytical hierarchical process (AHP) decision-making technique, are used to illustrate the differences between the opinions.

The findings imply that the most crucial element in the air transport supply quality model is service quality, from the viewpoints of most of the partners.

It should be noted that including additional numbers and operator groupings would provide a more complete generalization of the existing situation and more clearly emphasize its crucial components.

For a smoother investigation of more specific and detailed issues, those suggested and recommended steps could be achieved in the upcoming research. Additional studies using various MCDM methods could demonstrate more specific issues, such as using the analytical network process (ANP), which could demonstrate how each criterion and sub criteria could affect one another on various levels.

References

Akdag, H., et al. (2014). The evaluation of hospital service quality by fuzzy MCDM. *Applied Soft Computing*. Elsevier, *23*, 239–248. https://doi.org/10.1016/J.ASOC.2014.06.033

Aydin, N. (2017). A fuzzy-based multi-dimensional and multi-period service quality evaluation outline for rail transit systems. *Transport Policy*. Pergamon, *55*, 87–98. https://doi.org/10.1016/J.TRANPOL.2017.02.001

Bruno, G., Esposito, E., & Genovese, A. (2015). A model for aircraft evaluation to support strategic decisions. *Expert Systems with Applications*. Pergamon, *42*(13), 5580–5590. https://doi.org/10.1016/J.ESWA.2015.02.054

Chao, C. C., & Kao, K. T. (2015). Selection of strategic cargo alliance by airlines. *Journal of Air Transport Management*. Pergamon, *43*, 29–36. https://doi.org/10.1016/J.JAIRTRAMAN.2015.01.004

Dalkıran, A. et al. (2022). A review on thematic and chronological framework of impact assessment for green airports. *International Journal of Green Energy*. Taylor & Francis, 1–12. https://doi.org/10.1080/15435075.2022.2045298

Estrada, A., & Romero, D. (2016). A system quality attributes ontology for product-service systems functional measurement based on a holistic approach. *Procedia CIRP*. Elsevier, *47*, 78–83. https://doi.org/10.1016/J.PROCIR.2016.03.215

Kale, U., et al. (2021). Towards sustainability in air traffic management. *Sustainability, 13*, 5451. https://doi.org/10.3390/SU13105451

Kale, U., Rohács, J., & Rohács, D. (2020). Operators' load monitoring and management. *Sensors, 20*(17). https://doi.org/10.3390/s20174665

Nakagawa, T., & Sekitani, K. (2004). A use of analytic network process for supply chain management. *Asia Pacific Management Review*. 成功大學管理學院, *9*(5), 783–800. https://doi.org/10.6126/APMR.2004.9.5.02

Rezaei, J., Fahim, P. B. M., & Tavasszy, L. (2014). Supplier selection in the airline retail industry using a funnel methodology: Conjunctive screening method and fuzzy AHP. *Expert Systems with Applications. Pergamon, 41*(18), 8165–8179. https://doi.org/10.1016/J.ESWA.2014.07.005

Rohács, J., & Rohács, D. (2020). Total impact evaluation of transportation systems. *Transport*. Vilnius Gediminas Technical University, *35*(2), 193–202. https://doi.org/10.3846/TRANSPORT.2020.12640

Saaty, T. (1994). *Fundamentals of decision making and priority theory with the AHP*. RWS Publications.

Saaty, T. L. (1977). A scaling method for priorities in hierarchical structures. *Journal of Mathematical Psychology, 15*(3). https://doi.org/10.1016/0022-2496(77)90033-5

Saaty, T. L. (1990). How to make a decision: The analytic hierarchy process. *European Journal of Operational Research, 48*(1). https://doi.org/10.1016/0377-2217(90)90057-I

Saaty, T. L. (2002). Decision making with the analytic hierarchy process. *Scientia Iranica, 9*(3). https://doi.org/10.1504/ijssci.2008.017590

Saaty, T. L. (2008). Decision making with the analytic hierarchy process. *International Journal of Services Sciences, 1*(1), 83–98. Available at: https://www.inderscienceonline.com/doi/abs/10.1504/IJSSci.2008.01759. Accessed: 15 Feb 2022

Zietsman, D., & Vanderschuren, M. (2014). Analytic hierarchy process assessment for potential multi-airport systems – The case of Cape Town. *Journal of Air Transport Management*, Pergamon*, 36*, 41–49. https://doi.org/10.1016/J.JAIRTRAMAN.2013.12.004

A Comparative Study of the Reporting Approach for Corporate Social and Environmental Responsibility Between Iberia and Turkish Airlines

Eliezer José Arellano García, Rubén Pérez Fernández, César Montañés Alonso, and Gamze Orhan

Nomenclature

CSER	Corporate Social and Environmental Responsibility
CSR	Corporate Social Responsibility
SASB	Sustainability Accounting Standards Board
TCFD	Task Force on Climate Related Financial Disclosures
UN	United Nations

1 Introduction

Numerous studies have focused on corporate social responsibility, where environmental responsibility is an implicit part of social responsibility. Such studies have examined a wide range of approaches, e.g., what is the definition of CSR (corporate social responsibility), its history, companies' motivations for implementing CSR, among others (Othman & Ameer, 2009).

E. J. Arellano García · R. Pérez Fernández · C. Montañés Alonso
School of Aeronautical and Space Engineering, Universidad Politécnica
De Madrid, Madrid, Spain
e-mail: ej.arellano@alumnos.upm.es; ruben.perez.fernandez@alumnos.upm.es;
c.montanes@alumnos.upm.es

G. Orhan (✉)
Department of Aviation Management, Faculty of Aeronautics and Astronautics, Eskişehir
Technical University, Eskişehir, Türkiye
e-mail: gozsoy@eskisehir.edu.tr

Today, a high percentage of companies are aware of the importance of having a committed approach to corporate and social responsibility, so it is no longer a question of whether a company should have CSR (EU, 2011).

Many studies have already demonstrated and justified the benefits that this type of policy has for companies; this study aims to determine how the communication strategies of two companies in the airline industry can vary in terms of CSR, because corporate social responsibility loses much of its relevance if it is carried out but not communicated, and its credibility if the opposite happens.

Iberia in Spain and Turkish Airlines in Turkey operate a large majority of the flights in their respective countries. While these two carriers exhibit certain similarities, they also vary in how they approach management. Both airlines are excellent candidates for the study due to their strategic relevance in the airline industry and in each of their home markets.

Hence, this chapter will analyze what their CSR policy communication strategy is, which indicators they focus on, which part of CSR they give more importance to, how they present the information in their reports. It makes a comparative study of two leading airlines in each country, trying to identify similarities and differences in CSR communication styles, and trying to determine and make a correlation of the factors that may influence these differences. It is worth to mention that this study has been motivated and will follow the CSR reporting framework published by Amin (2021).

2 Literature Review

2.1 Defining CSR: Various Perspectives of a Single Aim

When it comes to define what CSR means we can find a wide range of literature available; however, no universally agreed-upon concept of corporate social responsibility is available. In truth, it has been described in a variety of ways, but they all have one thing in common: the unified company's commitment to methods of responsibility that go beyond economic profit. Corporate social responsibility, in this context, refers to a company's influence on the economic, social, and environmental elements.

The Green Paper of the Commission of the European Communities that aims to advance a European framework for CSR defines it as a concept whereby businesses voluntarily choose to make contributions to a better world and a cleaner environment, as well as the voluntary incorporation of environmental concerns into business operations and relationships with stakeholders. (EU, 2001).

According to World Business Council for Sustainable Development definition, "Corporate Social Responsibility is the continuing commitment by business to behave ethically and contribute to economic development while improving the quality of life of the workforce and their families as well as of the local community and society at large" (WBCSD, 2000).

Even though the vast majority of studies in literature use the term CSR, including (Abbott, 2011; Zivin & Small, 2005; Blowfield & Murray, 2008) and as it is stated by (Lynes & Andrachuk, 2008) the term "environment" is not included in the CSR acronym, environmental responsibility is an assumed aspect of social responsibility under this definition. However, there are also studies consider it another practice called CSER - Corporate Social and Environmental Responsibility (Amin, 2021). As Amin (2021) states it as that firms all over the world are now not only engaging in CSR initiatives, but also utilizing a range of media, including as annual reports, sustainability reports, websites, and integrated reports, to inform stakeholders about them. Companies voluntarily disclose their actions in relation to social issues including socioeconomic inequality, human rights, and environmental issues like pollution.

2.2   The Airline Industry's Interpretations and Understanding of CSER

CSR requires businesses to treat their social obligations with the same seriousness that they do their commercial goals, and the aviation sector is no different from other industries in this regard. The four components of CSR include economic, legal, ethical, and philanthropic responsibilities (Pinkston & Carroll, 1996). It is critical to emphasize the need of incorporating environmental considerations into the CSR term, introducing CSER (corporate social and environmental responsibility). The transport sector is the fourth largest polluter of all industries, just after the energy, textile, and food sectors.

Due to the increasing international tension and recent spike in crude oil prices, which is a key source of concern for airlines, fuel economy has become a top commercial goal. CSER programs have become an essential part of airlines' business strategy as a result of this, as well as increased concern about the environmental impact of air travel. Airlines have begun to employ broader tactics in order to satisfy fuel-saving targets and other CSER goals such as developing biofuels.

In general, there has been a close relationship between the aviation sector and social and environmental challenges. In the current airline business climate, CSR has emerged as a crucial competitive advantage and a strategy for gaining customer loyalty (Inoue & Lee, 2011; Hossain et al., 2012; Gard et al., 2009). As a result, many airlines are dedicated to conducting business ethically, abiding by local laws, implementing best practices where appropriate, and comparing their performance to industry benchmarks (Cowper-Smith & de Grosbois, 2010; Lynes & Andrachuk, 2008).

3   Methodology

In the airline industry, there is no standardized method of reporting CSER. Generally, the literature used for articles refers to CSR, but the importance of the environment is remarkable; for this reason, this chapter will consider the term CSER more broadly. CSER reporting framework will cover six areas of great importance: vision, safety and security, environment, community, marketplace, and workforce.

The methodology used focuses on nine core elements of corporate sustainability reporting: general business profile, strategy and policy, results, corporate social reporting policy, relevance of reported measures, clarity of the report, reliability of the report, stakeholder involvement, and contextual consistency (Heeres et al., 2011).

4   Results and Discussion

A comparison within the framework of the aforementioned subjects was conducted taking into account the social, environmental, and sustainability reports released by Iberia and Turkish Airlines in 2019, 2020, and 2021 (THY, 2019, 2020, 2021; IBE, 2019, 2020, 2021).

The evaluations of airlines for the general business profile, strategy and policy, results, corporate social reporting policy, relevance of reported measures, clarity of the report, reliability of the report, stakeholder involvement, contextual consistency are presented in Table 1.

5   Conclusions

The main objective of this work was to compare the cultural, social, and environmental and responsibility reporting patterns of two flag carriers from different countries. In this case, Iberia and Turkish Airlines were chosen for the study.

After analyzing several key points of both airlines based on the annual reports for the last 3 years, a general insight can be drawn. The reports published by Turkish airlines happen to be remarkably detailed, complete, extensive, and with a visual representation of graphs, tables, and diagrams that help to better understand the quantitative data. It is also worth noting the large difference between the two airlines in terms of size, from the fleet and staff to the entire administrative and corporate area. It should be noted that due to the complexity and the large size of Turkish Airlines, they decided to outsource a third company (PwC Turkey) to carry out the reports, whereas Iberia does so internally, from the sustainability directorate, which lead us to reflect on how beneficial it is for an enterprise to outsource another company for reporting.

Table 1 Comparative assessment of Iberia and Turkish Airlines within the framework of nine core elements of corporate sustainability reporting

Core element	Iberia	Turkish airlines
General business profile	Iberia describes the ambitions on market recovery of its three principal business activities: air transport of passengers and cargo, airport services, and aircraft maintenance. Also emphasizes the 50 different countries in which it operates while developing the organizational structure within the IAG group and its subsidiary airline (Iberia Express)	Turkish airlines clearly state the large size of the company and its network of flights across 127 countries, informing about its 18 subsidiaries in various fields of aviation, belonging to the star alliance group. It also provides very clear visual information through charts and graphs on the company's emissions, staff, company values, and financial performance
Strategy and policy	Outlines precisely the airline's past and evolution in terms of environmental reporting since 1990s to define the policies followed today in accordance with the United Nations Sustainable Development Goals. Furthermore, it links the sustainability plan with the post-pandemic recovery strategy	There is a strong focus on the importance of bringing the sustainability plan to all units of the organization in short, medium, and long terms in order to decide on improvements that will lead to increase its performance in the organization
Results	Throughout the document, it describes social commitment as one of the basic pillars of its organization and it can be clearly seen how it affects all units of its organization. Likewise, it is described how the pandemic has made a negative impact on the economy of the organization and how they plan to make a sustainable recovery on it	Along the document, it is fully detailed with graphs, tables, and diagrams to aid understanding how the company plans to address its environmental impact, engage stakeholders, and create equal social opportunities for female and male employees
Corporate social reporting policy	According to the document, Iberia follows since 2015 CSR included as part of United Nations sustainability goals	It is clearly defined with clear language and representative aids how they have taken into account the material issues of SASB as well as the working group TCFD
Relevance of reported measures	In general terms, the measures presented by Iberia are reduced, especially in terms of fuel efficiency, greenhouse gases, and number of passengers. In terms of waste, noise, and operational safety, there is an improvement in the quantity and quality of reporting	All the subsections mentioned in the methodology are satisfactorily fulfilled, presenting abundant information, especially on greenhouse gases and fuel efficiency, with very complete and detailed quantitative reports. It should be noted that the airline had its gas measurements verified by a third party in accordance with the TS EN ISO 14064-3: 2007 standard

Table 1 (continued)

Core element	Iberia	Turkish airlines
Clarity of the report	The report starts with a message in large letters, without any background photo as usual, making clear the real reasons for which the report is published, causing a visual impact. Something out of the ordinary and which brings a lot of originality to the report and the way of presenting it. This trend is followed in the rest of the document	The report has a classic structure and way of presenting the information, as we are normally used to. An easy and intuitive structure is defined, being even easier to follow than with the Iberia report. However, at certain times the information and especially the numerical data can make you feel overwhelmed, especially if you are not a user with a technical knowledge base
Reliability of the report	It does not explicitly state the total reliability of the information reported by a third party, but it does state the different audit committees of the organization which are repeatedly exposed The airline has a section in the report where it presents the different certifications it has, the scope and the certifying entity	According to the airline, PwC Turkey conducted an external audit of a subset of the report's metrics under a restricted assurance framework in compliance with ISAE 3000 and ISAE 3410 standards. In the report can be found an Independent Assurance Statement, which includes the list and scope of assured indicators
Stakeholder involvement	Stakeholders are a fundamental part of companies, and Iberia is aware of this. Although it devotes a small section of the report to this, it does so by indicating in the report that an area has been created, "the Shareholder and Investor Relations Office," where direct consultations can be made between shareholders and the highest governing body on economic, environmental, and social matters	Turkish Airlines has an impressive number of references to its stakeholders in the report. The airline is aware of their importance and makes this clear throughout the report, where they are made aware that they are a priority, and their voices are heard and taken into account
Contextual consistency	In general terms and in terms of context, Iberia's report follows the expected guidelines for a report based on the framework of the United Nations Sustainable Development Goals, without providing too much technical data but presenting a very clear and well-defined discursive line. As the years of the reports pass, the change in reporting style is obvious.	Turkish airlines, despite using the GIR framework, characterized by presenting a report with a more technical approach and has managed to present the information in the most didactic and easy to understand way. The airline, despite not belonging to the UN Global Compact, being the world's largest voluntary corporate sustainability initiative, has its own sustainability strategy, which is clearly defined in the reports, and supports the 17 sustainable development goals

Regarding the criteria and structure followed by Iberia, it shows its support to the United Nations Global Compact reaffirming its commitment to the 17 Sustainable Development Goals (SDGs). Since 2015, they have been following the CSR in line accordance to United Nations. Turkish Airlines, in contrast, follows the structure of global reporting initiative that Iberia previously utilized prior to embracing SDGs.

References

Abbott, P. (2011). Corporate responsibility: a critical introduction. *Action Learning: Research and Practice, 8*(1), 69–72.

Amin, A. (2021). Theories of Corporate Social and Environmental Reporting (CSER): An Overview. *The Cost And Management, 48*(05), 39–43.

Blowfield, M., & Murray, A. (2008). *Corporate responsibility: a critical introduction*. Oxford University Press.

Cowper-Smith, A., & de Grosbois, D. (2010). The adoption of corporate social responsibility practices in the airline industry. *Journal of Sustainable Tourism, 19*(1), 59–77.

EU. (2001). *Green paper: Promoting a European framework for corporate social responsibility Commission of the European Communities*. https://www.eumonitor.eu/9353000/1/j9vvik7m1 c3gyxp/vikqhjet6py6

EU. (2011). *Renewed EU strategy 2011–14 for Corporate Social Responsibility European Commisson*. https://www.eumonitor.eu/9353000/1/j4nvkkpftveemt7_j9vvik7m1c3gyxp/ vitwrzhm31gk

Gard McGehee, N., Wattanakamolchai, S., Perdue, R. R., & Onat Calvert, E. (2009). Corporate social responsibility within the US lodging industry: An exploratory study. *Journal of Hospitality & Tourism Research, 33*(3), 417–437.

Heeres, J., Kruijd, J, Montgomery, E., & Simmons, J. (2011). *Building trust in the air: Is airline corporate sustainability reporting taking off?* https://pwc.blogs.com/files/pwc_airlinescr_ web.pdf

Hossain, M. M., Rowe, A. L., & Quaddus, M. (2012). Drivers and barriers of corporate social and environmental reporting (CSER) practices in a developing country: Evidence from Bangladesh. In *Interdisciplinary Perspectives on Accounting Conference Proceedings*.

IBE. (2019). *Iberia sustainability reports*. https://grupo.iberia.es/sustainability/reports

IBE. (2020). *Iberia sustainability reports*. https://grupo.iberia.es/sustainability/reports

IBE. (2021). *Iberia sustainability reports*. https://grupo.iberia.es/sustainability/reports

Inoue, Y., & Lee, S. (2011). Effects of different dimensions of corporate social responsibility on corporate financial performance in tourism-related industries. *Tourism management, 32*(4), 790–804.

Lynes, J. K., & Andrachuk, M. (2008). Motivations for corporate social and environmental responsibility: a case study of Scandinavian airlines. *Journal of International Management, 14*(4), 377–390.

Othman, R., & Ameer, R. (2009). Corporate social and environmental reporting: Where are we heading? A survey of the literature. *International Journal of Disclosure and Governance, 6*(4), 298–320.

Pinkston, T. S., & Carroll, A. B. (1996). A retrospective examination of CSR orientations: have they changed? *Journal of Business Ethics, 15*(2), 199–206.

THY. (2019). *Turkish airlines annual report*. https://investor.turkishairlines.com/en/financial-and-operational/annual-reports

THY. (2020). *Turkish airlines annual report*. https://investor.turkishairlines.com/en/financial-and-operational/annual-reports

THY. (2021). *Turkish airlines annual report*. https://investor.turkishairlines.com/en/financial-and-operational/annual-reports

WBCSD. (2000). *Corporate social responsibility: Making good business sense*. World Business Council for Sustainable Development.

Zivin, J. G., & Small, A. (2005). A Modigliani-Miller theory of altruistic corporate social responsibility. *The BE Journal of Economic Analysis & Policy, 5*(1), 0000101515153806531369.

Fuel Efficient Flight Level Assignments Under Wind Uncertainties for the Conflict Resolution Problem at the En-Route Phase

Ramazan Kursat Cecen and Kadir Dönmez

Nomenclature

3D	3-Dimensional
ATM	Air Traffic Management
CDP	Conflict Detection Problem
CRP	Conflict Resolution Problem
EV	Expected Value Solution
FLC	Flight Level Change
GAMS	The General Algebraic Modeling System
HAC	Heading Angle Change
NA	Not Available
NM	Nautical Miles
RP	Here and Now Solution
SC	Speed Change
WSC	Wind Speed Coefficients

R. K. Cecen (✉)
Eskişehir Osmangazi University, Eskişehir, Türkiye
e-mail: ramazankursat.cecen@ogu.edu.tr

K. Dönmez
Samsun University, Samsun, Türkiye
e-mail: kadir.donmez@samsun.edu.tr

1   Introduction

Conflict resolution problem (CRP) can be solved using three different approaches: speed change (SC), heading angle change (HAC), and flight level change (FLC). SC and HAC do not affect the vertical position of aircraft. However, changing the flight level of an aircraft causes an interaction between different levels (Cecen & Cetek, 2020). Also, weather conditions may change between the levels, which can affect the ground speeds of aircraft. Even though FLC is performed with a single instruction, conflict resolution using this approach creates follow-up difficulties for the controllers due to the above-mentioned issues. Weather conditions must be considered to provide efficient and safe solutions for the CRP using FLC.

In general, the weather affects the predicted arrival or departure times of aircraft in two ways. The first one is bad weather conditions that affect the air traffic management (ATM) at a network level by causing no-fly zones, and the second one is atmospheric issues such as wind which may affect the individual routes of flights (Hernández-Romero et al., 2017). In such a situation, controllers may need to intervene to ensure minimum separations between aircraft. The wind is a weather component that significantly affects flight trajectories. It affects the trajectories through its speed element (Chaloulos & Lygeros, 2007). However, considering the uncertainties of both wind components (i.e., direction and speed) may provide more efficient and safe air traffic management (Dönmez, 2022).

In the literature, many studies handle conflict detection problem (CDP) and CRP, considering the wind uncertainties. Vela et al. provided a two-stage stochastic programming model for the CRP considering the wind uncertainties. They allowed only SC in their model to resolve the conflict (Vela et al., 2009). In addition, Matsuno et al. (2016) developed a stochastic near-optimal control method considering several uncertainties, including wind prediction errors, airspeed measurement errors, etc. Their model presented near-optimal heading maneuvers considering a two-dimensional horizontal plane (Matsuno et al., 2016). Matsuno et al. (2015) provided an optimal control model for determining three-dimensional conflict-free aircraft trajectories under wind uncertainty (Matsuno et al., 2015). Romero et al. presented a probabilistic approach for CDP and CRP considering the uncertainty of wind forecast. They assumed that the operations are realized with constant speed and flight level (Hernández-Romero et al., 2020). Most of the above-mentioned studies showed that robust and efficient conflict resolutions could provide considering the wind uncertainties.

The current study develops a two-stage stochastic mathematical model for the CRP for the en-route phase at a three-dimensional (3D) plane. Both wind direction and speed uncertainties are integrated into the model to validate the previous efforts. It is compared to the deterministic and expected value approaches to find out the possible gains of the developed stochastic programming model. Wind data from İZMİR (17220) station was added to a mathematical model to quantify the results, and various traffic samples were solved using GAMS (The General Algebraic Modeling System).

2 Method

We developed a two-stage stochastic programming model in a 3D plane for the CRP. FLC is used as the solution method. It is compared with the deterministic and expected solution approaches to find out possible gains of the presented model. The deterministic approach does not consider any wind uncertainty in the system while assigning the aircraft to the flight levels in the first stage of the problem. In the second stage, these assignment decisions are run under any uncertainty in the deterministic model. In the expected value solution (EV), on the other hand, the assignment decisions obtained from the first stage are applied under uncertainties. The first stage decisions of the deterministic and expected value solution are the same. The developed stochastic model considers the wind speed and direction uncertainties when assigning the aircraft to the FLs. Solutions of the stochastic model are obtained directly and referred to "as here and now solution" (RP). The methodology of the study is summarized in Fig. 1.

For all strategies, we assume that assignments are decided before sector entry points. Aircraft enter the system from the assigned flight levels. Figure 2 represents the operational concept of the models.

Generic airspace includes five different fight levels and two routes. For each flight level, there is one conflict point. The routes, entry and exit points, and flight level information are integrated to the mathematical model as parameters. The length of all air routes was determined as 100 nautical miles (NM) and the distance to the intersection point as 50 NM. The safe separation between the aircraft is specified as 5 NM and included in the mathematical model as time-based separations based on the aircraft velocities for each flight level. The aircraft speeds are constants for each flight level, and no speed change is allowed. In addition, deviation from the predetermined routes in the horizontal plane is not permitted after the sector entry points.
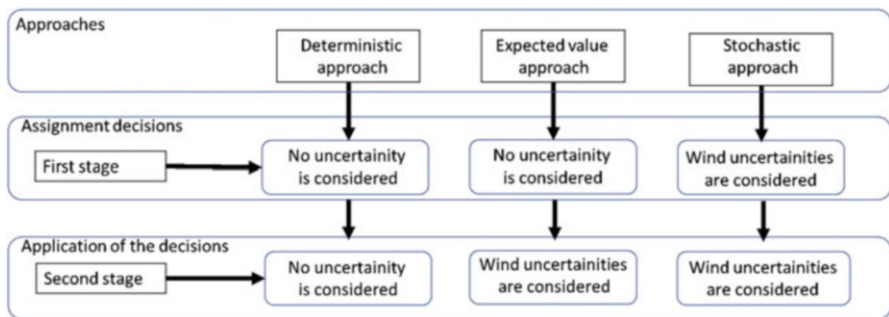
Fig. 1 Methodology
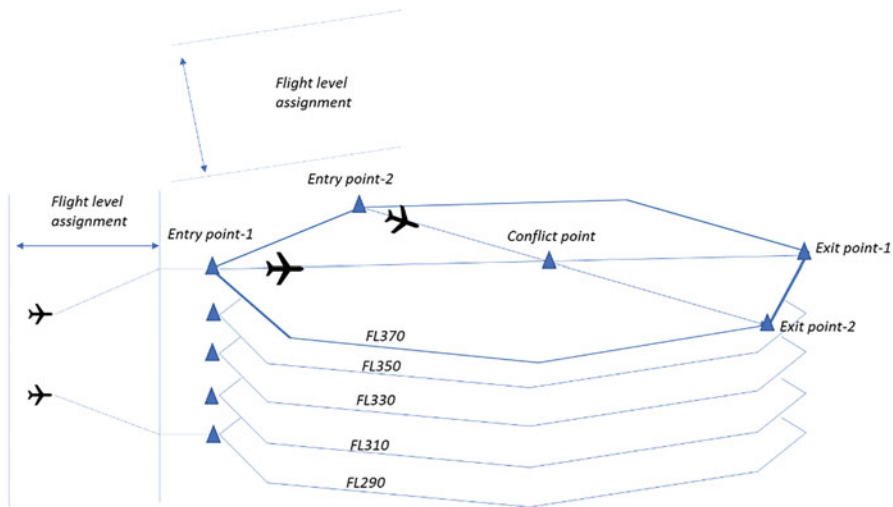
Fig. 2 Generic airspace and flight level assignments

2.1 Data Analysis

Wind data is obtained from the weather sound database of Wyoming University (Weatherdata, 2021). İzmir station (17220) data is used in this study. While the wind directions are considered at 60-degree intervals, wind speeds are considered at 20 kts intervals. A cross table of the wind speeds and directions that are observed together is given in Table 1.

As seen in Table 1, the frequency of some of the cells is equal to 0. This means no observation is found for these direction and speed intervals. Therefore, these scenarios were eliminated, and a total of 21 scenarios were included in the model. To represent all intervals and to generate reasonable scenarios for the mathematical model, medians and means of the wind directions and speeds are considered, respectively. Table 2 presents the wind scenarios with the probabilities.

As seen in Table 2, the highest probability is 15%, while the lowest probability is 0.013% among the scenarios. The highest wind speed is 121.63 kts, and the lowest is 13.05 kts. The above-mentioned scenarios are generated using the data for FL350 which is chosen as reference FL for wind scenarios. In addition, the flight levels' differences in wind speed are reflected in the model using the wind speed coefficients. These coefficients are obtained by comparing each flight level with the reference flight level regarding wind characteristics. Hence, we could extend the scenarios for all flight levels. Table 3 shows the differences between flight levels regarding wind direction and wind speeds.

As seen in Table 3, there are no significant differences between the flight levels regarding wind direction. Significant differences, however, are observed for wind speed. As a result, these differences are reflected in the mathematical model using

Table 1 Cross table of wind speeds and directions

İZMİR (17220)								
			Speed intervals (kts)					
			0–20	20–40	40–60	60–80	80+	Total
Direction intervals (degree)	0–60	Count	4	3	1	1	0	9
		%	5.0	3.8	1.3	1.3	0.0	11.3
	61–120	Count	1	0	0	0	0	1
		%	1.3	0.0	0.0	0.0	0.0	1.3
	121–180	Count	0	1	0	0	0	1
		%	0.0	1.3	0.0	0.0	0.0	1.3
	181–240	Count	5	4	3	2	3	17
		%	6.3	5.0	3.8	2.5	3.8	21.3
	241–300	Count	7	11	12	8	4	42
		%	8.8	13.8	15.0	10.0	5.0	52.5
	301–360	Count	3	4	1	1	1	10
		%	3.8	5.0	1.3	1.3	1.3	12.5
Total		Count	20	23	17	12	8	80
		%	25.0	28.8	21.3	15.0	10.0	100.0

Table 2 Wind scenarios

Scenario number	Probability	Direction	Speed
Scenario 1	0.050	30	13.05
Scenario 2	0.038	30	28.83
Scenario 3	0.013	30	48.82
Scenario 4	0.013	30	68.08
Scenario 5	0.013	90	13.05
Scenario 6	0.013	150	28.83
Scenario 7	0.063	210	13.05
Scenario 8	0.050	210	28.83
Scenario 9	0.038	210	48.82
Scenario 10	0.025	210	68.08
Scenario 11	0.038	210	121.63
Scenario 12	0.088	270	13.05
Scenario 13	0.138	270	28.83
Scenario 14	0.150	270	48.82
Scenario 15	0.100	270	68.08
Scenario 16	0.050	270	121.63
Scenario 17	0.038	330	13.05
Scenario 18	0.050	330	28.83
Scenario 19	0.013	330	48.82
Scenario 20	0.013	330	68.08
Scenario 21	0.013	330	121.63

Table 3 Wind differences between the flight levels

	Median of wind direction	Mean of wind speed	Wind speed coefficient (WSC)
FL290	269.00	25.58	0.58
FL310	259.50	29.71	0.67
FL330	271.50	33.66	0.76
FL350	275.00	44.30	1.00
FL370	275.00	46.22	1.04
Range	15.50	20.65	

wind speed coefficients (WSC). Including the differences in the model using coefficients decreases the computational load of the model compared to the additional scenarios (Dönmez et al., 2022).

2.2 Two-Stage Stochastic Model

The deterministic model developed by Dönmez and Cecen (2022) is enhanced to a stochastic model in this study (Dönmez & Cecen, 2022). They used SC and VM techniques with a deterministic approach in the model. They also considered a two-dimensional plane in the model. Their model is based on Cecen (2021); however, they enhanced the model by integrating improved speed restrictions and fuel calculations.

In the current model, FLC is considered a conflict resolution method. Also, 3D interactions between the aircraft are considered. The model's objective function is determined as the minimization of the total fuel consumption of aircraft. The fuel calculation regression model presented by Dönmez and Cecen 2022 is integrated to the mathematical modeling (Dönmez & Cecen, 2022). Additional speed and fuel calculations presented in previous study is maintained in the model. The fuel calculations using the regression models generated based on BADA 3.11 provide more realistic estimates than the only time-dependent ones. In the time-dependent calculation approach, fuel has a linear relationship with flight time. Provided regression models, however, consider the speed and altitude effect and flight time. The full form of the model is not presented here, but the deterministic version of the model can be reached from Cecen (2021), and extended speed and fuel calculations can be found in Dönmez and Cecen (2022).

3 Results

In this section, we first compared RP, deterministic, and EV strategies in fuel consumption. Then, we solved ten test problems to find out possible savings of the stochastic approach. Finally, Table 4 shows the models' total fuel consumption (kg) results.

As seen in Table 4, EV did not provide any feasible solution for the test problems. This means that the assignment decisions provided in the deterministic model in the first stage of the problem are not feasible when uncertainties occur. If we compare the results of the deterministic and RP solutions, we observed that RP provides an average improvement by 4.17% compared to deterministic in terms of fuel consumption. Table 5 shows the savings of the RP compared to the deterministic approach.

As seen in Table 5, an average of 1962.17 kg of fuel saving is provided in the stochastic model. This corresponds to approximately 39 kg fuel savings per aircraft. Note that this is not a clear comparison because the second stage of the problem is

Table 4 The results in terms of total fuel consumption (kg)

Test problems	Fuel consumption		
	Deterministic	RP	EV
1	39477.11	37829.27	NA
2	42732.87	40937.05	NA
3	45890.12	43998.91	NA
4	47258.73	45295.68	NA
5	50013.8	47918.41	NA
6	45734.51	43826.01	NA
7	51844.74	49690.98	NA
8	47512.18	45518.58	NA
9	50861.11	48750.74	NA
10	49384.46	47322.35	NA

NA Not available

Table 5 Savings of the stochastic approach

Test problems	kg	%
1	1647.83	4.17
2	1795.83	4.20
3	1891.21	4.12
4	1963.04	4.15
5	2095.39	4.19
6	1908.50	4.17
7	2153.77	4.15
8	1993.60	4.20
9	2110.37	4.15
10	2062.11	4.18
Average	1962.17	4.17

Table 6 Number of aircraft that provided non-conflicted routes in the EV model

Test problems	Feasible solutions for EV	
	Aircraft count	%
1	34	68
2	41	82
3	43	86
4	37	74
5	36	72
6	37	74
7	41	82
8	42	84
9	38	76
10	36	72
Average	38.50	77.00

not having any uncertainty in the deterministic model. Since no results were obtained in the EV model, the results of the stochastic model were directly compared with the deterministic approach.

We also examined the unfeasible solutions of the EV model in detail. Table 6 shows the number of aircraft that provided non-conflicted routes in the EV model for each scenario.

As seen in Table 6, the EV model provided non-conflicted routes for an average of 38.5 aircraft in each scenario. This means that approximately 12 aircraft's conflicts cannot solve by applying the first stage assignment decisions obtained from the deterministic model when the uncertainties are realized. Therefore, only delaying some of these 12 aircraft can solve the problem. However, we did not allow any delay in all strategies. Namely, suppose the deterministic assignment decisions obtained for the first stage of the problem are applied under the uncertainties. In that case, non-conflicted routes are provided for 77% of aircraft, while the others have a potential conflict that may be resolved by delaying some aircraft. However, in the RP model, feasible and better solutions are provided for all scenarios compared to deterministic and EV approaches. We also compared the deterministic and RP solutions regarding the number of aircraft assigned to the same altitude (Table 7).

Table 7 indicates that 65.2% of the aircraft is assigned to the same altitude in RP and deterministic approaches, and 34.8% of aircraft are assigned to different levels for these models. We also examined how many aircraft were assigned to each flight level for each test problem. Figure 3 shows the average number of aircraft assigned to each flight level for all test problems.

As seen in Fig. 3, 33.4 aircraft were assigned to FL370 in the deterministic model, while 28.6 aircraft were assigned to this flight level in the stochastic model. Although both models assigned most aircraft to higher flight levels because of fuel efficiency, the stochastic model used lower flight levels more than the deterministic approach. This is because wind speed increases as the flight level increases. Although the wind speed affects the aircraft positively or negatively according to the direction of wind and arrival, lower levels are preferable to higher flight levels

Table 7 Number of aircraft assigned to the same altitude in deterministic and stochastic models	Test problem	Count	%
	1	35	70
	2	29	58
	3	37	74
	4	35	70
	5	29	58
	6	29	58
	7	33	66
	8	33	66
	9	34	68
	10	32	64
	Average	32.60	65.20
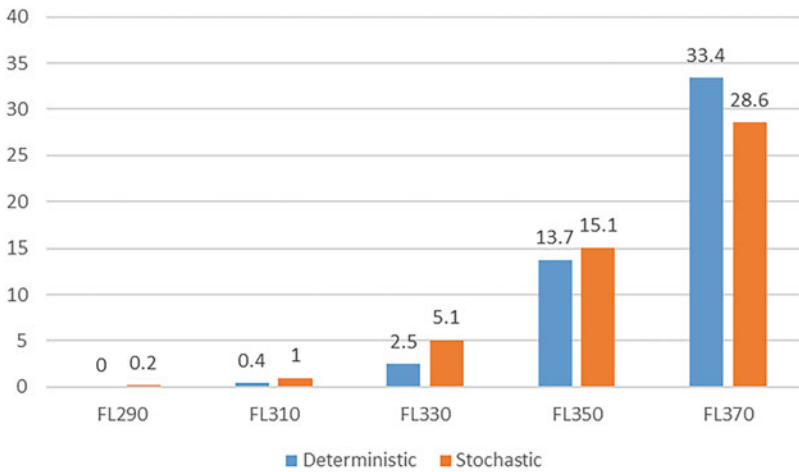
Fig. 3 Average flight level assignments

when the wind is involved in the problem because of uncertainty. Note that the stochastic model still prefers higher levels. The above statements are valid for comparisons made with the deterministic approach. Figures 4 and 5 show the rates of flight level assignments for stochastic and deterministic methods, respectively.

In Figs. 4 and 5, the highest rate of assignments was FL370 for both models. While assignments to FL330 and FL350 constituted approximately 40% of the aircraft in the stochastic model, this ratio remained at approximately 32% in the deterministic model. Table 8 examines the flight level assignments for each test problem given below.

As seen in Table 8, some of the test problems resulted in more different FL assignments. For example, for test problem 10, 35 aircraft were assigned to FL370 in the deterministic model, while 28 were assigned to this level in the stochastic model. For all test problems, it is observed that the lower levels are not preferred much in both models.

Fig. 4 Flight level
assignment rates for
stochastic model
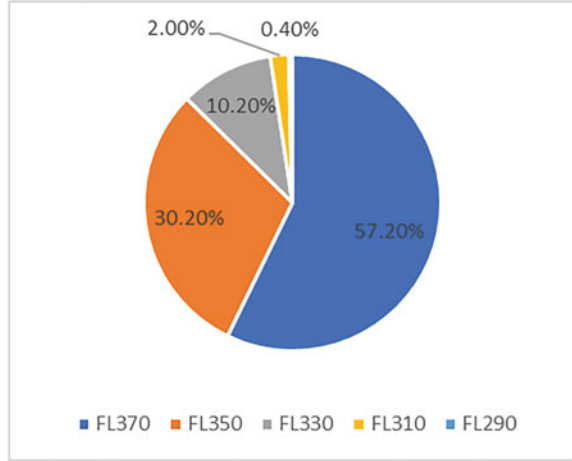
Fig. 5 Flight level
assignment rates for
deterministic model
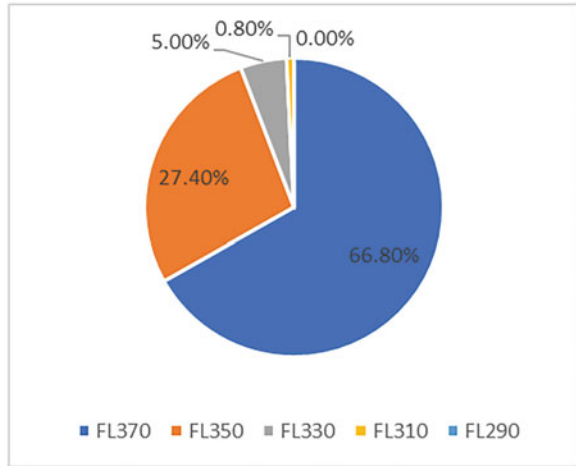
4   Discussion and Conclusion

This study develops a two-stage stochastic model for the conflict resolution problem
in the en-route phase. Also, flight level assignment is used as a conflict resolution
technique, and wind direction and speed uncertainties are reflected in the model. In
addition, the mathematical model uses real wind data to reflect wind speed differ-
ences between the levels. The developed model then, compared to deterministic and
expected value approaches in terms of fuel efficiency and the assignment decisions
of the stochastic and deterministic approaches, is examined in detail. As a result, it is
observed that the stochastic model provides an average of 4.17% fuel savings
compared to the deterministic model. In addition, it was observed that none of the
deterministic assignment decisions were applicable when the uncertainties occurred.

Table 8 Flight level assignments for each test problem

Model	Test problem	FL290	FL310	FL330	FL350	FL370
Stochastic	1	1	1	4	18	26
	2	0	2	5	17	26
	3	0	0	4	16	30
	4	1	2	6	12	29
	5	0	2	4	15	29
	6	0	2	6	14	28
	7	0	0	2	15	33
	8	0	0	6	15	29
	9	0	1	8	13	28
	10	0	0	6	16	28
Deterministic	1	0	1	1	16	32
	2	0	1	5	12	32
	3	0	0	2	13	35
	4	0	0	4	12	34
	5	0	1	1	13	35
	6	0	1	4	14	31
	7	0	0	0	12	38
	8	0	0	3	16	31
	9	0	0	4	15	31
	10	0	0	1	14	35

Therefore, any feasible solution for the EV model is not obtained, including applying the deterministic assignment decisions under uncertainties. The EV model provided non-conflicted routes for approximately 77% of aircraft. However, 23% of the conflicts were not solved without aircraft delays. On the other hand, the stochastic model solved all conflicts by flight level assignments without delay.

The assignment decisions of the models were examined in detail. It was observed that although both models assigned aircraft to higher flight levels because of fuel efficiency, it is seen that the stochastic model used lower flight levels more than the deterministic approach. This is because wind speed increases as the flight level increases. In future work, we will test the model efficiency for different wind characteristics by obtaining various data from other stations. In addition, flight level assignments after the sector entry points in the tactical phase will also be integrated into the model by using a dynamic model.

References

Cecen, R. K. (2021). A Mixed Integer Linear Programming Approach for Aircraft Conflict Detection and Resolution Problem. *International Journal of Engineering Research and Development, 13*(2), 350–358. https://doi.org/10.29137/umagd.736065

Cecen, R. K., & Cetek, C. (2020). Conflict-free en-route operations with horizontal resolution manoeuvers using a heuristic algorithm. *Aeronautical Journal, 124*(1275), 767–785. https://doi.org/10.1017/aer.2020.5

Chaloulos, G., & Lygeros, J. (2007). Effect of wind correlation on aircraft conflict probability. *Journal of Guidance, Control, and Dynamics, 30*(6), 1742–1752. https://doi.org/10.2514/1.28858

Dönmez, K. (2022). *A stochastic multi-objective programming model for the runway scheduling problem in the airport with the parallel point merge system and multiple runways*. Eskişehir Technical University. https://tez.yok.gov.tr/UlusalTezMerkezi/tezSorguSonucYeni.jsp

Dönmez, K., & Cecen, R. K. (2022). Comparison of the speed change and vector maneuver techniques for the conflict resolution problem: Fuel and flight time analysis. In *ISEAS'22 (International Symposium on Electric Aircraft and Autonomus Systems)*.

Dönmez, K., Cetek, C., & Kaya, O. (2022). Air traffic management in parallel-point merge systems under wind uncertainties. *Journal of Air Transport Management, 4*, 102268.

Hernández-Romero, E., Valenzuela, A., & Rivas, D. (2017). *Probabilistic aircraft conflict detection and resolution considering wind uncertainty*. SESAR Innovation Days.

Hernández-Romero, E., Valenzuela, A., & Rivas, D. (2020). Probabilistic multi-aircraft conflict detection and resolution considering wind forecast uncertainty. *Aerospace Science and Technology, 105*(105), 973. https://doi.org/10.1016/j.ast.2020.105973

Matsuno, Y., Tsuchiya, T., Wei, J., Hwang, I., & Matayoshi, N. (2015). Stochastic optimal control for aircraft conflict resolution under wind uncertainty. *Aerospace Science and Technology, 43*, 77–88. https://doi.org/10.1016/j.ast.2015.02.018

Matsuno, Y., Tsuchiya, T., & Matayoshi, N. (2016). Near-optimal control for aircraft conflict resolution in the presence of uncertainty. *Journal of Guidance, Control, and Dynamics, 39*(2), 326–338. https://doi.org/10.2514/1.G001227

Vela, A. E., Salaun, E., Solak, S., & Feron, E. (2009). A two-stage stochastic optimization model for air traffic conflict resolution under wind uncertainty. In *2009 IEEE/AIAA 28th digital avionics systems conference*, 2.E.5-1-2.E.5-13. https://doi.org/10.1109/DASC.2009.5347531

Weatherdata. (2021). *University of Wyoming College of Engineering*. http://weather.uwyo.edu/upperair/sounding.html

MCDM Risk Assessment in Ground Operation

Ilker Inan and Ilkay Orhan

Nomenclature

IATA	International Air Transport Association
IGOM	IATA Ground Operations Manual
MCDM	Multi-Criteria Decision-Making
PROMETHEE	The Reference Ranking Organization Method for Enrichment Evaluation

1 Introduction

Aviation occupies an important place in passenger transport compared to other sectors. In addition, 35% of all cargo is transported by aircraft (ICAO, 2019). It is estimated that the total number of passengers travelling will be around 4 billion in 2024 (IATA, 2022). In this regard, the demand for air transportation is increasing day by day. Departing thousands of aircraft on scheduled time is possible with correct management of pre-flight processes. The aim is to carry out many ground operations such as loading/offloading cargoes, mail and bags, refueling aircraft and providing caterings without compromising safety. Airlines with a complex fleet have to manage all processes safely while performing aircraft maintenance on time. Otherwise, many risk factors arise, and this will cost millions of dollars (Studic

I. Inan

Department of Civil Aviation, Graduate School of Sciences, Eskişehir Technical University, Eskişehir, Türkiye

I. Orhan (✉)

Faculty of Aeronautics and Astronautics, Eskişehir Technical University, Eskişehir, Türkiye
e-mail: iorhan@eskisehir.edu.tr

et al., 2017). There are many causes of accidents in ground operations related to safety. For instance, ramp workers are exposed to high noise levels from engines and auxiliary power units when loading/offloading the aircraft. Hearing problems may occur shortly if personal protective equipment is not used (Basner et al., 2017). In addition, all operations are expected to be achieved as scheduled during the ground time of the aircraft. Therefore, time pressure causes haste among ramp agents. Many ground accidents can occur due to these processes, both among personnel and aircraft. Low awareness may also lead to undesired incidents (Wenner & Drury, 2000). On the other hand, aircraft maintenance involves a high level of safety (Ward et al., 2010). Thus, equipment used in the hangar should be calibrated, and sometimes incorrect instructions during maintenance may derive from a lack of technical training. Environmental risks are also considered external factors, such as heavy rain, wind, snow, and icing, which may lead to safety weaknesses. For instance, irregularities in de-icing operations may cause deterioration of the aircraft's aerodynamic structure, affecting take-off performance in terms of safety (Cao et al., 2018).

2 Method

Decision-making is a process that has significant importance in getting accurate results. There are many MCDM methods, and one of the effective methods is PROTMETHEE (The Preference Ranking Organization Method for Enrichment Evaluation). The approach determines the alternatives to be decided according to preference functions and then calculates the partial and complete priorities of the alternatives through a pairwise comparison technique. There are six preference functions introduced by Brans in 1982 and are shown in Fig. 1 (Dagdeviren & Erarslan, 2013).

2.1 Data and Analyses

The risk weights resulting from sub-criteria assessment of "human factor," "communication," "job description," and "environment" are examined using AHP method as shown in Table 1.

2.2 Risk Impact on Ramp Operations

Risk factors implemented in AHP are scored in PROMETHEE to determine impact on ground operations as shown in Fig. 2.

Impact of main risk factors on five ground operations are illustrated in Fig. 3.
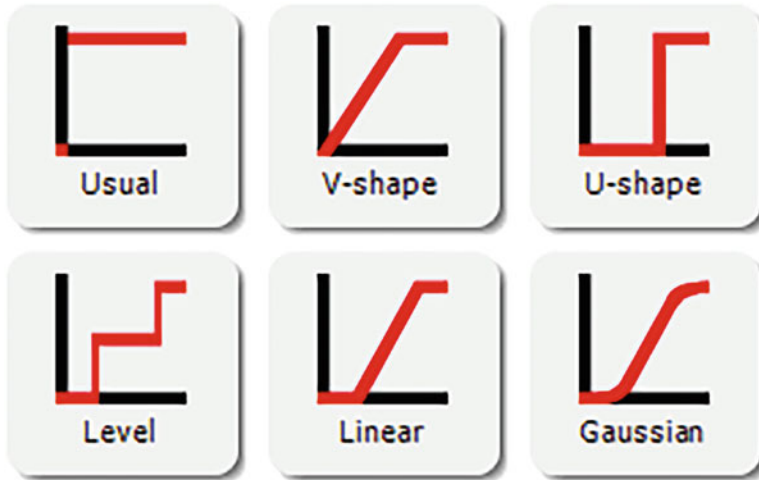
Fig. 1 Preference functions

Table 1 Risk factors in ground operation (Inan & Orhan, 2021)

Main factors	Sub-factors		Weight
Human factor	Fatigue	A1	0.70886
	Overconfidence	A2	0.17862
	Unattending	A3	0.11252
Communication	Lack of communication	B1	0.31081
	Marshalling	B2	0.49339
	Work shift	B3	0.19580
Job description	Kneeling/bending	C1	0.68698
	Overtime work	C2	0.18648
	Repetitive work	C3	0.12654
Environment	Bad weather	D1	0.45996
	Low visibility	D2	0.22113
	Noise	D3	0.31892

Each factor effect is examined and the impacts are shown based on operation in Figs. 4, 5, 6, and 7.

3 Results and Discussion

The sub-criteria obtained by comparing each one with the other through AHP method are shown in Table 1.

Results by grading and pairwise comparisons are evaluated according to the 5-point Likert scale with the PROMETHEE method, considering the expert opinions.

Fig. 2 Ground operations

The human factor, which covers fatigue, overconfidence, and unattended, has the highest rate in maintenance. Then ULD-BULK operation ranks second in loading/offloading due to fatigue (Fig. 4).

While the risks arising from communication has a significant effect on Pushback-Towing, it is also explored that accidents may occur due to marshalling in the de-anti icing process (Fig. 5).

Kneeling/bending movements have significant impact on ramp agents who are responsible for loading/offloading cargoes and bags in bulk aircraft operations. Similarly, technicians are also exposed to repetitive movements such as long-time working at height, bending/kneeling, holding the head in a fixed direction in maintanance action. Therefore, these sub-factors lead technician to take the second rank after the ramp workers in job description main factor (Fig. 6).

Weather conditions, considered external factors, have a more significant effect on ramp staff performing the operations while the aircraft is in the parking position. Moreover, exposure to excessive levels of noise is thought as a risk factor for both technicians and those working around the engines (Fig. 7).

4 Conclusion

Occupational accident causes and safety factors that may arise in ground operation have been examined based on the main items such as "human factor," "communication," "job description," and "environment." The risk factors calculated by pairwise comparisons are evaluated on a 5-point Likert scale according to the PROMETHEE method, taking weight percentages into account.
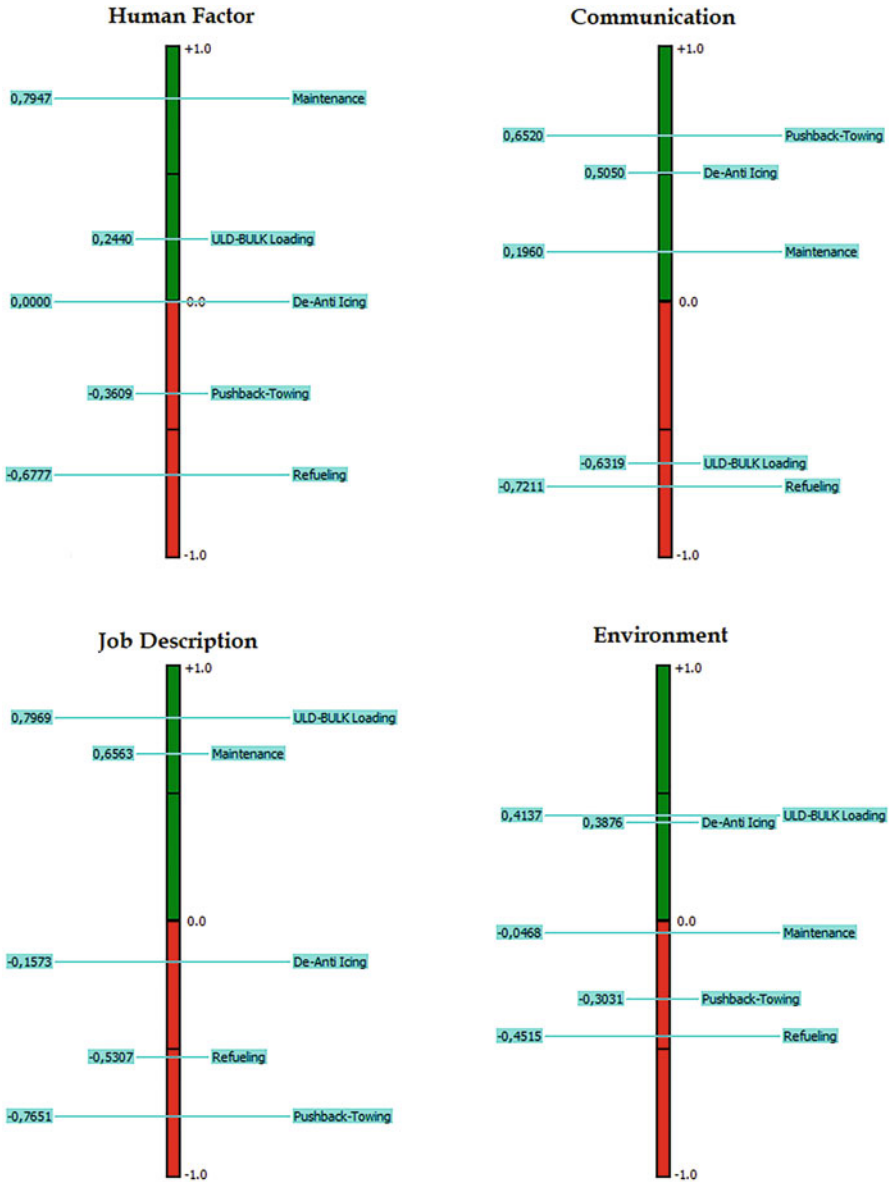
Fig. 3 Ranking analysis

This study, which can be recommended as a risk analysis method for airlines, presents an approach to the proactive accident prevention process.
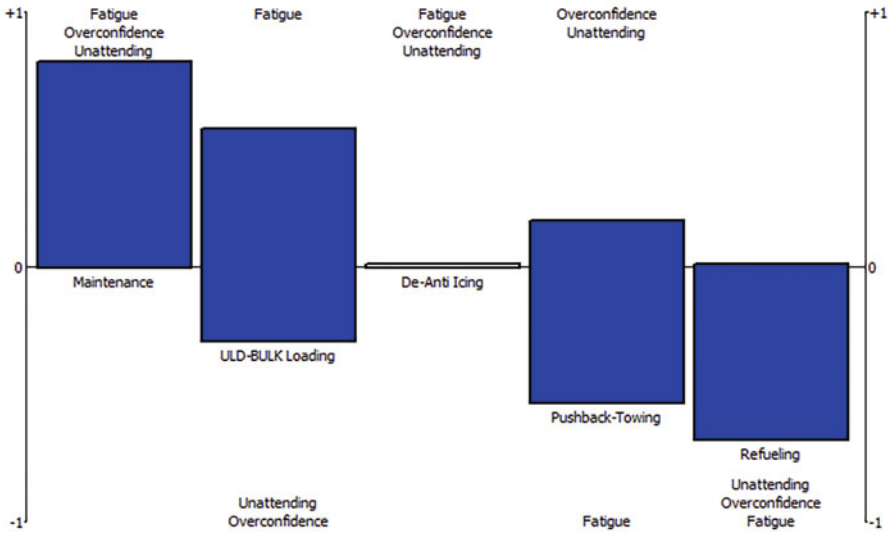
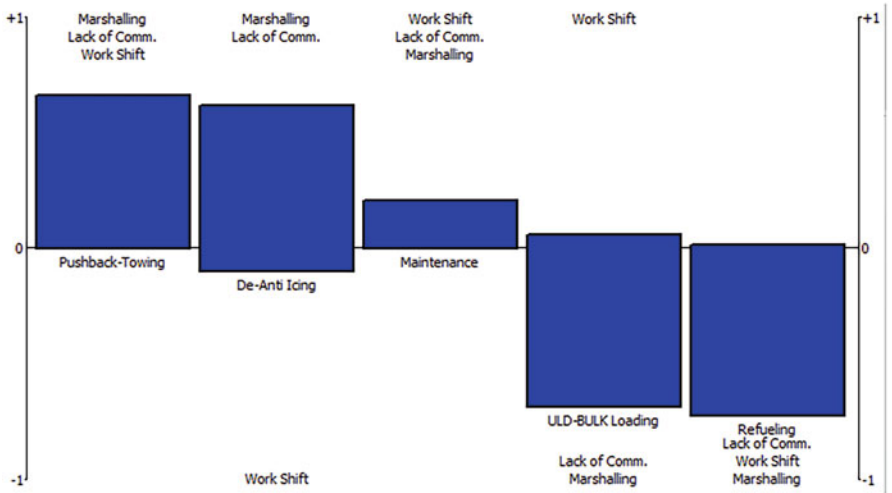**Fig. 4** Sub-factor analysis of human factor

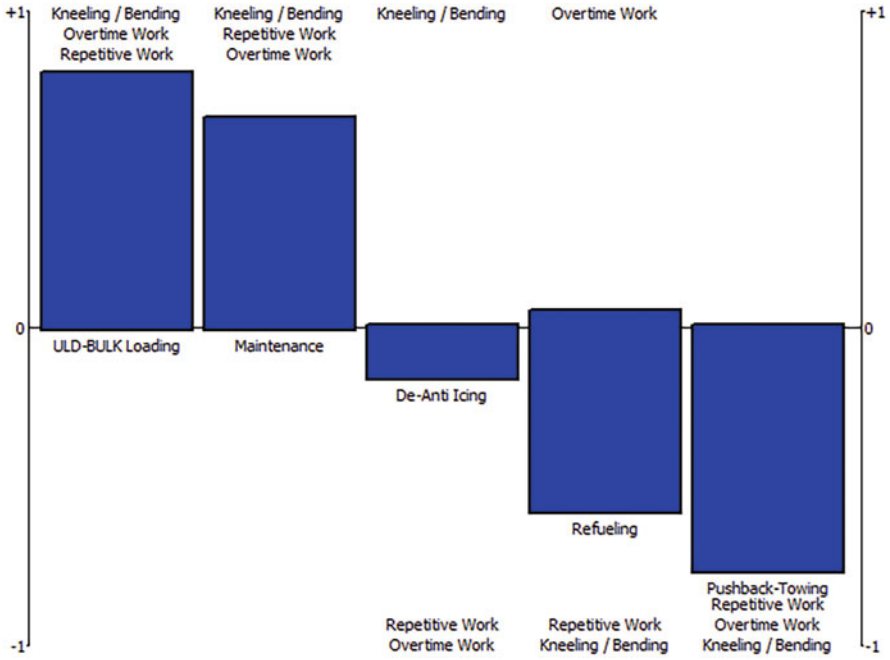**Fig. 5** Sub-factor analysis of communication

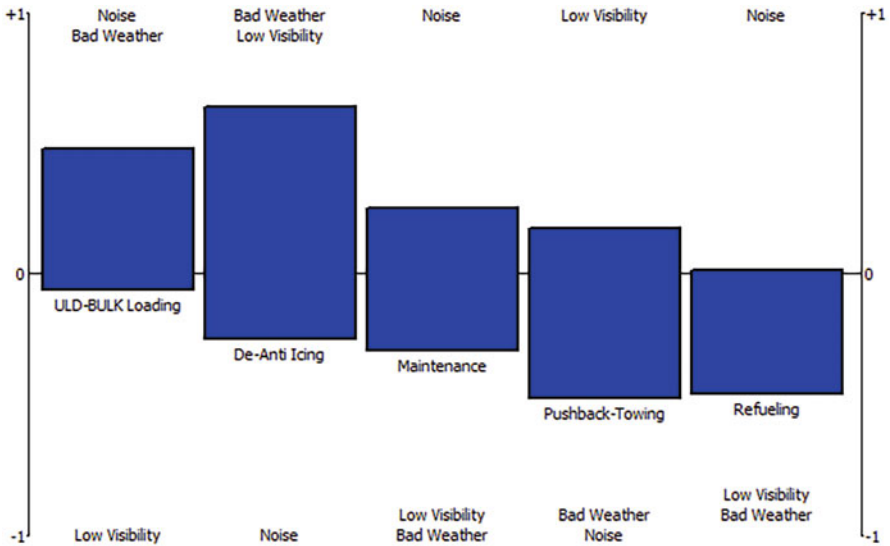**Fig. 6** Sub-factor analysis of job description

Fig. 7 Sub-factor analysis of environment

References

Basner, M., Clark, C., Hansell, A., Hileman, J. I., Janssen, S., Shepherd, K., & Sparrow, V. (2017). Aviation noise impacts: State of the science. *Noise & Health, 19*(87), 41–50. https://doi.org/10.4103/nah.NAH_104_16

Cao, Y., Tan, W., & Wu, Z. (2018). Aircraft icing: An ongoing threat to aviation safety. *Aerospace Science and Technology, 75*, 353–385. https://doi.org/10.1016/j.ast.2017.12.028

Dağdeviren, M., & Erarslan, E. (2013). PROMETHEE SIRALAMA YÖNTEMİ İLE TEDARİKÇİ SEÇİMİ. *Gazi Üniversitesi Mühendislik Mimarlık Fakültesi Dergisi, 23*(1). Available at https://dergipark.org.tr/en/pub/gazimmfd/issue/6675/88291

IATA. (2022). *Air passenger numbers to recover in 2024*. Available at https://www.iata.org/en/pressroom/2022-releases/2022-03-01-01/

ICAO. (2019). *International Civil Aviation Organisation. Aviation benefits report*. Available at https://www.icao.int/sustainability/Documents/AVIATION-BENEFITS-2019-web.pdf

Inan, I., & Orhan, I. (2021). *Safety factor analysis in Ramp operation with AHP approach*. Paper presented at the International Symposium on Sustainable Aviation, Kasetsart University, Bangkok, 25–27 November 2021.

Studic, M., Majumdar, A., Schuster, W., & Ochieng, W. Y. (2017). A systemic modelling of ground handling services using the functional resonance analysis method. *Transportation Research Part C: Emerging Technologies, 74*, 245–260. https://doi.org/10.1016/j.trc.2016.11.004

Ward, M., McDonald, N., Morrison, R., Gaynor, D., & Nugent, T. (2010). A performance improvement case study in aircraft maintenance and its implications for hazard identification. *Ergonomics, 53*(2), 247–267. https://doi.org/10.1080/00140130903194138

Wenner, C. A., & Drury, C. G. (2000). Analyzing human error in aircraft ground damage incidents. *International Journal of Industrial Ergonomics, 26*(2), 177–199. https://doi.org/10.1016/S0169-8141(99)00065-7

Optimization of Cutting Parameters in Face Milling of Waspaloy Superalloy

Oğuzhan Çakmakoğlu, Ahmet Demirer, Yakup Turgut, and Ömer Seçgin

Nomenclature

ANOVA   Analysis of Variance

1   Introduction

Waspaloy is a superalloy developed by Pratt and Whitney in the 1950s. It is used in parts that require high strength and good corrosion resistance at high temperatures, such as in the hot parts of turbine machines. Waspaloy's maximum operating temperature is as high as 750 °C. However, it is also an expensive alloy due to its high cobalt content. For this reason, a much cheaper alternative, "Alloy 718" is often used. However, the operating temperature of Alloy 718 is limited to 650 °C. Waspaloy is used in turbine parts, compressor discs, shafts, and turbine boxes of aircraft engines (Olovsjö et al., 2010). These superalloys also have an outstanding combination of toughness, high-temperature strength, creep resistance, excellent thermal fatigue, and resistance to degradation in oxidizing or corrosive media (Isik, 2017). Waspaloy is rich in nickel. It is a superior material because it maintains its high strength at high temperatures due to nano-scale precipitation hardening in the matrix phase. The gamma matrix, a face-centered cubic structure, nickel-based austenitic phase, contains high proportions of chromium, cobalt, molybdenum, and

O. Çakmakoğlu (✉) · A. Demirer · Ö. Seçgin
Technology Faculty, Sakarya University of Applied Sciences, Sakarya, Türkiye
e-mail: ademirer@subu.edu.tr; omersecgin@subu.edu.tr

Y. Turgut
Technology Faculty, Gazi University, Ankara, Türkiye
e-mail: yturgut@gazi.edu.tr

tungsten. Dislocation is inhibited when the amount of precipitates increases. This increases the hardness of the alloy (Veerappan et al., 2018).

In machining, the highest production amount is aimed at the lowest cost. This can be achieved by minimizing the cutting forces. Minimizing cutting forces depends on optimizing cutting parameters. When the literature studies are examined, it can be seen that there are studies on parameter optimization related to the milling process in academic and commercial fields. However, studies on Waspoloy are limited. Yıldırım et al., searched machinability of Nickel-based Waspaloy superalloy in milling. They used Taguchi's L_{16} $(4^2 \times 2^3)$ orthogonal array (Yıldırım et al., 2017). As a result, they reported that the minimum cutting force was achieved with a combination of vegetable-based cutting oil, flow rate of 100 ml/s, milling in the opposite direction (up), Type 1 nozzle, and 25 mm spray distance. Yıldırım et al. focused on tool life in milling (Yıldırım et al., 2019). From the experimental results using Taguchi, they determined that the optimum machining parameters for tool life were PVD coating, wet machining, 30 m/min cutting speed, and 0.1 mm/rev feed rate. Thirumalai et al. investigated the effectiveness of chilled coolant in machining the heat-resistant superalloy material Inconel 718. They reported that with the Taguchi experimental design, they reduced the number of experiments by one-third compared to the full factorial experimental setup. Bagci and Aykut used the Taguchi method for low surface roughness value in terms of cutting parameters in the surface milling process of cobalt-based superalloy (stellite 6) material and determined that the cutting speed was the most important parameter (Bagci & Aykut, 2006). Akhyar Ibrahim et al. stated that the most important factor of affecting the tool life of Inconel 718 by turning in dry conditions and at high speed: the depth of cut, feed rate, and cutting speed are respectively (Akhyar Ibrahim et al., 2011).

Motorcu et al. investigated the effects of cutting type, cutting speed, feed rate, and drill bit angle on surface roughness when drilling Waspaloy super alloy with coated (TiN) and uncoated drills. Köksal milled a nickel-based superalloy material named Waspaloy, which is used in the construction of some jet engine parts in the aircraft industry, with CVD-coated and uncoated carbide tips (Köksal, 2000). He measured and examined the subsurface microhardness of the machined surfaces. He discussed the effect of the insert types and process parameters used on this. Venkatesen et al. examined the tool wear of Inconel X-750 and Waspaloy in dry turning. They reported higher machining wear of Waspaloy compared to Inconel X-750 in all experiments. Velmurugan et al. analyzed the turning forces of Inconel X-750 and Waspaloy in dry turning (Vetri Velmurugan et al., 2019). They reported that the cutting force was much higher when processing Waspaloy. Işık investigated the effect of cutting speed on tool life and surface quality while machining Waspaloy (Isik, 2017).

In this experimental study, it was aimed to obtain optimum cutting parameters in the face milling process of Waspaloy superalloy. The effects of cutting parameters on the cutting force in face milling were investigated. The experimental data obtained in the study were optimized using the Taguchi method.

2 Material and Method

2.1 Materials and Experimental Setup

Nickel-based superalloys have high-temperature resistance and high corrosion resistance. Therefore, it is widely used in the aviation industry, especially in gas turbine engines. These alloys are known difficult materials to cut. The reasons for the difficult machining of nickel-based superalloys can be listed as follows (Dudzinski et al., 2004; Ezugwu et al., 1998; Jawaid et al., 2001; Sharman et al., 2001):

1. Due to its high-temperature resistance feature, a large part of its strength is preserved during machining.
2. During machining, work hardening occurs rapidly.
3. It has weak thermal conductivity.
4. During machining, a chemical reaction takes place with the cutting tool material.
5. Nickel alloys tend to bonding of the cutting tool.

In Table 1, physical properties of Waspaloy super alloy material are given.

For the experimental study, Waspaloy super alloy was prepared in the size of 40x40x50 mm. Experiments were made in Johnford VMC-550 CNC vertical machining center. The cutters were supplied by Sandvik company, and the cutting speed ranges recommended by the company for the cutting tool qualities were taken into account. In the study, four-level cutting speeds, two-level federates, and four-level indexable inserts, and a fixed depth of cut were determined (Table 2).

In the experiments, cutting tools (R245-12-T3-E-ML) and tool holder (R245-063Q22-12L) made by Sandvik company were used. The face milling tool diameter was 63 mm, the approach angle was 45°, and the up-milling method was used (Fig. 1). Milling was performed at a radial depth of cut (ae) of 10 mm using a single-edged cutting tool. In Table 3, important dimensions of the cutting tools used are given. In Table 4, coating properties of the used inserts are given.

The experimental setup is shown in Fig. 2. Test piece was attached to the dynamometer. The force data obtained from the experiments were taken from the

Table 1 Physical properties of Waspaloy (Köksal, 2000)

Density (g/cm^3)	8.19
Thermal conductivity (W/m°C)	~11(20 °C)
Hardness (HV)	454
Tensile strength (MPa)	1280
Coefficient of thermal expansion (10^{-6}/°C)	12.1 (21 °C)

Table 2 Cutting parameters

Cutting Speed (m/min)	20, 30, 40, 50
Federate (mm /tooth)	0.1, 0.12
Depth of cut (mm)	0.5
Cutting tool type	GC 1025, GC 1030, GC 2030, GC 2040
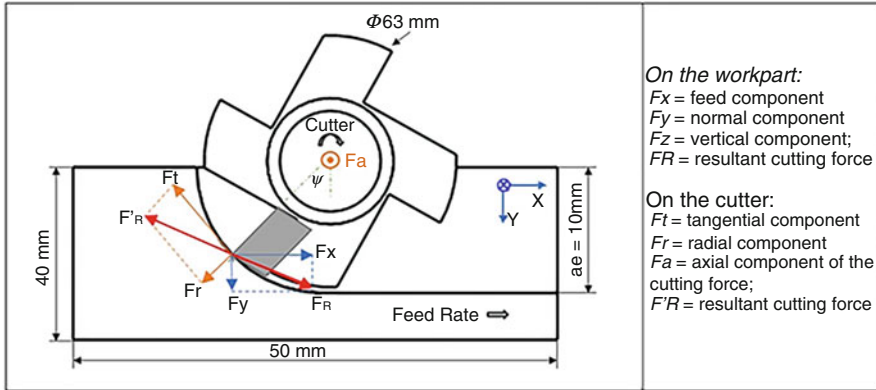
Fig. 1 Cutting forces in up-milling

Table 3 Cutting tool properties (Sandvik Coromant et al., 2010)

	GC 1025	GC 1030	GC 2030	GC 2040
Inscribed circle diameter	13.4 mm			
Cutting edge effective length	10 mm			
Insert thickness	3969 mm			
Wiper edge length	2.1 mm			
Corner radius	1.5 mm			
Major cutting edge angle	45°			

Table 4 Coating properties of inserts (Sandvik Coromant et al., 2010)

Grade	ISO area applications	Cutting material	Coating procedure and compositions	
GC1025	S15	HC	PVD	Ti (C, N) + TiN
GC1030	S15	HC	PVD	(Ti,Al) N + TiN
GC2030	S25	HC	PVD	(Ti,Al)N TiN
GC2040	S30	HC	CVD	MT-Ti (C,N) + Al_2O_3 + TiN

dynamometer. KISTLER 9272A 4 component dynamometer is used in the system. KISTLER Dynoware software was used to process the data and obtain the graphics. Because milling is an intermittent operation and chip thickness changes, cutting forces change. There are many cutting force estimation models. Two reference systems can be used to determine the cutting force components. A table reference system was used in the study (Köksal, 2000).

The cutting force components which occur in the face milling process are shown in Fig. 1. According to the table reference system, the cutting force is calculated according to the following formula (Alauddin et al., 1998; Köksal, 2000). The cutting force (F_R) was calculated from the F_x, F_y, F_z forces obtained from the dynamometer with the help of Eq. (1).
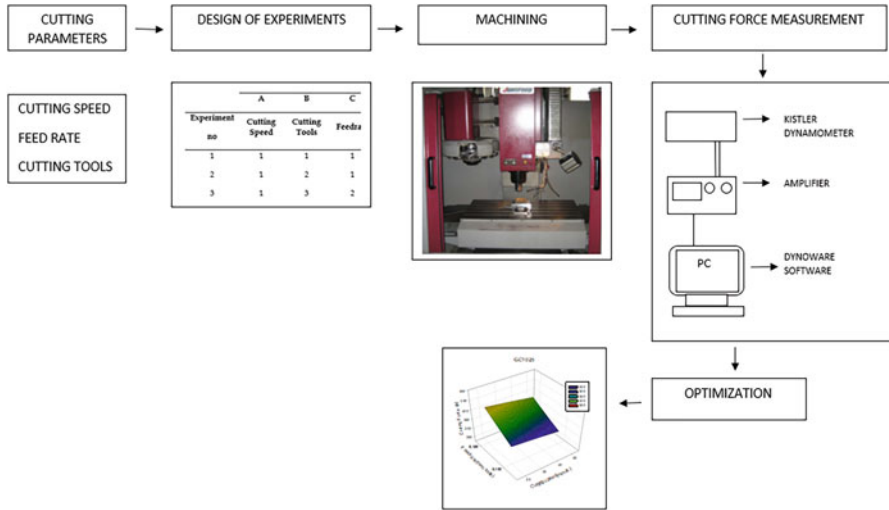
Fig. 2 Schema experimental setup

$$F_R = \sqrt{F_x{}^2 + F_y{}^2 + F_z{}^2} \tag{1}$$

3 Experimental Design and Optimization

3.1 The Taguchi Method and Design of Experiments

Traditional experimental design procedures are very complex and not easy to use. When the number of parameters increases, many experimental studies are required (Bagci & Aykut, 2006). Increasing the number of experiments means increasing time and costs. To eliminate this negative situation, Taguchi, a well-known academician, developed a method to reduce the number of experiments without affecting the results (Dutta & Kumar Reddy Narala, 2021). Parametric design experiments aim to find the ideal parameter set that optimizes the output and is least sensitive to noise (uncontrollable) factors. In this method, orthogonal arrays (OA) are used to formulate the combination of input variables during experiments (Ekici & Uzun, 2022). The Taguchi method is not only an experimental design technique, but also a useful technique for high-quality system design (Çiçek et al., 2012).

The Taguchi technique includes the following steps:

- Control factors are specified.
- The levels of each control factor are determined, and the appropriate orthogonal sequence is selected.

- Control factors are assigned to the selected orthogonal matrix and experiments are performed.
- Data is analyzed and optimal levels of control factors are determined.
- Validation experiments are performed, and the confidence interval is obtained.

The Taguchi method uses a loss function to determine quality characteristics. Loss function values are also converted to a signal-to-noise (S/N) ratio. In general, there are three different quality characteristics in S/N ratio analysis: "nominal is best," "bigger is better," and "smaller is better." For each process parameter level, the signal-to-noise ratio is calculated based on the S/N analysis (Çiçek et al., 2012; Ekici & Uzun, 2022). In an ideal situation, the cutting force (FR) should be at minimum levels. Therefore, the S/N ratios were calculated with the formula given in Eq. 2.

$$S/N = -10 \left[\frac{1}{n} \times \sum_{i=1}^{n} y_i^2 \right] \tag{2}$$

where y_i represents the characteristic value (cutting force) measured under that test conditions and n represents the number of tests performed under that test conditions.

4 Analysis and Evaluation of Experimental Results

4.1 Analysis of the Signal-to-Noise (S/N) Ratio

In this study, cutting tools, cutting speed, and feed rate were selected as control factors and their levels were determined as shown in Table 2. The first step of the Taguchi method is to choose a suitable orthogonal array. L_{16} ($4^2 \times 2^1$) was chosen to determine the optimal cutting parameters and to analyze the effects of these parameters. Cutting parameters were assigned to each column and sixteen cutting parameter combinations were generated as shown in Table 5.

The Taguchi method uses the S/N ratio to measure variations of the experimental design. Since the lowest cutting force values are the desired results for good product quality, the equation "smaller is better" (Eq. 2) was chosen for calculating the S/N ratio. S/N and mean response values for cutting force are shown in Table 5. As a results of sixteen experiments, the average value of the cutting force was calculated as 358.875 N, and the average S/N ratio for the cutting force value was −50.94 dB.

Table 6 gives the S/N (a) and average response table (b) for the cutting forces. This table gives the S/N ratio for the parameters. The level with the biggest S/N ratio indicates the optimum level for that parameter. In the line named "delta," the difference between the maximum S/N ratio of the parameters and the minimum S/N ratio is given. The parameter with the biggest delta value is the most important parameter affecting the cutting force (Sen et al., 2020).

Table 5 Taguchi L$_{16}$ ($4^2 \times 2^{1)}$ experimental design

| Experiment no. | Factors and levels | | | | | | Cutting force (N) | S/N ratio (dB) |
	A Cutting speed	B Cutting tools	C Feed rate	A Cutting speed	B Cutting tools	C Feed rate		
1	1	1	1	20	GC1025	0.1	323	−50,1841
2	1	2	1	20	GC1030	0.1	415	−52,361
3	1	3	2	20	GC2030	0.12	288	−49,1878
4	1	4	2	20	GC2040	0.12	366	−51.2696
5	2	1	1	30	GC1025	0.1	315	−49,9662
6	2	2	1	30	GC1030	0.1	449	−53,0449
7	2	3	2	30	GC2030	0.12	303	−49.6289
8	2	4	2	30	GC2040	0.12	365	−51,2459
9	3	1	2	40	GC1025	0.12	400	−52,0412
10	3	2	2	40	GC1030	0.12	429	−52,6491
11	3	3	1	40	GC2030	0.1	252	−48,028
12	3	4	1	40	GC2040	0.1	408	−52,2132
13	4	1	2	50	GC1025	0.12	387	−51,7542
14	4	2	2	50	GC1030	0.12	418	−52,4235
15	4	3	1	50	GC2030	0.1	229	−47,1967
16	4	4	1	50	GC2040	0.1	395	−51,9319

Table 6 S/N Response and average response table for cutting force

(a) S/N table

Level	Cutting speed	Cutting tool	Feed rate
1	**−50.75**	−50.99	**−50.62**
2	−50.97	−52.62	−51.28
3	−51.23	**−48.51**	
4	−50.83	−51.67	
Delta	0.48	4.11	0.66
Rank	3	1	2

(b) Average response table

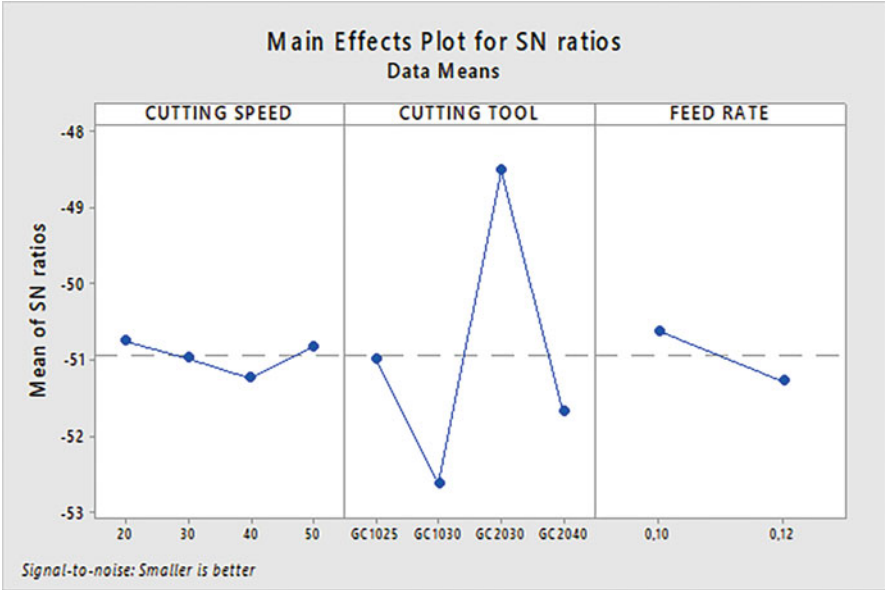| Level	Cutting speed	Cutting tool	Feed rate
1	**348.0**	356.3	**348.3**
2	358.0	427.8	369.5
3	372.3	**268.0**	
4	357.3	383.5	
Delta	24.3	159.8	21.3
Rank	2	1	3

Fig. 3 Main effects plot for S/N ratios

Another requirement in calculating optimum values is to determine optimum levels. The S/N ratios of the cutting force are given in the Fig. 3. Fig. 3 shows the optimum levels at which the lowest cutting force can be obtained in the processing of Waspaloy super alloy: 20 m/ min cutting speed (A1), GC 2030 cutting tool (B3), 0.1 mm/tooth feed rate (C1). Levels and S/N ratios of the factors that give the lowest cut-off value are shown in in Table 7: factor A: Level 1, $S/N = -50.75$ dB; factor B: Level 3, -48.51 dB; and factor C: Level 1, -50.62 dB.

4.2 Analysis of Variance (ANOVA) Method

In this study, ANOVA was used to analyze the effects of experimental parameters on cutting force. ANOVA is a statistical method used to determine the individual interactions of all control factors. Table 7 presents the ANOVA results revealing the effects of cutting speed, feed rate, and cutting tool control factors on cutting force at 95% confidence level and 5% significance level.

ANOVA table shows the importance of the factors. The results showed that factor B (cutting tool) had a high (82.99%) effect on the cutting force. This factor was followed by factor C (feed rate) with a rate of 2.75%. The results of factors and their interactions with a P value less than 0.05 are statistically significant. Factor C (feed

Table 7 Analysis of variance

Source	DF	Seq SS	Contribution	Adj SS	Adj MS	F-Value	P-Value
Cutting speed	3	1202	1.83%	1202	400.7	0.39	0.761
Cutting tool	3	54,461	**82.99%**	54,461	18153.8	17.82	**0.001**
Feed rate	1	1806	2.75%	1806	1806.3	1.77	**0.220**
Error	8	8152	12.42%	8152	1019.0		
Total	15	65,622	100.00%				

rate) and factor A (cutting speed) was not found to be statistically significant. The second-order model was used to examine the effectiveness of the parameters used in the experiments and to measure the predictive efficiency of the test results, and the determination coefficient $R^2 = 87.58\%$.

Figure 4 shows the cutting force graphs for four cutting tools. These graphs were obtained from the experiments performed as a result of the Taguchi method (Table 6). It is known that cutting force decreases with increasing cutting speed in conventional materials, but it has been observed in academic studies that cutting force increases with increasing cutting speed in machining superalloys (Mia 2018; Sharman et al. 2001; Thrinadh et al. 2020). In Fig. 4c, it is seen that the GC2030 cutting tool has lower cutting force than other cutting tools. In general, the cutting force increased as the chip volume increased with an increase in the feed rate. This result is in line with the literature (Hoier et al. 2017, 2018).

4.3 Estimation and Verification Experiment of Optimum Cutting Force

A validation experiment is required to verify the optimized condition with the Taguchi optimization technique. Figure 3 shows the estimation of the optimum cutting force. The optimum combination of control factors is calculated by the following equation, taking into account A1B3C1.

$$F_{R_{opt}} = F_{R_{avg}} + \left(A_1 - F_{R_{avg}}\right) + \left(B_3 - F_{R_{avg}}\right) + \left(C_1 - F_{R_{avg}}\right) \tag{3}$$

In the Table 6, the average of the cutting forces $(F_{R_{opt}})$ was calculated as *358.875 N*. Calculation result of $F_{R_{opt}}$ was found *246.55 N* with using Eq. 3. Confidence interval is used to validate the quality characteristics of the validation experiment (Mia, 2018; Motorcu et al., 2016). The confidence interval for the estimated optimal values is calculated with the help of Eqs. 4 and 5. The value obtained as a result of the validation experiment should be within the confidence interval (Çiçek et al. 2012; Şen et al. 2020).
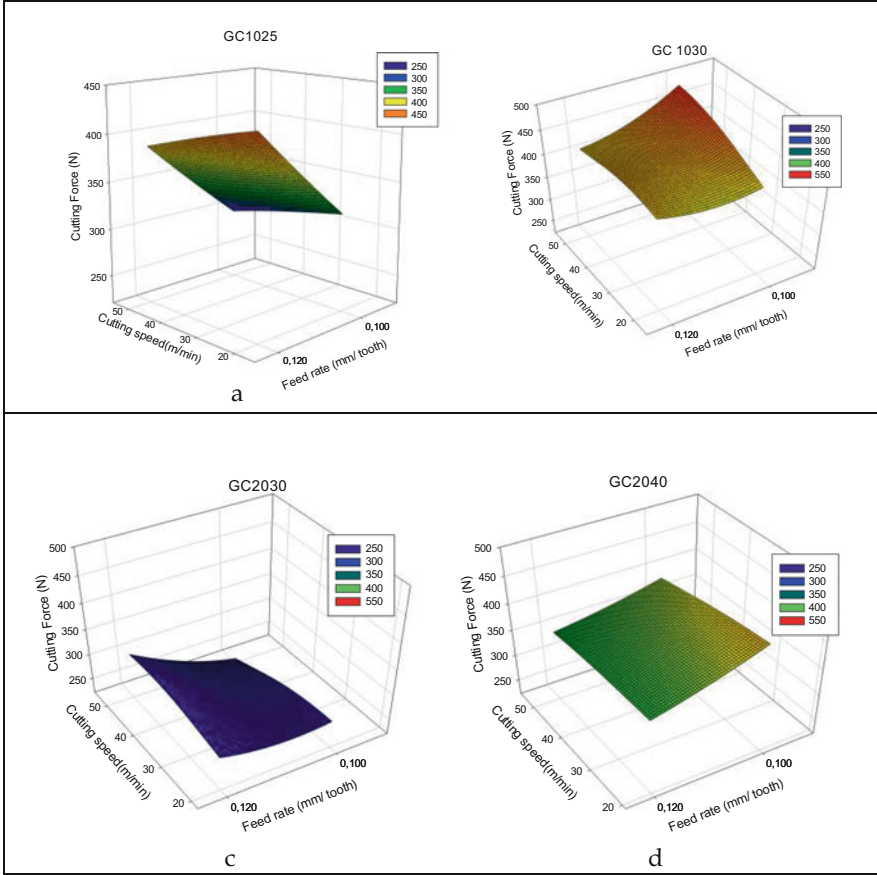
Fig. 4 Effect of cutting speed and feed rate on cutting force for cutting tools

$$CI = \sqrt{F_{\alpha;1;fe} \; Ve\left[\frac{1}{n_{\text{eff}}} + \frac{1}{r}\right]} \tag{4}$$

$$n_{\text{eff}} = \frac{N}{1 + T_{\text{dof}}} \tag{5}$$

In Eqs. 4 and 5, $F_{\alpha;1;\;fe}$ is the *F* ratio at *95%* confidence level (*F distribution table*), α is the significance level, n_{eff} is the effective iteration number, *fe* is the error degree of freedom, *r* is the *number of* validation experiments, *Ve* is the error variance, *N* is the total number of experiments, and T_{dof} is the total master factor degrees of freedom.

Consider that $F_{0.05;1;8} = 5.32$, $Ve = 8152$, $R = 2$, $N = 16$, $T_{dof} = 7$ and $n_{eff} = 2$. Confidence interval calculated using Eqs. 4 and 5 is $CI = \pm 208,251$. The optimum level of *A1B3C1* was not present in the experiments in the experimental design. Therefore, two replicate verification experiments were performed using the GC 2030 cutting tool, and the cutting force value was found to be *227.94 N*. Estimated average optimum cutting force with 95% confidence interval is as follows:

$$\left(F_{Ropt} - CI\right) \leq F_{Rexperimental} \leq \left(F_{Ropt} + CI\right)$$
$$\left(246.55 - 208,251\right) \leq 227.94 \leq \left(246.55 + 208,251\right)$$
$$38.298 \leq 227.94 \leq 454.801$$

5 Conclusions

In this study, optimum cutting parameters in the face milling process of Waspaloy super alloy were obtained, and the effects of cutting parameters on the cutting force in face milling were investigated. The experimental data obtained in the study were optimized using the Taguchi method. The remarkable results of the study are listed below:

- Quadratic model was used to measure the predictive adequacy of the test results and the coefficient of determination was $R^2 = 87.58\%$.
- ANOVA analysis showed that among the cutting parameters (cutting tool, cutting speed, and feed rate) used to determine the cutting force, "cutting tool" was observed to be more effective by 82.99%.
- The optimum levels at which the lowest cutting force was obtained in the machining of Waspaloy super alloy using the Taguchi method were as follows: cutting tool GC 2030, cutting speed 20 m/min, feed rate 0.1 mm/tooth.
- The value obtained as a result of the validation experiment (227.94 N) was within the confidence interval.

References

Akhyar Ibrahim, G., Che Haron, C. H., Abdul Ghani, J., Said, A. Y. M., & Abu Yazid, M. Z. (2011). Performance of PVD-coated carbide tools when turning inconel 718 in dry machining. *Advances in Mechanical Engineering, 2011*. available at: https://doi.org/10.1155/2011/790975

Alauddin, M., Mazid, M. A., El Baradi, M. A., & Hashmi, M. S. J. (1998). Cutting forces in the end milling of Inconel 718. *Journal of Materials Processing Technology, 300*(3–4), 153–159.

Bagci, E., & Aykut, Ş. (2006). A study of Taguchi optimization method for identifying optimum surface roughness in CNC face milling of cobalt-based alloy (stellite 6). *International Journal of Advanced Manufacturing Technology, 29*(9–10), 940–947.

Çiçek, A., Kıvak, T., Samtaş, G., Kivak, T., & Samtas, G. (2012). Application of Taguchi method for surface roughness and roundness error in drilling of AISI 316 stainless steel. *Strojniški Vestnik – Journal of Mechanical Engineering, 58*, 165–174.

Dudzinski, D., Devillez, A., Moufki, A., Larrouquère, D., Zerrouki, V., & Vigneau, J. (2004). A review of developments towards dry and high speed machining of Inconel 718 alloy. *International Journal of Machine Tools and Manufacture, 44*(4), 439–456.

Dutta, S., & Kumar Reddy Narala, S. (2021). Optimizing turning parameters in the machining of AM alloy using Taguchi methodology. *Measurement: Journal of the International Measurement Confederation*, Elsevier Ltd*., 169*, 108340.

Ekici, E., & Uzun, G. (2022). Effects on machinability of cryogenic treatment applied to carbide tools in the milling of Ti6AI4V with optimization via the Taguchi method and grey relational analysis. *Journal of the Brazilian Society of Mechanical Sciences and Engineering, 44*-(7) Available at: https://doi.org/10.1007/s40430-022-03572-1

Ezugwu, E. O., Wang, Z. M., & Machado, A. R. (1998). The machinability of nickel-based alloys: A review. *Journal of Materials Processing Technology, 86*(1–3), 1–16.

Hoier, P., Klement, U., Tamil Alagan, N., Beno, T., & Wretland, A. (2017). Flank wear characteristics of WC-Co tools when turning Alloy 718 with high-pressure coolant supply. *Journal of Manufacturing Processes*, The Society of Manufacturing Engineers*, 30*, 116–123.

Hoier, P., Malakizadi, A., Stuppa, P., Cedergren, S., & Klement, U. (2018). Microstructural characteristics of Alloy 718 and Waspaloy and their influence on flank wear during turning. *Wear*, Elsevier B.V*., 400–401*, 184–193.

Isik, Y. (2017). Effect of Cutting Speed on the Pvd-Coated Carbide Insert in the Machining on Waspaloy. *International Journal of Research in Engineering and Technology, 06*(08), 48–52.

Jawaid, A., Koksal, S., & Sharif, S. (2001). Cutting performance and wear characteristics of PVD coated and uncoated carbide tools in face milling Inconel 718 aerospace alloy. *Journal of Materials Processing Technology, 116*(1), 2–9.

Köksal, S. (2000). *Face milling of nickel-based superalloys with coated and uncoated carbide tools*, No. October.

Mia, M. (2018). Mathematical modeling and optimization of MQL assisted end milling characteristics based on RSM and Taguchi method. *Measurement*. Elsevier Ltd. Available at: https://doi.org/10.1016/j.measurement.2018.02.017

Motorcu, A. R., Ekici, E., & Kuş, A. (2016). Investigation of the WEDM of Al/B4C/Gr reinforced hybrid composites using the Taguchi method and response surface methodology. *Science and Engineering of Composite Materials, 23*(4), 435–445.

Olovsjö, S., Wretland, A., & Sjöberg, G. (2010). The effect of grain size and hardness of Waspaloy on the wear of cemented carbide tools. *International Journal of Advanced Manufacturing Technology, 50*(9–12), 907–915.

Sandvik Coromant. (2010). *Technical guide and product catalogues*.

Şen, N., Taşdemir, V., & Seçgin, Ö. (2020). Investigation of formability of HC380LA material via the TPIF-RL incremental forming method. *Ironmaking and Steelmaking*, Taylor & Francis*, 47*(10), 1199–1205.

Sharman, A., Dewes, R. C., & Aspinwall, D. K. (2001). Tool life when high speed ball nose end milling Inconel 718™. *Journal of Materials Processing Technology, 118*(1–3), 29–35.

Thrinadh, J., Mohapatra, A., Datta, S., & Masanta, M. (2020). Machining behavior of Inconel 718 superalloy: Effects of cutting speed and depth of cut. *Materials Today: Proceedings*, Elsevier Ltd*., 26*, 200–208.

Veerappan, G., Ravichandran, M., & Marichamy, S. (2018). Mechanical properties and machinability of waspaloy for aerospace applications – Review. *IOP Conference Series: Materials Science and Engineering, 402*(1) Available at: https://doi.org/10.1088/1757-899X/402/1/012039

Velmurugan K, V., K, V., S, D. & Mathew, A. (2019). Investigation of parameters for machining a difficult-to-machine superalloy: Inconel X-750 and Waspaloy. *Lecture Notes in Mechanical Engineering Innovative Design, Analysis and Development Practices in Aerospace and Automotive Engineering (I-DAD 2018)*, 199–215. Available at: https://doi.org/10.1007/978-981-13-2718-6_19

Yıldırım, Ç. V., Kıvak, T., Sarıkaya, M., & Erzincanlı, F. (2017). Determination of MQL parameters contributing to sustainable machining in the Milling of Nickel-Base Superalloy Waspaloy. *Arabian Journal for Science and Engineering, 42*(11), 4667–4681.

Yıldırım, Ç. V., Kıvak, T., & Erzincanlı, F. (2019). Tool wear and surface roughness analysis in milling with ceramic tools of Waspaloy: a comparison of machining performance with different cooling methods. *Journal of the Brazilian Society of Mechanical Sciences and Engineering*, Springer Berlin Heidelberg*, 41*(2), 83.

The Role of Additive Manufacturing Towards Sustainable Aerospace Structures

Joshua Rodrigues, Simon Barter, and Raj Das

Nomenclature

AM   Additive Manufacturing
TO   Topology Optimisation
CAD   Computer-Aided Design
ISS   International Space Station
ISRU   In-Situ Resource Utilisation

1 Introduction

The ambition to achieve a more sustainable aerospace sector is critical to future aerospace operations and research. The aerospace industry is a significant contributor to environmental air pollution and greenhouse gas emissions, epitomising the importance of focusing on the sector's sustainability. The unprecedented growth in aerospace has led to a surge in operations, significantly increasing local air pollution (Psanis et al., 2017). With an increase in demand for more efficient structures, engines and operations, innovative technologies are continuously being developed to realise these goals. In the case of structures (including engine components), additive manufacturing (AM) is a leading example of such innovation that has revolutionised how structures are designed and created. Since its initial use for rapid prototyping, AM technology has matured to become an established fabrication method, providing significant benefits to the aerospace industry (Attaran, 2017). The adoption of this technology has embarked on a new era for an advanced ecological

J. Rodrigues (✉) · S. Barter · R. Das
School of Engineering, RMIT University, Melbourne, Australia
e-mail: joshua.rodrigues@student.rmit.edu.au; simon.barter@rmit.edu.au; raj.das@rmit.edu.au

sector, producing structures that are less damaging to the surrounding environments through better resource usage and high structural efficiencies.

In this chapter, the role of AM technology in a more sustainable aerospace sector is viewed. An overview of AM technology is initially portrayed, highlighting the numerous advantages this technology presents, particularly, its unique ability to create highly customised components through structural optimisation, the potential for novel materials that are not currently possible to produce by conventional methods and the introduction of functionally graded structures. The influence of these properties on sustainable aerospace is then emphasised, addressing how these benefits contribute to a more sustainable outlook. With this, the future opportunities of AM presents are outlined, including the prospective abilities of in-space manufacturing and in-situ resource utilisation (ISRU) that will be crucial for future progression in the aerospace sector.

2   Additive Manufacturing Technology

As opposed to conventional, subtractive processes, whereby material is removed from a bulk source to reveal the final structure, AM fabricates components by adding material, commonly through a layer-by-layer process. Several classes of material can be used for AM fabrication, including polymers, ceramics, and metals. These materials often come in the form of a powder or wire feedstock that is typically melted by a heat source and deposited to form the item being built. This is usually achieved in successive layers to produce the defined component geometry. Due to this unique, generative nature, AM technology greatly enhances the design freedom of complex structures and removes many of the constraints imposed by traditional manufacturing methods (Dordlofva & Törlind, 2017). Unprecedented control over the shape, function and composition of components is enabled through AM, allowing for structures with incredibly complex geometries and internal features to be created that would be otherwise difficult via conventional techniques (Huang et al., 2015).

With this ability, methods of structural optimisation have become widely applied to a variety of applications to create highly customised components tailored to suit specific loading conditions. Methods of optimisation, encompassing size, shape and topology, as well as cellular lattice designs have utilised the advanced abilities of AM, performing synergistic advantages to fabricate structures that are entirely unique to the application with effective material distribution (Tejani et al., 2018). Various methods of topology optimisation (TO) exist that can produce lightweight parts without comprising the mechanical properties required for the application (Prathyusha & Babu, 2022). Structures can be optimised for a variety of objectives, such as to minimise mass, strain or displacement, or to maximise stiffness, while enhancing the performance and mechanical properties of the structure. Multiple objectives can be incorporated simultaneously with various weightings, resulting in several potential design iterations of a single component.

3 Advantages of AM for Sustainable Aerospace

With the plethora of advantages realised through AM, it is widely considered an exceptional candidate to progress the aerospace industry towards a more sustainable sector. The space industry is poised to gain the maximum benefit of AM technology, where most parts created for spacecraft structures are highly customised with low volume part production (Sacco & Moon, 2019). Stemming from the realised complexity achievable through AM, TO and cellular designs have demonstrated numerous advantages in aerospace applications, particularly the ability to reduce component weight, part count, material wastage and the associated supply chain issues that arise with small production runs. Each of these inherent benefits significantly contributes toward more sustainable aerospace, domain as discussed in the following.

3.1 Weight Reduction

One of the primary advantages that arise from component optimisation is the ability to fabricate structures with less material, resulting in significant weight reduction. Aerospace and space applications are highly sensitive to mass, which is directly proportional to the fuel required for an intended mission. Large structures, such as aircraft and rockets, require ample amounts of fuel to transport their payloads safely and complete their objective. In terms of an orbital rocket launch, the propellant component alone can contribute to almost 95% of the total mass of the rocket. This is to ensure that the structure and payload can produce enough thrust to reach orbit safely, overcoming the associated drag and gravitational resistances. The emissions from the combustion of fuels containing hydrocarbons and/or aluminium powder, primarily carbon dioxide, black carbon and alumina, present significant harm to the surrounding environments and atmosphere (Ryan et al., 2022). Gases and particles emitted from burning fuel have been shown to damage the ozone layer through heating of the middle and upper atmospheres (Kokkinakis & Drikakis, 2022).

Using TO techniques, structures can be reimagined and redesigned in a way that can reduce their mass by 50–80%, significantly decreasing the related fuel requirements (Joshi & Sheikh, 2015). Various components for spacecraft applications have demonstrated significant weight reductions through optimisation processes, including satellite antennas, brackets and CubeSats (Blakey-Milner et al., 2021). Lattice panel designs have also been shown to achieve weight reductions of 50% compared to their conventional counterparts (Blachowicz et al., 2021). Lesser fuel requirements thus, in turn, further minimise the associated environmental impact. This continual cycle of optimisation to reduce the contributed pollution from aerospace structures is highly beneficial as further developments are made in the aerospace sector. As the demand for longer, farther missions increase, structures with reduced weight will also allow for more fuel to be carried without exceeding the initial weight constraints at launch.

3.2   Reduced Material Processing Energy Requirements

The use of structural optimisation also contributes to a reduction in material usage and processing costs. While casting manufacturing techniques may be considered a direct competitor to AM, the additive nature of AM processes that do not require the need for moulds or other casting additions; runners, risers, vents, cores, is clearly advantageous. Additionally, conventional subtractive manufacturing techniques, such as milling or turning, remove material from a bulk object to realise the final structure within, and this method results in significant material wastage that is often non-recyclable for subsequent parts. AM, on the other hand, only fabricates the required geometry necessary to create the final structure, ensuring minimal material wastage. High buy-to-fly ratios also exist in subtractive manufacturing techniques, commonly exceeding 20:1, as opposed to almost 1:1 for most AM processes (Joshi & Sheikh, 2015). The abundance of material wastage further contributes to many process-related impacts including higher energy requirements and gaseous emissions that are produced.

Along with the reduction of material required for fabrication, AM technology also has the added benefit of high material reusability efficiency, which is uncommon in most other manufacturing methods. In AM processes that use powder feedstock, the unmelted feedstock can be collected after the fabricated part is removed, and then put through a filtration processes system to remove unusable or partially melted particles, producing a quantity of feedstock for reuse. Such filtration processes can recycle 95–98% of the feedstock, which is unparalleled in the manufacturing industry (Petrovic et al., 2011).

3.3   Supply Chain Reduction

AM technology provides significant advantages towards a more sustainable sector through a much simpler supply chain process. For the construction of unique components and assemblies, manufacturers, often more than one, that have the required workforce and machinery are tasked to complete the construction. These structures are then transported, either domestically or internationally, often between manufacturers and finally reach the designated buyer. This can present several obstacles to projects, including lengthy delays due to manufacturer's capability limitations, logistics costs and setbacks, and unnecessary environmental impact due to the transportation. AM enables a reconfiguration of this supply chain as parts may now be fabricated locally to the final destination using a single supplier and at more affordable costs (Ford & Despeisse, 2016). Rather than exporting the required manufacturing, industries and institutions can access AM machines to fabricate structures where they are needed. This not only reduces the associated environmental impact from component transportation but also enables industries to act independently and more responsively.

Furthermore, AM technology is ideal to enable the notion of on-demand component manufacturing. Rather than maintaining a populous inventory of large structures and repair components, AM can be used to fabricate components as needed. This minimises the necessity to transport multiple structures that can lead to potential inventory waste and risk. Traditionally, when a component is damaged, it requires either repair or replacement, depending on the severity. Obtaining these components from the manufacturer or distributor is often costly and may involve long delays, which is inefficient for limited component numbers. The economics of AM make the one-off production of parts attractive, with significant cost-effectiveness (Ford & Despeisse, 2016).

3.4 Prototyping Ability

The unique nature of AM to fabricate components directly further enables the ability to prototype components before implementation in full-scale critical structures. In AM processes, parts are geometrically created using computer-aided design (CAD) technology, where structures are modelled to a high degree of accuracy and strict structural requirements. During fabrication, dimensional tolerances are critical to ensure that the final component is suitable for the application. These models can be adjusted with ease through CAD software, compared to traditional methods, scaling and modifying their shape as required. This allows smaller structures to be produced with the same relative ratios and dimensions that can be initially tested. Using this as a proof-of-concept approach, these structures can be fabricated much faster than full-scale models. This can also eliminate the potential risk of wastage if the final model is not suitable.

Through CAD technology, models of structures can easily be shared once created. Associated contributors can easily view and modify these models to ensure the structure is suitable for their requirements. This is much more favourable as opposed to an entire redesign of a system after fabrication (Ford & Despeisse, 2016).

4 Future Opportunities

As the aerospace and space industries grow, the use of AM will be imperative for future operations. With the increase of interest in space exploration and research, future mission objectives will aim to explore deeper into untouched areas of space with significantly longer mission durations. For this to occur, however, innovative structures and techniques must be realised to reduce costs and increase capabilities. The uniqueness of the AM processes has already reimagined how components are fabricated, which has further enabled the ingenious use of AM for in-space manufacturing capabilities and ISRU. With the versatile process of AM, launch vehicles now do not necessarily have to be designed to support large payloads as part

of the mission launch but can be fabricated during the mission timeline, resulting in longer and further exploration profiles. Both of these innovative uses of AM are outlined in the following.

4.1 In-Space Manufacturing Capability

With the urge to explore further into space, it is evident that innovative structures that have the capability to do so are necessary. One option for this is to increase the size and capacity of current structures to accommodate larger payloads such as satellites. However, this is not a sustainable method to progress aerospace operations; larger structures will require more manufacturing and production, as well as even larger amounts of fuel to achieve launch. Both of these factors are already significant contributors to environmental damage from aerospace operations. Stemming from this, AM technology provides the unique ability to fabricate complex structures in space, presenting an abundance of opportunities for future in-space manufacturing and sustainment concepts.

Rather than developing large launch vehicles to accommodate larger payloads, compact material feedstock can be supplied and components can be fabricated once in space. This provides several advantages for future missions, where it can enable the fabrication of components on-demand required for extended missions without the need to return to Earth (Mitchell et al., 2018). Alongside the economic advantages of not requiring a larger launch structure, sensitive and ultra-lightweight structures can be fabricated that do not need to survive the harsh conditions of launch. The material feedstock can be supplied with maximum volume efficiency, and these optimised structures can be manufactured in orbit without the risk of damage during launch.

Whilst in-space manufacturing capabilities have already been utilised for smaller, less critical applications, such as for manufacturing spare parts and tools on the International Space Station (ISS), the fabrication of large-scale structures is yet to be explored in depth (Zocca et al., 2022). Space stations, much like the ISS, can be used as development platforms, where structures can be fabricated through on-board AM machines, and then launched from there. An added advantage is access to the vacuum of space during the build, a condition that is often difficult to achieve on Earth. AM in space will allow ultra-lightweight and optimised components to be created, without the need to endure an orbital launch, with materials that may be difficult to use in any other atmosphere other than a vacuum. Such components will require less fuel to explore further into deep space. The potential for entire space station platforms to be developed in orbit can also transpire, whereby a plethora of these structures can be used as a constellation system for future missions and possible habitation for extended periods.

4.2 In-Situ Resource Utilisation

Stemming from the potential for large-scale in-space manufacturing, the ability of ISRU through AM technology also presents several opportunities for future exploration. For long-duration interplanetary missions, the creation of large-scale infrastructure is necessary. The concept of ISRU takes full advantage of the surrounding conditions by using natural regolith as the feedstock for AM processes, where with the abundance of this material on inter terrestrial planets, structures and components can be used as a self-sustaining method of construction (Isachenkov et al., 2021). Through this technology, the weight of launch vehicles can be reduced furthermore, as only the AM machine itself is required. The significant mass saving of material will also lead to more efficient launches, reducing the associated environmental impact.

5 Conclusion

Whilst still in the research and development phase for many applications, AM technologies demonstrate great potential for significant advancements towards a more environmentally conscious aerospace sector. The unique combination of AM and TO techniques provides several advantages that will further contribute to a sustainable industry. Through optimisation methods, component weight and material processing can be significantly reduced, leading to less fuel and energy consumption, respectively. The ability to manufacture components and prototypes on demand reduces the associated supply chain and transportation impact, and the innovation of in-space manufacturing capabilities and ISRU also provides an abundance of future opportunities for the advancement of this technology. With the constantly evolving aerospace industry, the use of AM technology will inevitably become an essential tool in progressing this sector towards a more sustainable outlook.

References

Attaran, M. (2017). The rise of 3-D printing: The advantages of additive manufacturing over traditional manufacturing. *Business Horizons, 60*(5), 677–688. https://doi.org/10.1016/j.bushor.2017.05.011

Blachowicz, T., Ehrmann, G., & Ehrmann, A. (2021). Metal additive manufacturing for satellites and rockets. *Applied Sciences, 11*(24), 12036. https://doi.org/10.3390/app112412036

Blakey-Milner, B., Gradl, P., Snedden, G., Brooks, M., Pitot, J., Lopez, E., Leary, M., Berto, F., & du Plessis, A. (2021). Metal additive manufacturing in aerospace: A review. *Materials & Design, 209*, 110008. https://doi.org/10.1016/j.matdes.2021.110008

Dordlofva, C., & Törlind, P. (2017). Qualification challenges with additive manufacturing in space applications. In *Proceedings of the 28th annual international solid freeform fabrication symposium – An additive manufacturing conference*. The University of Texas, Austin.

Ford, S., & Despeisse, M. (2016). Additive manufacturing and sustainability: An exploratory study of the advantages and challenges. *Journal of Cleaner Production, 137*, 1573–1587. https://doi.org/10.1016/j.jclepro.2016.04.150

Huang, Y., Leu, M. C., Mazumder, J., & Donmez, A. (2015). Additive manufacturing: Current state, future potential, gaps and needs, and recommendations. *Journal of Manufacturing Science and Engineering, 137*(1), 014001. https://doi.org/10.1115/1.4028725

Isachenkov, M., Chugunov, S., Akhatov, I., & Shishkovsky, I. (2021). Regolith-based additive manufacturing for sustainable development of lunar infrastructure – An overview. *Acta Astronautica, 180*, 650–678. https://doi.org/10.1016/j.actaastro.2021.01.005

Joshi, S. C., & Sheikh, A. A. (2015). 3D printing in aerospace and its long-term sustainability. *Virtual and Physical Prototyping, 10*(4), 175–185. https://doi.org/10.1080/17452759.2015.1111519

Kokkinakis, I. W., & Drikakis, D. (2022). Atmospheric pollution from rockets. *Physics of Fluids, 34*, 056107. https://doi.org/10.1063/5.0090017

Mitchell, A., Hołyńska, U. L. M., & Semprimoschnig, C. (2018). Additive manufacturing – A review of 4D printing and future applications. *Additive Manufacturing, 24*, 606–626. https://doi.org/10.1016/j.addma.2018.10.038

Petrovic, V., Gonzalez, J. V. H., Ferrando, O. J., Gordillo, J. D., Puchades, J. R. B., & Griñan, L. P. (2011). Additive layered manufacturing: Sectors of industrial application shown through case studies. *International Journal of Production Research, 49*(4), 1061–1079. https://doi.org/10.1080/00207540903479786

Prathyusha, A. L. R., & Babu, G. R. (2022). A review on additive manufacturing and topology optimization process for weight reduction studies in various industrial applications. *Materialstoday: Proceedings, 62*(1), 109–117. https://doi.org/10.1016/j.matpr.2022.02.604

Psanis, C., Triantafyllou, E., Giamarelou, M., Manousakas, M., Eleftheriadis, K., & Biskos, G. (2017). Particulate matter pollution from aviation-related activity at a small airport of the Aegean Sea Insular Region. *Science of the Total Environment, 596-597*, 187–193. https://doi.org/10.1016/j.scitotenv.2017.04.078

Ryan, R. G., Marais, E. A., Balhatchet, C. J., & Eastham, S. D. (2022). Impact of rocket launch and space debris air pollutant emissions on stratospheric ozone and global climate. *Earth's Future, 10*(6), e2021EF002555. https://doi.org/10.1029/2021EF002612

Sacco, E., & Moon, S. K. (2019). Additive manufacturing for space: Status and promises. *The International Journal of Advanced Manufacturing Technology, 105*(10), 4123–4146. https://doi.org/10.1007/s00170-019-03786-z

Tejani, G. G., Savsani, V. J., Patel, V. K., & Savsani, P. V. (2018). Size, shape, and topology optimization of planar and space trusses using mutation-based improved metaheuristics. *Journal of Computational Design and Engineering, 5*(2), 198–214. https://doi.org/10.1016/j.jcde.2017.10.001

Zocca, A., Wilbig, J., Waske, A., Günster, J., Widjaja, M. P., Neumann, C., Clozel, M., Meyer, A., Ding, J., Zhou, Z., & Tian, X. (2022). Challenges in the technology development for additive manufacturing in space. *Chinese Journal of Mechanical Engineering: Additive Manufacturing Frontiers, 1*(1), 100018. https://doi.org/10.1016/j.cjmeam.2022.100018

Aerodynamic Performance Analysis of Penguin-Inspired Biomimetic Aircraft Wing

Mahadi Hasan Masud and Peter Dabnichki

Nomenclature

Re	Reynolds number
AOA	Angle of attack
CD	Coefficient of drag
CL	Coefficient of lift
RANS	Reynolds-averaged Navier–Stokes
NURBS	Non-uniform rational basis spline
CFL	Courant–Friedrichs–Lewy

1 Introduction

Improved aerodynamic efficiency through reduction in the drag force complemented by increased lift force has been the objective of the aerospace industry. Traditional large-scale aircrafts have had their wing profiles substantially altered in the last decade and the lift to drag ratio considerably reduced while operating at low Reynolds number (Re). Moreover, the introduction of micro aerial vehicles posed further challenges as they run at low Re, where stall occurs at a very low AOA. A substantial volume of research explores an increased aerodynamic efficiency for a wide range of AOA and Re using modified aerofoil's shape and surface. In search of such solutions, sinusoidal leading edge and dimpled surface have been introduced, inspired by biomimetic research. One of the most significant biomimetics aerodynamic applications in recent years is the modified aerofoil inspired by the humpback

M. H. Masud (✉) · P. Dabnichki
School of Engineering, RMIT University, Bundoora Campus, Melbourne, Australia
e-mail: masud.08@me.ruet.ac.bd; peter.dabnichki@rmit.edu.au

whale flipper structure. The bumps along the leading edge of the humpback whale flippers are arranged sinusoidally as rounded tubercles. Protuberances along the leading edge, known as LEP, help the flipper hydrodynamically by functioning as a passive flow controller (Watts & Fish, 2001). Malipeddi et al. analyzed modified NACA2412 foil with a sinusoidal leading edge and found that the maximum lift coefficient can be increased by up to 48% at an angle of attack of 16 deg when compared to baseline aerofoil (Malipeddi et al., 2012). Miklosovic et al. examined modified NACA0020 wing at a Re= 5.2×10^5 and found that the lift coefficient increases by 60%, while the drag coefficient decreased by 32% (Miklosovic et al., 2004). Furthermore, extensive research on surface modification is ongoing by introducing vortex generators that help to reduce the pressure drag at a high AOA and bring overall performance improvement (Huang & Lin, 1995; Bearman & Owen, 1998; Akbari & Price, 2003).

There is, however, a much broader scope for research on underwater "flying" features that could potentially deliver improved aerodynamic performance, in particular for small-scale aircrafts that require agility and high-energy efficiency due to their limited energy supply. Based on kinematic data analysis of numerous penguin dives, Masud et al. showed that penguin species offer efficient underwater propulsion (Masud et al., 2022). Hence, we hypothesize that their blade-shaped wings would offer a higher stall angle. However, to date, no study investigated the drag and lift characteristics of a penguin-inspired biomimetic wing under different flow conditions. In this work, computational fluid dynamics analysis of aerodynamic forces of a penguin-inspired wing is performed to assess its suitability for aircraft application with a focus on AOA and stall.

2   Penguin-Inspired Wing Model and Numerical Procedure

The wing model was devised from a scan of a dead little (aka fairy penguin) penguin. The carcass was provided from the Philp Island research group (Permit no.: 10009208 under Wildlife Act 1975) and scanning of the little penguin carcass was performed using a HandySCANTM® 3D (Volumetric accuracy: 0.020 mm + 0.100 mm/m) scanner. The 3D scan of a little penguin carcass was transformed into a NURBS solid. For converting the STL (mesh) files into non-uniform rational basis spline (NURBS) SOLID, Autodesk Meshmixer® and GEOMAGIC DESIGNX® 2016 software were used. Then we scaled the dimension two times that make the wingspan 0.24 m, and correspondingly, the chord length across the span also changed. After converting the STL (mesh) into NURBS, we took a cross-section from the mid-plane (spanwise) of the wing having a chord length of 0.108 m and extruded it up to the length of 0.108 m. That means the generated penguin-inspired wing has a chord*span of ($C = 0.108$ m * $S = 0.108$ m), as shown in Fig. 1 at an AOA = 10 deg.

The computer-aided design model was transferred to ANSYS Fluent® 2021, and the computational domain's dimensions were set to 30C*20C*10C
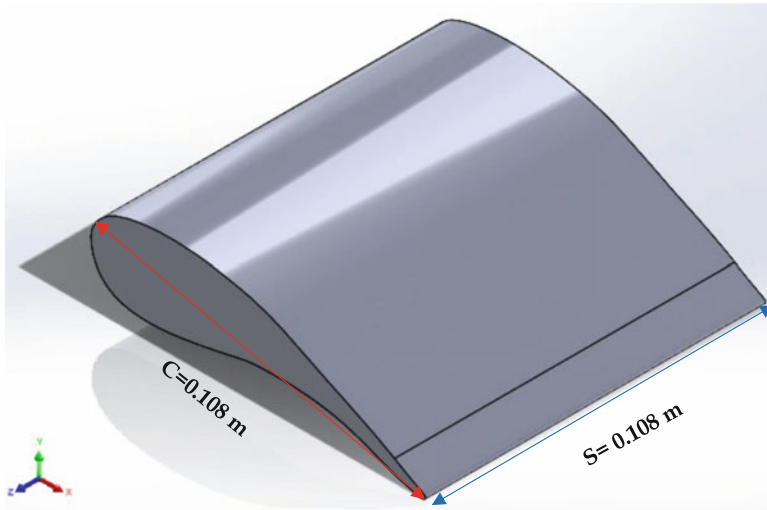
Fig. 1 Penguin-inspired biomimetic wing

(length*height*depth). The boundary's inflow and outflow are 10C upstream and 20C downstream from the wing's leading edge and trailing edge, respectively. In relation to the height, it is placed precisely in the middle of the computational domain. The simulation was performed at a chord-based $Re = 5 \times 10^5$ related to air velocity for $V_{avg} = 67.7$ m/s at an angle of attack ranging from 0 to 30 deg. In order to compare the results with the available experimental data of the conventional baseline NACA0012 wing (Critzos et al., 1955) at the same Reynolds number, $Re = 5 \times 10^5$ was selected. Furthermore, Kowalczuk et al. stated that Courant–Friedrichs–Lewy (CFL) also known as Courant with a value of 1 is adequate for sufficiently accurate results (Kowalczuk & Tatara, 2021). Hence, CFL of 1 was used, and for that, the time step was fixed at 10^{-3} s. Each solution was conducted for a minimum duration of 2 s, and the initial 100 steps were eliminated to mitigate the effect of initial flow conditions.

In meshing, 15 inflation layers were defined with a growth ratio of 1.2 to accurately resolve the boundary layer. Delayed detached Eddy simulation along with improved delayed detached Eddy simulation as shielding function was used, where SST K-ω model was applied as RANS model. Thus, to determine the turbulence near the wall, we needed to obtain the average Y+ value ≤1, and to obtain desired Y+ value, the first layer thickness of the inflation layer was set at 4.8×10^{-6} for an air velocity of 67.7 m/s. The maximum skewness and orthogonal quality of the generated mesh were 0.83 and 0.998, respectively. Finally, the mesh sensitivity analysis was performed following the procedure mentioned in Elsayed and Lacor (2011).

3   Results and Discussion

The lift coefficient (C_L) of the baseline aerofoil shows linear relationship up to about 10 deg AOA and has a better drag to lift ratio when compared with the findings of Critzos et al. (1955). The penguin-inspired profiles are also streamlined bodies and flow separation occurs beyond 20 deg AOA at a $Re = 5 \times 10^5$, after which point, C_L begins to decrease with further rise of the AOA. In other words, nearly 100% increase in the flow separation threshold is achieved compared to the NACA0012 threshold value. Hence, there is a strong suggestion that penguin-inspired biomimetic aerofoil promises better performance compared to almost all aerofoils in relation to stall effect (Airfoil Tools, 2022). It is already stated in the literature that protuberances along the leading edge of the aerofoil display better performance compared to the baseline aerofoils, specifically at higher AOA; this improved performance is owing to a notable reduction/delay of the flow separation (Levshin et al., 2006; Johari et al., 2007; Cai et al., 2019; Wang et al., 2021). This additional modification on a modified NACA aerofoil delivers inferior performance compared to the penguin-inspired biomimetic aircraft wings in terms of regulating flow separation at higher AOA.

The drag coefficient is proportional to the AOA for streamlined bodies (Masud et al., 2017; Islam et al., 2018), which is also the case in this work (see Fig. 2 for details). For AOA of 30 deg, a maximum drag coefficient of 0.35 is reached, which is still 71.4% lower than the baseline aerofoil of 0.60 (Critzos et al., 1955). Hence, it can be concluded that the penguin-inspired biomimetic aircraft wings offer superior performance compared to the baseline aerofoil beyond 10 deg AOA. Furthermore, the lift-to-drag ratio for penguin-inspired biomimetic aircraft wings is maximum when AOA is at 10 deg, and it is anticipated that the efficiency will also be the highest at that point. The combination of those results points to overall better maneuverability at lower energy cost.

4   Conclusion

We have numerically evaluated the aerodynamic performance of the penguin-inspired biomimetic aircraft wing, compared the results with the experimental data of baseline NACA0012 aerofoil for $Re = 5 \times 10^5$, and found that the stall occurs for NACA0012 at around 10 deg AOA. It is notable that for a penguin-inspired biomimetic aircraft wing, stall occurs at 20 deg (at the same Reynolds number). Moreover, in the post-stall region, the penguin-inspired biomimetic aircraft wing provides superior results compared to baseline NACA0012 aerofoil. At 15 deg and 20 deg AOA, penguin-inspired biomimetic aircraft wings provide 30.43% and 52.11% greater lift compared to the reported lift for NACA0012 aerofoil, respectively. Moreover, under the same conditions, penguin-inspired biomimetic aircraft wings generate 6.25% and 9.1% lesser drag compared to the reported drag for
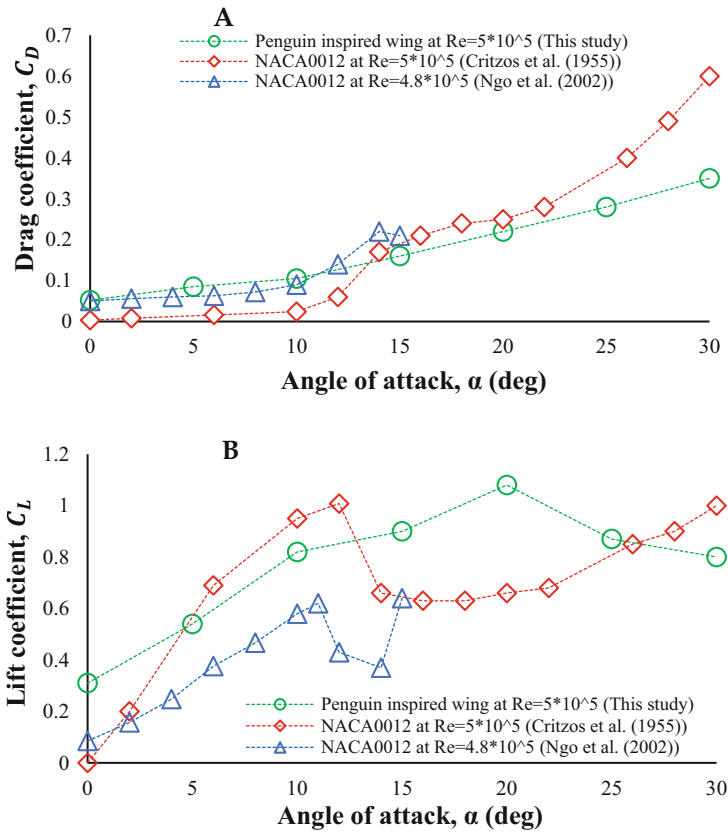
Fig. 2 Aerodynamic forces of a penguin-inspired biomimetic aircraft wing at different AOA. (**a**) Variation in drag coefficient with varying AOA, (**b**) variation in lift coefficient with varying AOA

NACA0012 aerofoil, respectively. Finally, it can be concluded that although penguin-inspired biomimetic aircraft wings show potential to be implemented as biomimetic aircraft wings for high maneuverability aircraft with potentially reduced energy requirements due to the demonstrated drag reduction, these are initial results, and further numerical and experimental analysis at varying flow conditions is required to fully assess their suitability for practical applications.

References

Airfoil Tools. (2022). *NACA 4 digit Airfoil database*. Available at http://airfoiltools.com/search/index?m%5Bgrp%5D=naca4d&m%5Bsort%5D=1. Accessed 4 Apr 2022.

Akbari, M. H., & Price, S. J. (2003). Simulation of dynamic stall for a NACA 0012 airfoil using a vortex method. *Journal of Fluids and Structures*. Elsevier, *17*(6), 855–874.

Bearman, P. W., & Owen, J. C. (1998). Reduction of bluff-body drag and suppression of vortex shedding by the introduction of wavy separation lines. *Journal of Fluids and Structures*. Elsevier, *12*(1), 123–130.

Cai, C., Liu, S., Zuo, Z., Maeda, T., Kamada, Y., Li, Q. A., & Sato, R. (2019). Experimental and theoretical investigations on the effect of a single leading-edge protuberance on airfoil performance. *Physics of Fluids*. AIP Publishing LLC, *31*(2), 27103.

Critzos, C. C., Heyson, H. H., & Boswinkle, R. W., Jr. (1955). *Aerodynamic characteristics of NACA 0012 airfoil section at angles of attack from 0 deg to 180 deg*. National Aeronautics and Space Administration.

Elsayed, K., & Lacor, C. (2011). Numerical modeling of the flow field and performance in cyclones of different cone-tip diameters. *Computers & Fluids*. Elsevier, *51*(1), 48–59.

Huang, R. F., & Lin, C. L. (1995). Vortex shedding and shear-layer instability of wing at low-Reynolds numbers. *AIAA Journal, 33*(8), 1398–1403.

Islam, M. T., Arefin, A. M., Masud, M. H., & Mourshed, M. (2018). The effect of Reynolds number on the performance of a modified NACA 2412 airfoil. In *AIP conference proceedings*. https://doi.org/10.1063/1.5044325

Johari, H., Henoch, C., Custodio, D., & Levshin, A. (2007). Effects of leading-edge protuberances on airfoil performance. *AIAA Journal, 45*(11), 2634–2642.

Kowalczuk, Z., & Tatara, M. S. (2021). Analytical 'steady-state'-based derivation and clarification of the Courant-Friedrichs-Lewy condition for pipe flow. *Journal of Natural Gas Science and Engineering*. Elsevier, *91*, 103953.

Levshin, A., Custodio, D., Henoch, C., & Johari, H. (2006). Effects of leading edge protuberances on airfoil performance. In *36th AIAA fluid dynamics conference and exhibit* (p. 2868).

Malipeddi, A., Mahmoudnejad, N., & Hoffmann, K. (2012). Numerical analysis of effects of leading-edge protuberances on aircraft wing performance. *Journal of Aircraft, 49*(5), 1336–1344.

Masud, M. H., Naim-Ul-Hasan, Arefin, A. M. E., & Joardder, M. U. (2017). Design modification of airfoil by integrating sinusoidal leading edge and dimpled surface. In *AIP conference proceedings*. https://doi.org/10.1063/1.4984677

Masud, M. H., La Mantia, M., & Dabnichki, P. (2022). Estimate of Strouhal and Reynolds numbers for swimming penguins. *Journal of Avian Biology*. Wiley Online Library, *2022*(2), e02886.

Miklosovic, D. S., Murray, M. M., Howle, L. E., & Fish, F. E. (2004). Leading-edge tubercles delay stall on humpback whale (Megaptera novaeangliae) flippers. *Physics of Fluids, 16*(5), 39–42. https://doi.org/10.1063/1.1688341

Wang, T., Feng, L.-H., & Li, Z.-Y. (2021). Effect of leading-edge protuberances on unsteady airfoil performance at low Reynolds number. *Experiments in Fluids*. Springer, *62*(10), 1–13.

Watts, P., & Fish, F. (2001). The influence of passive, leading edge tubercles on wing performance. In *Proceedings of the twelfth international symposium on unmanned untethered submersible technology (UUST)*. Autonomous Undersea Systems Institute.

Leading and Trailing Edge Configuration for Distributed Electric Propulsion Systems

Mithun Eqbal, Matthew Marino, and Patrick Farley

Nomenclature

BLDC	Brushless direct current
BLI	Boundary layer ingestion
DA	Drag from the airframe
DEP	Distributed electric propulsion
ESC	Electronic speed control
GUI	Graphic user interface
I_R	Ingestion ratio
P_L	Power of the leading edge
P_T	Power of the trailing edge
P_{useful}	Useful power
PSC	Power saving coefficient
Re	Reynolds number
RPAS	Remotely piloted aircraft systems
T	Thrust
W	Watt
∂	Boundary layer length
u_J	Propeller airflow
u_w	Airframe drag
u_∞	Free stream velocity
u_1 and u_2	Airstream velocity
x	Length of the cross-section

M. Eqbal (✉) · M. Marino
RMIT University, Melbourne, Australia
e-mail: mithun.eqbal@rmit.edu.au; matthew.marino@rmit.edu.au

P. Farley
Deutsche Zentrum für Luft- und Raumfahrt e. V. (DLR), Weßling, Germany
e-mail: partick.farley@dlr.de

121

1   Introduction

DEP (distributed electric propulsion) and BLI (boundary layer ingestion) provide a significant advantage on the aerodynamic efficiency of the aircraft (Davies et al., 2013; Hendricks, 2018; Plas et al., 2007; Rothhaar et al., 2014; Zhang et al., 2019). Studies were conducted, placing multiple propellers on leading-edge using advanced computational fluid dynamics (CFD). It is found that there are benefits like an increase in lift and reduction in drag; however, the advantages depend on the location of the propeller (Huang et al., 2018; Sinnige et al., 2019; Wang et al., 2018, 2019). Based on this, various leading-edge DEP concept prototypes are built and tested (Berg et al., 2015; Borer et al., 2016; Gohardani et al., 2011; Ko et al., 2003; Wang et al., 2018, 2019). Previous research has shown that a turbofan and boundary layer propulsion system on the wing's trailing edge capitalizes on BLI (Hall et al., 2017; Plas et al., 2007; Zhang et al., 2019) has demonstrated significant increases in propulsive efficiency. Combining both concepts proposes a new question: can an increase of propulsive efficiency be achieved by placing the propeller on the trailing edge of the wing to capitalize on the aerodynamic benefits of BLI? Few 2D CFD studies conducted similar comparisons and have shown improved propulsive efficiency but have created different losses in the process (El-Salamony & Teperin, 2017; Mantič-Lugo et al., 2013; Valencia et al., 2020). No conclusive wind tunnel or experimental studies have been conducted at this stage using propeller systems.

1.1   Theoretical Explanation

There is a connection between BLI and the benefits of the trailing edge, which leads to speed (Hall et al., 2017). The primary advantage of BLI is re-energizing the aircraft's wake, capitalizing on low-speed boundary layers, and enabling more efficient thrust when the flow is accelerated to generate propulsion (Tiseira Izaguirre et al., 2021). These two idealized solutions are shown in Fig. 1, where the flow is increased for a propeller situated in the front. As the flow traverses the top and bottom surfaces of the wing, a portion of its velocity is lost to frictional forces. This loss of velocity is transmitted to the surfaces of the wings and results in friction drag. This energy transfer is called energy recovery. Energy transmission and energy recovery are distinct for a propeller located on the wing's trailing edge. The wing is exposed to unbroken flow; however, when a boundary layer of flow builds across the surfaces, the momentum of the flow is diminished, similar to the preceding illustration. This boundary layer is composed of slower-moving flow; hence, when exposed to the propellor, it is propelled much faster than the surrounding flow, which travels at freestream velocity. As a result, boundary layer flow offers a mechanism for higher thrust. The slower flow is accelerated at more significant rates, therefore recovering a portion of the energy lost due to friction. This may be discussed in further detail using propulsion theory (Plas, 2006).
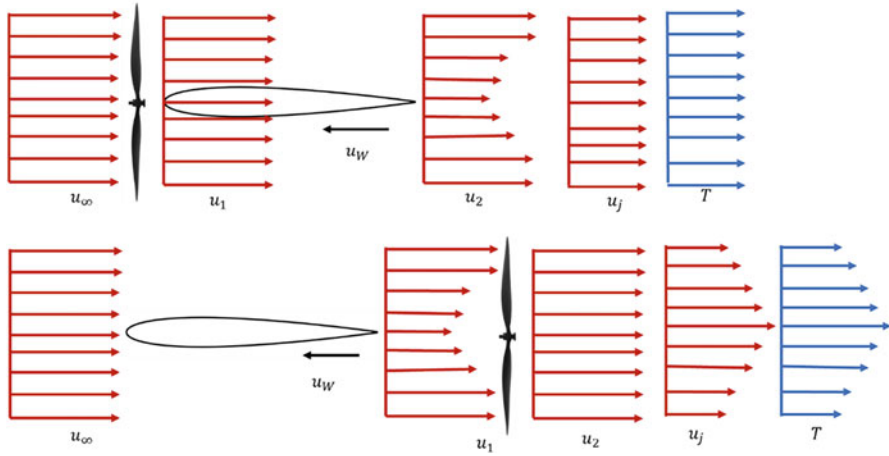
Fig. 1 Aerofoil with the leading edge and trailing edge with velocity

Where, u_∞ is the free stream velocity, u_J is the propeller air flow, T is the thrust, u_w is the airframe drag, u_1 and u_2 are airstream velocities through different phases.

Figure 1 shows that the flow is entering the propeller at freestream velocity (u_∞). The propeller accelerates the airflow to a velocity u_j, creating excess momentum to balance the momentum deficit (Plas, 2006). The momentum excess created by the propeller on the leading edge is equal to the momentum deficit of the airframe and is clearly defined by Plas (2006).

Due to the drag from the airframe D_A

$$T_p = m_* \left(u_j - u_\infty\right) = \frac{T}{2} \left(u_\infty - u_w\right) = D_A \tag{1}$$

The rate of mechanical energy added P_{Added} given to the flow by the propeller is provided by

$$P_{\text{Added},L} = \frac{m_*}{2} \left(u_j^2 - u_\infty^2\right) = \frac{T}{2} \left(u_j + u_\infty\right) \tag{2}$$

The power required for the flight (P_{useful}) is given by

$$P_{\text{useful}} = D_A u_\infty = m_* (u - u_\infty) u_\infty \tag{3}$$

Suppose all the boundary layer is ingested and the propeller accelerates the wake back to freestream. The force provided by the propeller is

$$T_p = m_* \left(u_j - u_\infty \right) = m_* \left(u_\infty - u_w \right) = D_A \tag{4}$$

The rate of energy given to the flow by the propeller, $P_{\text{added, BLI}}$, is

$$P_{\text{added},T} = \frac{m_*}{2} \left(u_j{}^2 - u_w{}^2 \right) = \frac{m_*}{2} \left(u_j{}^2 - u_\infty{}^2 \right) = \frac{F}{2} \left(u_w + u_\infty \right) \tag{5}$$

The power required for flight is the same as when the propeller is on the leading edge

$$P_{\text{useful}} = D_A u_\infty = m_* \left(u_j - u_\infty \right) u_\infty \tag{6}$$

Since $u_i > u_w$, comparison of Eqs. 4 and 5 shows,

$$P_{\text{added},L} > P_{\text{added},T} \tag{7}$$

It shows trailing edge needed less power to sustain the same drag on the airframe due to BLI.

This can be explained as follows: for a less specific force, less power needs to be added to a flow that enters the propeller with a lower velocity. Consider a flow that enters a propeller at velocity u_1 and exits at a velocity u_2. The thrust created by the propeller is:

$$T = m_*(u_2 - u_1) = m_* \Delta u \tag{8}$$

The power put to the flow is

$$P = \frac{m_*}{2} \left(u_2{}^2 - u_1{}^2 \right) = T \frac{u_1 + u_2}{2} = T \left(u_1 + \frac{\Delta_u}{2} \right) \tag{9}$$

For a constant mass flow and constant propulsive force, Δ_v is constant. A decrease in u_1 results in a decrease in power. That means for lower velocity, in the case of BLI fluid in trailing edge, less power input can create the same propulsive force.

To simplify, all this data can be written as power saving coefficient (PSC) as described by Blumenthal et al. (2019), Budziszewski and Friedrichs (2018), Gray et al. (2018) and Hall et al. (2017):

$$\text{PSC} = \frac{P_L - P_T}{P_L} \tag{10}$$

Where P_L is the leading edge and P_T is the trailing edge which has the direct influence on BLI.

Similarly thrust and power can be simplified as

$$T = m_* (u_{\text{out}} - u_{\text{in}}) = m_* (\Delta_u) \tag{11}$$

$$P = \frac{1}{2} m_* \left(u_{\text{out}}^2 - u_{\text{in}}^2\right) = \frac{1}{2} m_* (\Delta_u)) \tag{12}$$

In terms of propulsion efficiency, it can be defined as

$$n_p = \frac{u_\infty}{u_j + u_{in}} \tag{13}$$

2 Method

The wind tunnel used for the experiment is given in Fig. 2. It's a closed-circuit wind tunnel with a maximum speed of 140 km/h powered by a 380 kW DC motor. The tunnel has very low noise as it consists of anechoic turning vanes. Airflow can be changed using the speed controller located in the control room. The tunnel is equipped with an MKS differential pressure measuring system. The pitot static tube can be connected to calibrate the flow speed at different locations in the test section. The air temperature within the wind tunnel can be captured with the equipment provided.

An RC benchmark dynamometer 1520 (Benchmark, 2019) in Fig. 3 is used to measure the test power as it is designed for BLDC motor.

Fig. 2 Picture of the wind tunnel

Fig. 3 RC benchmark mark
dynamometer 1520
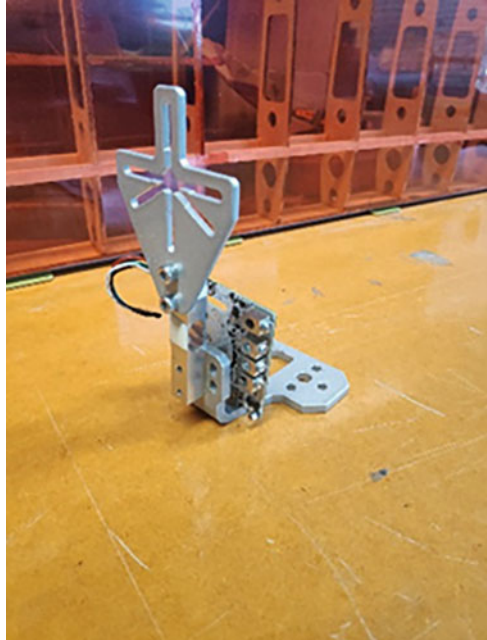
A constant supply power source is used to power the motor. The motor is controlled through electric speed control (ESC), where the ESC is throttled manually by using the graphics software interface (GUI) (Benchmark, 2019). An arbitrary velocity of 50 km/h is used to test the experiment. At the velocity of 50 km/h, the tip velocity of the propeller is under Mach 1, which is an essential consideration for the actuator disk theory so that the results can be verified without anomalies. Similarly, there is no propeller interference. If the interaction is there, the results need to consider aerodynamics and power integration, which are of future interest. Also, it needs more power and propeller integration factors, which gives a higher margin of error. Additionally, the test is only done for a zero angle of attack to reduce the complexities associated, but one angle of attack is enough to prove the test result (Stoll et al., 2014).

A brushless direct current (BLDC) 1650 KV motor as in Table 1 and three propeller configurations as given in Table 2 are studied to effectively determine the area's impact on power, thrust, and propulsive efficiency.

The propeller arrangement is given in Figs. 4 and 5. The trailing edge propeller is arranged not on the edge of the wing but close enough to conceal the motor inside the wing to avoid extra drag for the arrangement, more explanation is given in Sect. 3.

Table 1 Details of the BLDC motor and ESC used for testing

Parameters	Number
Dimension (motor)	28 mm × 25 mm
Weight	49 g
KV	1650 rpm/V
Voltage	7.2 v ~ 11.1 v (2 s ~ 3 s)
Max power Max current	180 W 17.5 A
Dimension (ESC)	30 × 17.5 × 10 mm
Weight	14.5 g
Voltage	2 ~ 4 S (8.4 ~ 16.8 V)
Max current	20 A

Table 2 Details of the propeller used for testing

| Propeller	Type and specifications	Brand
7x6	2 blade plastic with 0.50 inch hub diameter, 0.32 hub thickness, ¼ inch shaft diameter and 0.18 oz weight	APC 7x6 slow flyer propeller
8x6	2 blade plastic with 0.50 inch hub diameter, 0.30 inch hub thickness, ¼ inch shaft diameter, and 0.25 oz weight	APC 8x6 slow fly propeller
9x6	2 blade plastic with 0.50 inch hub diameter, 0.30 inch hub thickness, ¼ inch shaft diameter, and 0.32 oz weight.	APC 9x6 slow fly propeller
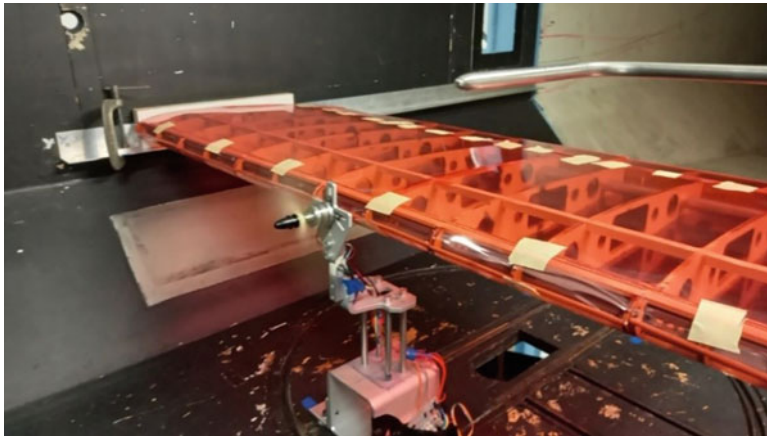
Fig. 4 Wind tunnel testing setup for a leading-edge test

2.1 Calculation of Power Saving Coefficient and Ingestion Ratio

The explanation of power saving is defined in Eq. 10 (Gray et al., 2018) as an effect of BLI. A thrust setting is chosen to explain the power saving coefficient at a specific point. Similarly, the effective area of the propeller can be defined in the trailing edge
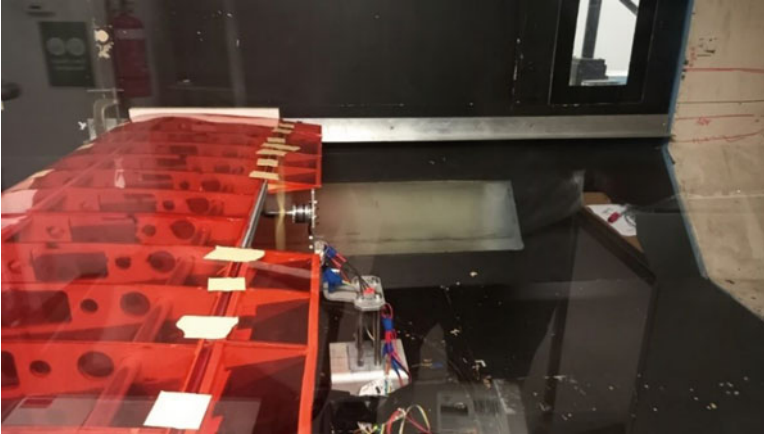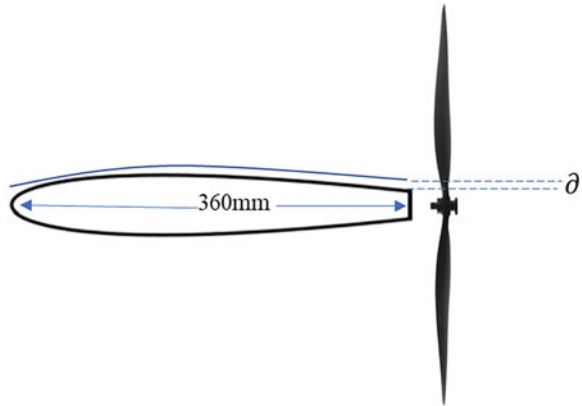
Fig. 5 Wind tunnel testing setup for a trailing-edge test

Fig. 6 Boundary layer

arrangement. Figure 6 gives a cross-section representation of the aerofoil used for the experiment and propeller.

A typical UAS flight occurs at low Reynolds Numbers and within the atmospheric boundary layer. This flight regime increases the probability of a turbulent boundary layer formation. A turbulent boundary layer model is assumed and is likely to produce a conservative estimate of the growth of the boundary layer for a typical UAS flight. From Itoh et al. (2005), the length of the boundary layer can be explained by Eq. (14)

$$\partial = \frac{0.37x}{\mathrm{Re}^{0.2}} \tag{14}$$

Where, ∂ is the boundary layer length, x is the length of the cross section, where this is chord length and Re is the Reynolds number, where it is defined as
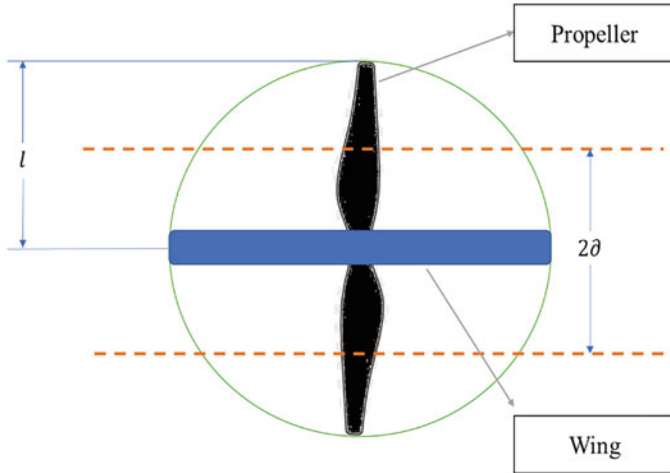
Fig. 7 Area of propeller relative to wing

$$\text{Re} = \frac{\rho\, u\, L}{\mu} \tag{15}$$

From Eq. (15), the boundary layer can be calculated, and the length of the propeller is known from the manufacturers data (Table 2).

As given in Fig. 7 and with known data, the area of propeller and the boundary layer can be calculated. This is defined as ingestion ratio (I_R).

$$I_R = \frac{\text{Area of the Boundary layer}}{\text{Area of the Propeller}} \tag{16}$$

From Eqs. 10, 11, 12, 13, 14, 15, and 16, the factors power saving coefficient (PSC) and ingestion ratio (I_R) are defined. These equations form a base to explain the performance of the experimental analysis or leading and trailing edge. The drag created by the leading edge and trailing edge is different, which needs an explanation not to add more drag to the arrangement.

3 Drag Estimation and Motor Arrangement

One of the significant factors to consider is whether the installation arrangement needed for anchoring the motor on the trailing edge can create additional drag and overrun the gains made by trailing edge propulsive efficiency. However, this can be easily solved by designing the installation mount, as in Fig. 8.

Figure 8 shows the dimension of the aerofoil used for the testing and the electric motor's measurement. The length of the aerofoil near the trailing edge at the
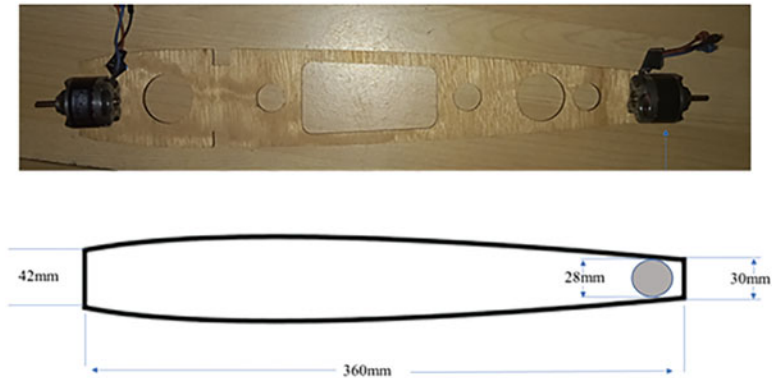
Fig. 8 Aerofoil and motor arrangement

outermost tip is 30 mm, while the diameter of the motor is 28 mm. So, the motor can be easily concealed inside the aerofoil to avoid drag from the installation with some proper mount design. The experimental testing of the drag is for future work where the aerofoil coupled to the motor will be tested in the wind tunnel.

Previously, Junzi described the use of the drag estimation in open aerodynamic model, where he deliberately avoided utilizing manufacturer data (unless they are freely accessible) and looked for another method to estimate the drag, i.e., the actual energy model often represents energy change by multiplying every force by the corresponding direction's speed.

4 Results and Discussion

In this section, the experiment results are discussed in more detail. The issue is simplified by reflecting on the assumptions that were made in an attempt to make it more manageable. Finally, we also discuss the restrictions and ambiguities of the offered approaches. This study aims to investigate the impact on power savings and advancements in propellant efficiency that would result from mounting the propeller on the trailing edge of the wing rather than the leading edge of the wing. Using a brushless direct current (BLDC) engine and various propeller configurations, a scaled-down remotely piloted aircraft systems (RPAS) wing is put through its paces in a wind tunnel. The impact that the change in propeller size has on the amount of electricity that may be saved is referred to as the ingestion ratio (IR), which is a brand new word. The PSC is connected to the reduced intake velocity of the trailing edge, which helps to boost the propulsive efficiency of the trailing arrangement efficiently. It is essential to have a solid understanding that every parameter is treated as a random variable (described by probability density functions) in the hierarchical model that has been provided. Testing uses almost all of the
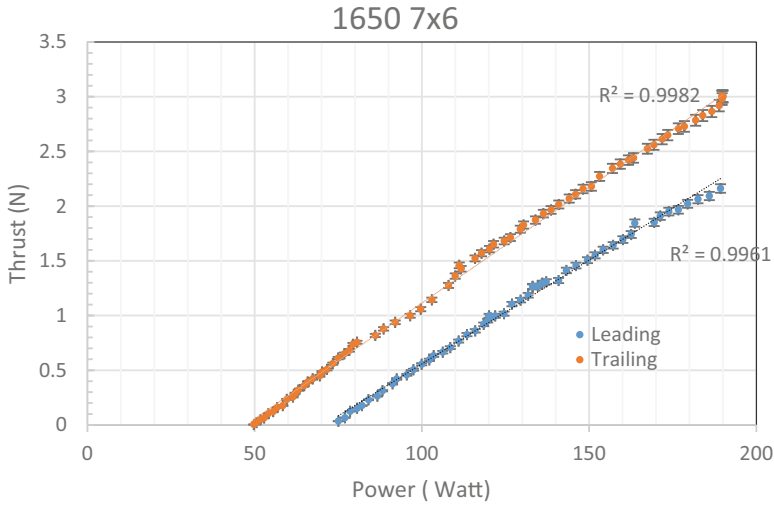
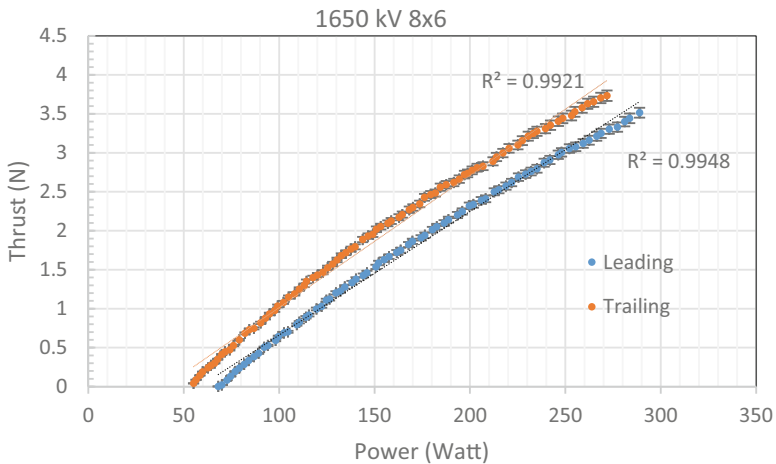**Fig. 9** Thrust by power for a 7x6 propeller configuration

Fig. 10 Thrust by power for an 8x6 propeller configuration

settings of the BLDC motor and the ESC. The tests conducted with various propeller configurations were represented as multi-dimensional probability density functions.

In addition, there is a downward tendency in the PSC when there is a rise in the propeller's surface area. This helps to explain why the ingestion ratio offered by the smaller wing area is more significant than that provided by the larger wing area since the boundary layer directly affects the smaller wing area.

The experiment results for the 7x6, 8x6, and 9x6 for the 50 km/h wind setting are given in Figs. 9, 10, and 11, respectively.
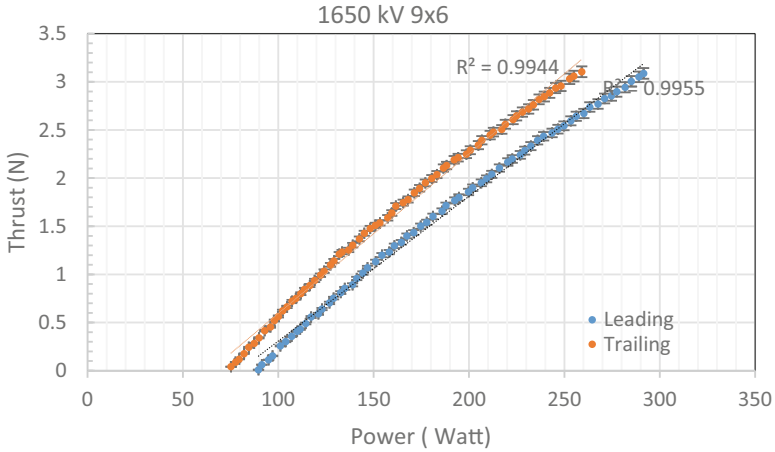
Fig. 11 Thrust by power for a 9x6 propeller configuration

Table 3 Summary of the test results for the test with different propeller configuration

Propeller type for thrust 1.6–1.8 N	Ingestion ratio	PSC	Power savings (W)	Propulsive efficiency savings
7x6	7.02	0.22	33.98	5.80
8x6	5.37	0.15	29.36	3.82
9x6	4.32	0.13	24.70	2.81

In all the cases, the thrust and power didn't start from zero. This is because of electrical losses, idle power as well as the thrust stand only starts recording at a specific thrust to overcome the drag associated with the flowing wind.

Figures 9, 10, and 11 show a decrease in power consumption when the propeller is placed on the trailing edge throughout the throttle setting. An effective reduction in power consumption is evident. Now using the Eqs. 13, 14, 15, and 16, the ingestion ratio, PSC, power savings, and propulsive efficiency are calculated from the experiment for a thrust setting between 1.6 and 1.8 N and are tabulated in Table 3.

As explained in Eq. 10, the PSC is related to the lower inlet velocity for the trailing edge and effectively increases the propulsive efficiency for the trailing arrangement. Also, there is a reducing trend in the PSC with increase in propeller area. This explains the ingestion ratio provides a higher the ingestion ratio provided by the smaller wing area, which is directly affected by the boundary layer.

5   Conclusion

The experiment demonstrated that mounting the propeller on the trailing edge of the wing results in greater propulsive efficiency and a reduction in the amount of power used by taking advantage of BLI. This has significant repercussions for aircraft that use distributed electric propulsion. It is validated on various BLDC motor and propeller combinations using wind tunnel testing at a predetermined speed. A new factor ingestion ratio has been created to describe the effect ratio of boundary layer and propeller area on trailing edge efficiency. For a single motor propeller arrangement, the ingestion ratio may contribute to a power savings of 24.7% and propulsive efficiency of 5.8%. The higher the ingestion ratio, the more significant the improvement in propulsive efficiency and power savings.

References

Benchmark, R. (2019). https://cdn-docs.rcbenchmark.com/datasheets/series-1520/Datasheet-RCbenchmark-Series-1520.pdf

Berg, F., Palmer, J., Miller, P., Husband, M., & Dodds, G. (2015). HTS electrical system for a distributed propulsion aircraft. *IEEE Transactions on Applied Superconductivity, 25*(3), 1–5.

Blumenthal, B. T., Elmiligui, A. A., Geiselhart, K. A., Campbell, R. L., Maughmer, M. D., & Schmitz, S. (2019). Computational investigation of a boundary-layer ingesting propulsion system for the common research model. *Journal of Aircraft, 55*(3), 1141–1153.

Borer, N. K., Patterson, M. D., Viken, J. K., Moore, M. D., Bevirt, J., Stoll, A. M., & Gibson, A. R. (2016). Design and performance of the NASA SCEPTOR distributed electric propulsion flight demonstrator. In *16th AIAA aviation technology, integration, and operations conference* (p. 3920).

Budziszewski, N., & Friedrichs, J. (2018). Modelling of a boundary layer ingesting propulsor. *Energies (Basel), 11*(4), 708.

Davies, K., Norman, P., Jones, C., Galloway, S., & Husband, M. (2013). *A review of turboelectric distributed propulsion technologies for N+ 3 aircraft electrical systems* (pp. 1–5). IEEE.

El-Salamony, M., & Teperin, L. (2017). 2D numerical investigation of boundary layer ingestion propulsor on Airfoil. In *7th European conference for aeronautics and aerospace sciences*, Milan, Italy.

Gohardani, A. S., Doulgeris, G., & Singh, R. (2011). Challenges of future aircraft propulsion: A review of distributed propulsion technology and its potential application for all electric commercial aircraft. *Progress in Aerospace Sciences, 47*(5), 369–391.

Gray, J. S., Mader, C. A., Kenway, G. K. W., & Martins, J. R. R. A. (2018). Modeling boundary layer ingestion using a coupled aeropropulsive analysis. *Journal of Aircraft, 55*(3), 1191–1199.

Hall, D. K., Huang, A. C., Uranga, A., Greitzer, E. M., Drela, M., & Sato, S. (2017). Boundary layer ingestion propulsion benefit for transport aircraft. *Journal of Propulsion and Power, 33*(5), 1118–1129.

Hendricks, E. S. (2018). *A review of boundary layer ingestion modeling approaches for use in conceptual design*. NASA Glenn Research Center.

Huang, X., Zhao, X., & Huang, J. (2018). A simplified model for predicting the propeller-wing interaction. *Aircraft Engineering and Aerospace Technology, 90*(1), 196–201.

Itoh, M., Tamano, S., Yokota, K., & Ninagawa, M. (2005). Velocity measurement in turbulent boundary layer of drag-reducing surfactant solution. *Physics of Fluids (1994), 17*(7), 1–9.

Ko, A., Schetz, J., & Mason, W. (2003). Assessment of the potential advantages of distributed propulsion for aircraft. In *XVI international symposium on air breathing engines*, Cleveland, Ohio.

Mantič-Lugo, V., Doulgeris, G., & Singh, R. (2013). Computational analysis of the effects of a boundary layer ingesting propulsion system in transonic flow. *Proceedings of the Institution of Mechanical Engineers, Part G: Journal of Aerospace Engineering, 227*(8), 1215–1232.

Plas, A. (2006). *Performance of a boundary layer ingesting propulsion system*. Master of Science thesis, Massachusetts Institute of Technology. https://dspace.mit.edu/handle/1721.1/35568

Plas, A., Crichton, D., Sargeant, M., Hynes, T., Greitzer, E., Hall, C., & Madani, V. (2007, January). Performance of a boundary layer ingesting (BLI) propulsion system. In *AIAA 2007–450. 45th AIAA aerospace sciences meeting and exhibit*.

Rothhaar, P. M., Murphy, P. C., Bacon, B. J., Gregory, I. M., Grauer, J. A., Busan, R. C., & Croom, M. A. (2014). NASA Langley distributed propulsion VTOL tiltwing aircraft testing, modeling, simulation, control, and flight test development. In *14th AIAA aviation technology, integration, and operations conference* (p. 2999).

Sinnige, T., Stokkermans, T. C. A., Arnhem, N., & Veldhuis, L. L. M. (2019). Aerodynamic performance of a wingtip-mounted tractor propeller configuration in windmilling and energy-harvesting conditions. In *AIAA aviation 2019 forum* (p. 1624105890).

Stoll, A. M., Bevirt, J., Moore, M. D., Fredericks, W. J., & Borer, N. K. (2014). Drag reduction through distributed electric propulsion. In *Aviation technology, integration, and operations conference*, 16–20 June 2014, Atlanta, Georgia.

Tiseira Izaguirre, A. O., García-Cuevas González, L. M., Quintero Igeño, P., & Varela Martínez, P. (2021). Series-hybridisation, distributed electric propulsion and boundary layer ingestion in long-endurance, small remotely piloted aircraft: Fuel consumption improvements. *Aerospace Science and Technology, 2021*, 107227.

Valencia, E., Alulema, V., Rodriguez, D., Laskaridis, P., & Roumeliotis, I. (2020). Novel fan configuration for distributed propulsion systems with boundary layer ingestion on an hybrid wing body airframe. *Thermal Science and Engineering Progress, 18*, 100515. ISSN 2451-9049.

Wang, H., Zhou, Z., Xu, X., & Zhu, X. (2018). Influence analysis of propeller location parameters on wings using a panel/viscous vortex particle hybrid method. *The Aeronautical Journal, 122*(1247), 21–41.

Wang, K., Zhou, Z., Zhu, X., & Xu, X. (2019). Aerodynamic design of multi-propeller/wing integration at low Reynolds numbers. *Aerospace Science and Technology, 84*, 1–17.

Zhang, J., Kang, W., & Yang, L. (2019). Aerodynamic benefits of boundary layer ingestion for distributed propulsion configuration. *Aircraft Engineering and Aerospace Technology, 91*(10), 1285–1294.

Cost and Weight Optimization of Recyclable Honeycomb Sandwich Panels

Sanjeev Rao and Jeremy Chen

Nomenclature

φ	Relative density of the core
FC	Facesheet cracking
IB	Intracellular buckling
CY	Cell wall yielding
CB	Core buckling

1 Introduction

A typical sandwich panel construction consists of thin and stiff facings bonded to a relatively thick, low-density core. A wide variety of core materials (aluminum, Kevlar, polypropylene, etc.) are available, each having its own advantages and disadvantages. Sandwich panels are commonly used in flexural applications where they behave similar to an I-beam, where the facings similar to the flanges sustain the bending stresses and the core similar to the webbing takes the shear. Using a weak core assumption (Wicks & Hutchinson, 2004), common modes of failures observed in such panels under flexural loading are faceplate fracture, shear failure in the core, wrinkling of the faceplate into the core or outward due to delamination at their

S. Rao (✉)

Department of Aerospace Engineering, Khalifa University of Science and Technology, Abu Dhabi, UAE
e-mail: sanjeev.rao@ku.ac.ae

J. Chen
Department of Mechanical Engineering, University of Auckland, Auckland, New Zealand
e-mail: j.chen@auckland.ac.nz

interface. Analytical closed form solutions for each of the modes are well established and are readily available for the designers (Gibson, 2005).

Though several materials and core configurations are available, the failure modes for sandwich panels are more or less similar with their occurrence depending primarily on the relative density of the core (Ashby et al., 2000). The optimization of sandwich panels and plates with various cores are usually estimated based on their failure modes, such as the performance optimization of metallic sandwich plates with truss cores by Wicks and Hutchinson (2001, 2004), design of metallic sandwich panels with textile cores (Zok et al., 2003), pyramidal truss cores by Zok et al. (2004), and corrugated cores by Valdevit et al. (2006). Rathbun et al. (2005) developed a general methodology for the weight optimization of metallic sandwich panels subjected to flexural loads. Zhang et al. (2006) showed that the optimized performances of the prismatic cores are comparable to that of a honeycomb core. More recently, Banerjee et al. (2010) have derived expressions to optimize shear strength of reinforced honeycomb core materials. Extensive study of various cores and sandwich structures can be found in the monograph of Zenkert (1995) and review article by Noor et al. (1996). The main goal of this work is to develop a technique to maximize the strength to weight ratio of the honeycomb materials under flexural loading. The methodology developed in this study is based on the failure criteria derived in terms of relative density of the cell wall material of the core, differing from the existing literature where researchers have focussed on the optimization of sandwich panel as a whole.

The aim of the panel optimization is to predict the lowest weight of the sandwich panels and the corresponding values of the geometrical parameters, when the panel is subjected to a prescribed bending load. Therefore, the objective function for the optimization is the panel self-weight or panel cost, and the failure criteria are the constraints. The failure criteria are derived considering the core material to be either isotropic or specially orthotropic (as a result of fiber reinforcement). The optimum weight of the sandwich panel beam can then be obtained at the confluence of any four failure criteria in a four parameter optimization. Five failure criteria in total are chosen, and five different combinations of four failure criteria are established which are evaluated to obtain five optimal weight values, of which one is the global optimum.

2 Geometrical Parameters of a Honeycomb

A schematic of a unit cell is shown in Fig. 1 as indicated in dotted red triangle. The hexagonal core consists of cell walls of length 'l,' thickness 't,' and height 'H,' and as two half hexagonal profiles are bonded to make a complete cell, two cell walls are of the thickness '$2t$'. As the hexagonal cores consisted of symmetrical hexagonal cells that are periodic, they can be represented as a single unit cell with cell wall length '$l/2$', thickness 't' and '$2t$' of the single and double cell wall, respectively which can be translated to form a complete core.

Fig. 1 Honeycomb cell and associated geometric parameters
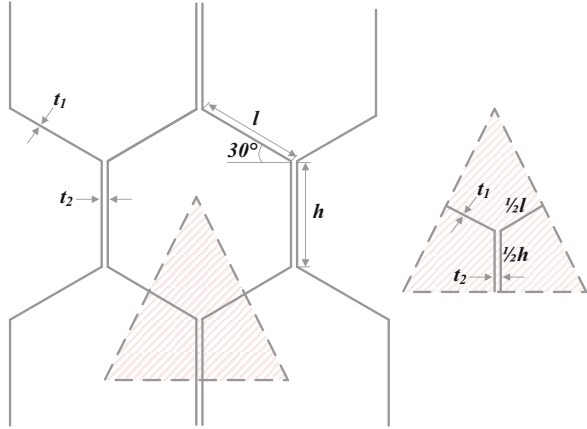
Therefore, the effective area of a honeycomb unit cell can be expressed as the area of the triangle shown in Fig. 1.

$$A_{\text{eff}} = (h + l \sin \theta)l \cos \theta \tag{1}$$

and the effective area of the cell walls is:

$$\frac{h}{2} t_2 + l t_1 \tag{2}$$

Let ρ^* and ρ_s be the densities of the honeycomb core and the solid from which the honeycomb is made of, respectively. The equation for equating the mass per unit thickness of the unit cell and the cell walls is given as

$$[(h + l \sin \theta)l \cos \theta] \rho^* = \left[\frac{h}{2} t_2 + l t_1\right] \rho_s \tag{3}$$

and can be expressed in the form

$$\varphi = \frac{\rho^*}{\rho_s} = \frac{t_1}{l} \left[\frac{\left(\frac{h}{l}\right)\left(\frac{t_2}{t_1}\right) + 2}{2\left(\left(\frac{h}{l}\right) + \sin \theta\right) \cos \theta} \right] \tag{4}$$

where, h/l, θ, t_1/l, and t_2/t_1 are the non-dimensional parameters that define the geometry of a hexagonal cell and φ is the relative density of the honeycomb core (Gibson & Ashby, 1997; Gibson et al., 1982).

3   Failure Criteria Establishment

Six failure criteria have been considered in the analysis of a sandwich beam under four-point bending (quarter-span) as shown in Fig. 2. The derivations for these are covered in the following sections. It is assumed that the facesheets are much thinner and stiffer than the core ($t_f/t_c \leq 0.1$, $E_f/E_c \geq 10$).

Five non-dimensional parameters were obtained using a method outlined by White to relate a failure load index of the beam to several geometric parameters:

$$
\begin{aligned}
\text{Load index} \quad & \Pi_1 = \frac{2P_{cr}}{LE_f} \\
\text{Facesheet thickness} \quad & \Pi_2 = \frac{t_f}{L} \\
\text{Core thickness} \quad & \Pi_3 = \frac{t_c}{L} \\
\text{Cellwall thickness} \quad & \Pi_4 = \frac{t_{\text{cell}}}{L} \\
\text{Core relative density} \quad & \Pi_5 = \frac{\rho^*}{\rho_s}
\end{aligned}
\tag{5}
$$

3.1   Facesheet Cracking (FC)

The normal stress generated in the facesheets under four-point bending (quarter span) can be expressed in terms of the non-dimensional parameters in (6). Failure will not occur as long as the inequality is satisfied.

$$
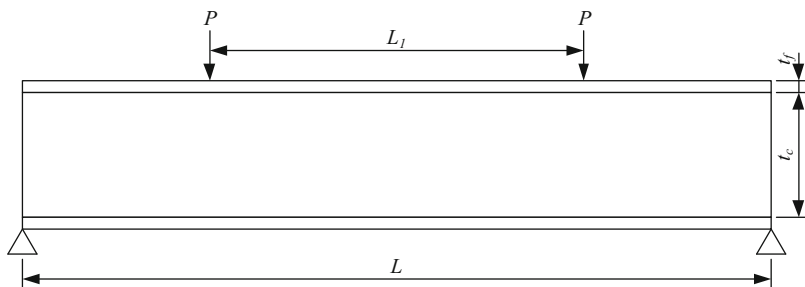\frac{1}{8}\Pi_1\left(\frac{E_f}{\sigma_{f,cr}}\right)(\Pi_2\Pi_3)^{-1} \leq 1
\tag{6}
$$

Fig. 2 Four point (quarter-point) bending scheme of the sandwich panel considered in this study

3.2 Intracellular Buckling (IB)

The stress at which intracellular buckling occurs is given in the following equation:

$$\frac{\Pi_1 \Pi_4^2 \left(1 - \nu_f^2\right)}{9\Pi_2^3 \Pi_3 \Pi_5^2} \leq 1 \tag{7}$$

3.3 Cell Wall Shear Yielding (CY)

Cell wall shear yielding occurs when the shear stress in an individual cell wall exceeds the shear strength of the cell wall material. Thus, the failure load of the beam for this failure mode is given by

$$\frac{2\Pi_1}{3\Pi_3 \Pi_5} \frac{E_f}{\tau_s} \leq 1 \tag{8}$$

3.4 Cell Wall Shear Buckling (CB)

The in-plane shear load at which a cell wall undergoes Euler's buckling as per elastic buckling of a plate under shear. This failure criterion can then be expressed in terms of the non-dimensional parameters for isotropic material as (8):

$$\left(\frac{512}{27}\right) \frac{\Pi_1}{\Pi_3 \Pi_5^3} \left(\frac{E_f}{E_s}\right) \frac{(1 - \nu^2)}{K\pi^2} \leq 1 \tag{9}$$

A method for calculating the shear buckling load of a simply supported orthotropic plate has been presented by Leissa (1980), using results from Fogg (1981). This method uses two non-dimensional parameters, provided in (8), to calculate the value of the shear buckling parameter, as given in (10), in terms of non-dimensional parameters in (11):

$$\theta = \frac{\sqrt{D_{11}D_{22}}}{D_{12} + 2D_{66}}, B = \frac{l_{\text{cell}}}{t_c} \left(\frac{D_{11}}{D_{22}}\right)^{\frac{1}{4}} \tag{10}$$

$$P_{cr} = \frac{2}{\sqrt{3}} \frac{k_s \pi^2 \left(D_{11} D_{22}^3\right)^{\frac{1}{4}}}{l_{\text{cell}}^3} t_c \tag{11}$$

where,

$$k_s = 3.32 + 2.17\left(\frac{1}{\theta}\right) - 0.163\left(\frac{1}{\theta}\right)^2 + B^2\left(1.54 + 2.36\left(\frac{1}{\theta}\right) + 0.1\left(\frac{1}{\theta}\right)^2\right) \text{ and}$$

$$\tau_{xy}^* = \frac{k_s \pi^2 \left(D_{11} D_{22}^3\right)^{\frac{1}{4}}}{t_{\text{cell}} l_{\text{cell}}^2}$$

$$\Pi_1 \left(\frac{512}{27\pi^2}\right) \left(\frac{E_f}{\left(Q_{11} Q_{22}^3\right)^{\frac{1}{4}}}\right) \left(A\Pi_3\Pi_5^3 + C\Pi_3^{-1}\Pi_4^2\Pi_5\right)^{-1} \le 1 \tag{12}$$

where,

$$A = 3.32 + 2.17(1/\varnothing) - 0.163\left(1/\varnothing\right)^2$$

$$C = \frac{64}{27}\sqrt{\frac{Q_{11}}{Q_{22}}\left(1.54 + 2.36(1/\varnothing) + 0.1\left(1/\varnothing\right)^2\right)}$$

$$\varnothing = \frac{\sqrt{Q_{11}Q_{22}}}{Q_{12} + 2Q_{66}}$$

4 Optimization Procedure

The optimum weight of the sandwich beam can be obtained at the confluence of any four failure criteria in a four parameter optimization. As there are five failure criteria in total, there are five different combinations of four failure criteria which need to be evaluated to obtain five optimal weight values, of which one is the global optimum. The five combinations to be evaluated are summarized in Table 1, with the equations describing the different failure modes.

Objective functions, defined to be either a weight or cost index (chosen depending on whether cost or weight is to be optimized), are given by

$$w = 2\rho_f\Pi_2 + \rho_s\Pi_3\Pi_5 \left[\frac{\text{kg}}{\text{m}^3}\right] \tag{13}$$

$$c = 2c_f\rho_f\prod_2 + c_s\rho_s\prod_3\prod_5 \left[\text{USD/m}^3\right] \tag{14}$$

Table 1 Combinations of failure criteria used to obtain optimal parameters

1. FC-FW-IB-CY	2. FC-FW-IB-CB	3. FC-FW-CY-CB	4. FC-IB-CY-CB	5. FW-IB-CY-CB

5 Material Properties

Aluminum (5052-H34 alloy) was chosen as the facesheet material to be paired with all core materials (Table 2).

Unreinforced and reinforced polypropylene was considered as a core material. However, in this study, only the polypropylene core has been evaluated (Table 3).

Closed form solutions for the in-plane shear strength of a fiber-reinforced polymer are not available. As such, the shear strength of all cell wall materials has been assumed to be 0.6 times the tensile strength of the material.

6 Results

6.1 Manual Optimization

The optimal parameters for each combination of four failure modes are first computed using the equations provided along with the weight index, Table 4.

Once the four optimal parameters have been determined for each combination of four failure modes, the fifth failure mode not included in each combination must be evaluated to assess the overall feasibility of the solution. Furthermore, the ratio of the facesheet and core thicknesses must be evaluated to ensure it does not exceed 0.1. The results for this step are shown in Table 5.

Based on the results of Tables 4 and 5, combination 2 is identified as the optimal solution that provides the lowest weight index and satisfies all failure criteria.

The variation in critical load indices for different failure modes with relative density was plotted, and for the sake of comparison, the load index of $\Pi_1 = 1 \times 10^{-8}$ was chosen. Fig. 3 shows that the dominant mode of failure for these panels at lower relative densities closer to 10^{-4} is intracellular bucking, which changes to core buckling when the relative densities are getting close to 10^{-3}, and at higher relative

Table 2 Properties of aluminum

Density, ρ [**kg/m³**]	2680
Modulus of elasticity, E [**GPa**]	70.3
Poisson's ratio, ν	0.33
Ultimate tensile strength, $\sigma_{f, cr}$ [**MPa**]	262
Cost [**USD/kg**]	4.65

Table 3 Properties of polypropylene

Density, ρ [kg/m³]	900
Modulus of elasticity, E [GPa]	1.4
Poisson's ratio, ν	0.33
Shear strength, τ_s [MPa]	16.5
Tensile strength, $\sigma_{f, cr}$ [MPa]	33.7
Cost [NZD/kg]	1.40–1.95

Table 4 Results from manual optimization for $\Pi_1 = 1 \times 10^{-8}$

Combination	w	Π_2	Π_3	Π_4	Π_5
1. FC-FW-IB-CY	1.7374	3.1938×10^{-4}	1.0502×10^{-3}	1.5899×10^{-4}	2.7047×10^{-2}
2. FC-FW-IB-CB	0.4194	4.1791×10^{-5}	8.0257×10^{-3}	2.0804×10^{-5}	2.7047×10^{-2}
3. FC-FW-CY-CB	1.7374	3.1938×10^{-4}	1.0502×10^{-3}	5.5384×10^{-5}	2.7047×10^{-2}
4. FC-IB-CY-CB	1.2443	2.2737×10^{-4}	1.4751×10^{-3}	8.0580×10^{-5}	1.9255×10^{-2}
5. FW-IB-CY-CB	1.4723	2.6991×10^{-4}	1.7398×10^{-3}	9.5967×10^{-5}	1.6326×10^{-2}

Table 5 Failure criterion for manual optimization for $\Pi_1 = 1 \times 10^{-8}$

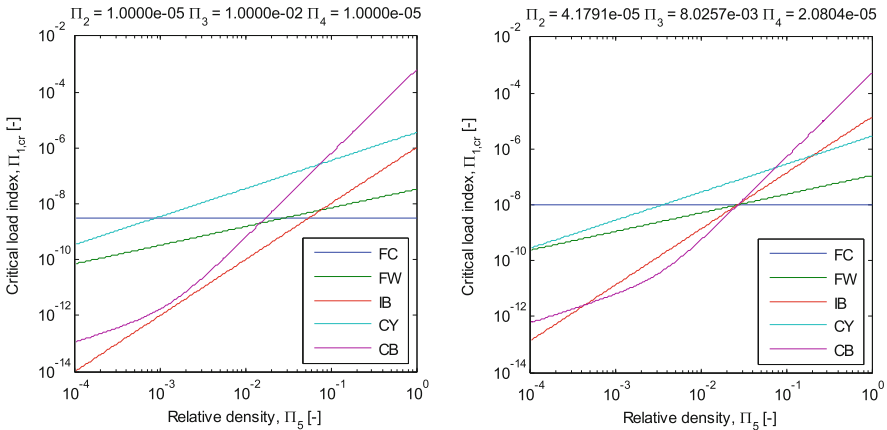| Combination	FC	FW	IB	CY	CB	Π_2/Π_3	Feasible?
1. FC-FW-IB-CY	1.0000	1.0000	.0000	.0000	.1368	0.3041	No
2. FC-FW-IB-CB	1.0000	1.0000	1.0000	0.1309	1.0000	0.0052	Yes
3. FC-FW-CY-CB	1.0000	1.0000	0.1214	1.0000	1.0000	0.3041	No
4. FC-IB-CY-CB	1.0000	1.2542	1.0000	1.0000	1.0000	0.1541	No
5. FW-IB-CY-CB	0.7142	1.0000	1.0000	1.0000	1.0000	0.1551	No

Fig. 3 Variation in critical load indices for different failure modes with relative density. Arbitrary values are used for the other geometric parameters on the left, while optimal values (obtained using the manual 4-parameter optimization for $\Pi_1 = 1 \times 10^{-8}$) are used on the right

densities, this changes to facings cracking in tension. The optimal value obtained in this study is pertinent to sandwich panels with isotropic aluminum facings and polypropylene cores having properties as listed in Tables 2 and 3, respectively.

6.2 Matlab Optimization

The same optimization is now run using the Optimization Toolbox in Matlab. All five failure criteria are considered at the same time, with the optimal weight index found using the *fmincon* function, which finds the minimum of a constrained nonlinear multivariable function, in the form shown in (15).

$$\min_{x} f(x) \text{ such that } \begin{cases} c(x) \leq 0 \\ ceq(x) = 0 \\ A \cdot x \leq b \\ Aeq \cdot x \leq beq \\ lb \leq x \leq ub \end{cases} \tag{15}$$

x is the vector of variables, with *A*, *Aeq*, *b* and *beq* used to define linear equality and inequality constraints. *c* and *c*eq are used to define nonlinear inequality and equality constraints, respectively, with *lb* and *ub* defining the lower and upper bounds, respectively. In addition to the five failure criteria, a sixth criterion, to ensure the correct facesheet to core thickness ratio, was also implemented. The bounds and starting points for the optimization procedure are provided in Table 6.

Results from the optimization procedure run using Matlab are provided in Tables 7 and 8. From these results, it can be seen that the optimal weight predicted by the manual procedure is 1.01% higher than that predicted by Matlab, which is extremely close. Matlab predicts that the optimal weight can be obtained at the confluence of the FW, IB, and CB failure criteria, as opposed to the confluence of the FC, FW, IB, and CB failure criteria obtained with the manual optimization method.

Table 6 Bounds and starting point that are defined for validation of manual optimization procedure

Parameter	Lower bound	Upper bound	Starting point
Π_2	1×10^{-6}	1×10^{-2}	1×10^{-4}
Π_3	1×10^{-5}	1×10^{-1}	1×10^{-3}
Π_4	1×10^{-6}	1×10^{-2}	1×10^{-4}
Π_5	1×10^{-4}	1×10^{0}	1×10^{-2}

Table 7 Results of optimization procedure run using Matlab for $\Pi_1 = 1 \times 10^{-8}$

Parameter	Optimal value
Π_2	3.5852×10^{-5}
Π_3	9.7525×10^{-3}
Π_4	1.7120×10^{-5}
Π_5	2.5411×10^{-2}
Weight index	Optimal value
w	0.4152

Table 8 Failure indices for optimization procedure run using Matlab for $\Pi_1 = 1 \times 10^{-8}$

	FC	FW	IB	CY	CB	Π_2/Π_3	Feasible?
Failure index	0.9593	1.0000	1.0000	0.1461	1.0000	0.0037	Yes

7   Summary

Results from the manual optimization procedure and MATLAB routine were obtained for the case of a sandwich beam with an aluminum facesheet and polypropylene honeycomb core. The optimal weight index was determined for a range of load indices from 1×10^{-8} to 1×10^{-6}. This load index range corresponds to a load (per unit width) between 703 and 70300N/m.

The dominant mode of failure for these panels at lower relative densities closer to 10^{-4} is intracellular bucking, which changes to core buckling when the relative densities get closer to 10^{-3}, and at higher relative densities the mode changes to facesheet cracking in tension. From the results of the manual four-parameter optimization, FC-FW-IB-CB combination provides feasible optimal solution. However, Matlab predicts the optimal weight to be at the confluence of only three failure modes (FW, IB, and CB), as opposed to the confluence of four parameters considered in manual optimization method. The lowest achievable panel density for a sandwich panel with aluminum facings and polypropylene core is 0.42 kg/m^3.

References

Ashby, M., Evans, A. G., Fleck, N., Gibson, L. J., Hutchinson, J. W., & Wadley, H. N. G. (2000). *Design analysis for material selection*. Butterworth-Heinemann. https://doi.org/10.1016/B978-075067219-1/50007-6

Banerjee, S., Battley, M., & Bhattacharyya, D. (2010). Shear strength optimization of reinforced honeycomb core materials. *Mechanics of Advanced Materials and Structures, 17*(7), 542–552. https://doi.org/10.1080/15376490903398714

Fogg, L. (1981). Stability analysis of laminated materials. In *State of the art design and analysis of advanced composite materials* (p. 162). Lockheed California Company, Sessions I and II.

Gibson, L. J. (2005). Biomechanics of cellular solids. *Journal of Biomechanics, 38*(3), 377–399. https://doi.org/10.1016/j.jbiomech.2004.09.027

Gibson, L., & Ashby, M. (1997). *Cellular solids: Structure and properties* (Cambridge solid state science series) (2nd ed.). Cambridge University Press. https://doi.org/10.1017/CBO9781139878326

Gibson, L. J., Ashby, M. F., Schajer, G. S., & Robertson, C. I. (1982). The mechanics of two-dimensional cellular materials. *Proceedings of the Royal Society of London. Series A: Mathematical and Physical Sciences, 382*(1782), 25–42. https://doi.org/10.1098/rspa.1982.0087

Leissa, A. W. (1980). *Buckling of laminated composite plates and shell panels*. Final report, 20 November 1980–20 January 1985. United States.

Noor, A. K., Burton, W. S., & Bert, C. W. (1996). Computational models for sandwich panels and shells. *ASME. Applied Mechanics Reviews, 49*(3), 155–199. https://doi.org/10.1115/1.3101923

Rathbun, H. J., Zok, F. W., & Evans, A. G. (2005). Strength optimization of metallic sandwich panels subject to bending. *International Journal of Solids and Structures, 42*(26), 6643–6661. https://doi.org/10.1016/j.ijsolstr.2005.06.044

Valdevit, L., Wei, Z., Mercer, C., Zok, F. W., & Evans, A. G. (2006). Structural performance of near-optimal sandwich panels with corrugated cores. *International Journal of Solids and Structures, 42*(16), 4888–4905. https://doi.org/10.1016/j.ijsolstr.2005.06.073

Wicks, N., & Hutchinson, J. W. (2001). Optimal truss plates. *Hutchinson. International Journal of Solids and Structures, 38*(30–31), 5165–5183. https://doi.org/10.1016/S0020-7683(00)00315-2

Wicks, N., & Hutchinson, J. W. (2004). Performance of sandwich plates with truss cores. *Journal of Mechanics of Materials, 36*(8), 739–751. https://doi.org/10.1016/j.mechmat.2003.05.003

Zenkert, D. (1995). *An introduction to sandwich construction*. Engineering Materials Advisory Services.

Zhang, W., Zok, F., & Evans, A. G. (2006). Design of sandwich panels with prismatic cores. *Journal of Engineering Materials and Technology-transactions of The ASME, 128*. https://doi.org/10.1115/1.2172279

Zok, F. W., Rathbun, H. J., Wei, Z., & Evans, A. G. (2003). Design of metallic textile core sandwich panels. *International Journal of Solids and Structures, 40*(21), 5707–5722. https://doi.org/10.1016/S0020-7683(03)00375-5

Zok, F. W., Waltner, S. A., Wei, Z., Rathbun, H. J., McMeeking, R. M., & Evans, A. G. (2004). A protocol for characterizing the structural performance of metallic sandwich panels: Application to pyramidal truss cores. *International Journal of Solids and Structures, 41*(22-23), 6249–6271. https://doi.org/10.1016/j.ijsolstr.2004.05.045

Negative Emission Technologies: Miraculous Solution or Aberrant Blindness?

Derya Soysal

Nomenclature

NET   Negative emission technologies
CCS   Carbon capture and storage
BECCS   Bioenergy associated with carbon capture and storage
GHG   Greenhouse gases

1 Introduction

As we enter the third millennium, the observation of the consequences of global warming is leading some organizations to continue to think and work on ways to address it. By signing the Paris Agreement in 2015, the international community recently committed to limiting the increase in global temperature to a level "below" +2 °C compared to the pre-industrial period. The agreement therefore implies a management of global climate policies and significant decreases in greenhouse gas (GHG) emissions. This objective seems unlikely to be achieved by current climate measures, which is why nearly 87% of the Intergovernmental Panel on Climate Change (IPCC) 2 °C scenarios include "negative emission techniques" (NETs) (Fuss et al., 2014). Effectively, 344 of the 400 scenarios rely on the rapid deployment of NETs in a context in which current national climate commitments are insufficient and GHG emissions will lead to an overshoot of the 2 °C target.

Carbon Market Watch defines negative emission technologies (NETs) as "*the removal of greenhouse gases from the atmosphere and their storage on land,*

D. Soysal (✉)
Free University of Brussels ULB, Brussels, Belgium
e-mail: derya.soysal@ulb.be

underground or in the oceans." These technologies therefore capture and reduce the CO_2 in the atmosphere. There are many ways to achieve negative emissions such as massive reforestation, fertilization of the oceans to increase phytoplankton populations, production of biochar (charcoal made from plant material with a negative net carbon balance), bioenergy associated with carbon capture and storage (BECCS), whose goal is to make bioenergy capture and store carbon from the atmosphere, or the direct capture of CO_2 (direct air capture) from the air to store it. The European climate law legally binds the EU to achieve a balance between greenhouse gas emissions and carbon removals by 2050 at the latest (European Commission, 2018). Today, NETs and other CCS technologies are beginning to gain traction. Indeed, it is possible to observe that CCS technologies are increasingly promoted by countries at international conferences. A question arises from this: How do academics and experts concerned with global warming represent NETs and what are their opinions about these technologies?

The following scientists participated in the survey: (1) Hervé Jeanmart, civil engineer; (2) Sandrine Selosse, PhD in economics; (3)two Belgian climate experts; (4) Audrey-Laude Depezay, mechanical engineer; (5) Rodolphe Meyer, environmental engineer; and (6) Zeki Yılmazoğlu, mechanical engineer.

2   Analysis and Interpretation of Results

2.1   The Environmental Dimension

Most of the representations on the environmental dimension of NETs point to their environmental impacts, which leads to a criticism of NET, but not always to a rejection. R. Meyer specifies the local impacts of NET such as the modification of water chemistry and the impact on biodiversity. Belgian climate experts point out the problems that this could cause in terms of biodiversity for BECCS and ocean acidification. S. Selosse points out that when deploying NETs, care must be taken not to create a bad impact on the other side. H. Jeanmart calls them "*aggressive*" and this adjective he uses to describe the consequences of NETs shows how reluctant he is about NET. Laude-Depezay, A., uses the term "*perverse effect*" to highlight the negative outcome of NET deployment. On the other hand, it is also possible to see that the representation of NETs is not univocal. According to climate expert R., nature has been "violated" for a long time. She adds that despite the environmental impacts, solutions must be found to deal with global warming such as BECCS while trying to reduce environmental impacts. NETs must be deployed according to S. Selosse and climate experts, but care should be taken not to generate more environmental impacts. However, H. Jeanmart and Laude-Depezay, A., are more critical of NETs. They consider that they could considerably impact the environment, that they are aggressive, and that they have perverse effects. They favor reforestation to obtain negative emissions. Differences remain in the representation

of the place that NETs would occupy in our environment and the argument of environmental impact is present in the criticism of NETs.

2.2   The Economic Dimension

Regarding the economic dimension of the representations, the criticism of economic systems refers directly to the criticism of energy systems. The criticism of energy systems, for its part, refers to the environmental and climatic consequences of the latter (GHG emissions). Among the need to change our economic systems, the expressions "*reduction of emissions*" and "*the need to decarbonize*" can be highlighted. A positive representation of degrowth can also be observed. Economic growth should stop, and we must reduce our economic production and consumption according to H. Jeanmart, A. Laude-Depezay, and R. Meyer. These three respondents give a definition close to degrowth and evoke it through the following expressions: "*produce less, consume les*s" by Jeanmart; "*reduce the production of objects and energy*" by Depezay; and "*reduce the production or extraction of resources*" by Meyer. In the representations, NETs are not perceived as the main solution to reduce socio-ecological problems (significant GHG emissions causing global warming). They are perceived as being useful for sectors that are difficult to decarbonize. On the other hand, economic costs are presented as an obstacle. The criticism of NETs in the economic dimension refers to the economic problems of their deployment. Convergences appear regarding the place of NETs in this "transformation" of economic systems. Indeed, S. Selosse, the climate experts M. and R., Z. Yilmazoglu are more pessimistic than R. Meyer with regard to our capacities to change our economic systems. As a result, they are more likely to support the place of NETs among the solutions for dealing with global warming. A more important criticism appears: H. Jeanmart and A. Laude-Depezay, proponents of degrowth, do not believe in the very important contribution of NETs to global warming. H. Jeanmart asserts that they have been developed with a vision of infinite growth in economic production. A. Laude-Depezay added that NETs and other geoengineering technologies are promoted by people with economic interests.

Nevertheless, the observed support is only a partial deployment of NETs, and this for the residual emissions of sectors that are difficult to decarbonize. To summarize, the interviewees advocate a change in our current economic systems, and this does not inevitably lead to a total rejection of CCS or NET. The latter are nevertheless considered as potentially useful for sectors that are difficult to decarbonize.

3   Conclusion

The purpose of this study was to study the dynamics of social representations of NETs among academics. This research focused on the representations of NETs by seven experts and the relationship of representations of the environment, the economy, and NETs. The idea was to analyze which arguments were in the positive and negative opinions about NET. The research methodology of this paper was essentially qualitative and exploratory, i.e., it was based on semi-directive interviews. This study, although not generalizable, yields interesting observations and conclusions. Even if it is difficult to extract a single strong trend, the survey reveals that the environment, the economic cost, and representations about the possibility of changing our economic systems are at the heart of the discourses about NETs.

A social representation is shared: nature is a physical environment affected by human intervention and it must be protected. The people interviewed systematically pointed out the environmental impacts of NETs and the need to be vigilant about them when they are deployed. Concerns about the environmental impacts of NETs, such as ocean acidification and deforestation, are central to the social representation of NETs. Although criticism of the environmental impacts that NETs might have has been frequent, this does not lead to an outright rejection of NETs. For example, the Belgian climate expert R. defends the idea that BECCS should be implemented in order to meet Belgium's commitments while ensuring that nature and biodiversity are protected.

Another constant came up in the climate dimension and brought to light another central core of the social representation: the interviewees point out that NETs alone cannot contribute to dealing with global warming and that the high cost of these technologies is an obstacle to their deployment. In this case, technologies are not perceived as the main solution to address the socio-ecological problems related to high GHG emissions causing global warming. Renewable energies are promoted more than NETs by all interviewees. Some of the interviewees consider that NETs will be necessary to accompany the transformation of our energy systems, while the others find that they could be useful for the residual emissions of sectors that are difficult to decarbonize. However, the latter point out that there are easier solutions to implement such as energy efficiency and building insulation.

Ultimately, to answer the title of the brief: NETs, miraculous solution or aberrant blindness? Based on the discourse analysis, the social representation that can be captured shows a fundamental concern about global warming and recognition of the need to reduce GHG emissions. None of the interviewees believe that NETs are a miraculous solution that will single-handedly save humanity from global warming. Total and unanimous opposition is not a social representation that emerges from the interviews either. Indeed, interviewees did not generally view these technologies as impossible to deploy or as unnecessary. Support for NETs is greater when they are coupled with other solutions than when they are considered in isolation. Indeed, support for NETs and CCS is conditional on the implementation of a range of other decarbonization options, particularly renewables and energy efficiency. The panel

advocates an integrated approach to decarbonization, in which all options are considered, such as social changes, changes in production systems, and less carbon-intensive technology options such as renewables. There was consensus that NETs may be useful for hard-to-decarbonize sectors. The core social representation of NETs is that they can be useful for local deployment and residual emissions but will not be able to fully address global warming.

Experts do not have a vision of technological solutionism, a notion developed by Morozov (2014). Gilli (2019) defines the notion of technological solutionism as "the belief that problems can be solved simply and quickly with new technologies.

Debating NETs does not necessarily reflect a consequence of technological solutionism and social representations placing great trust in technologies. Global warming often confronts the experts involved with dilemmas, difficulties, etc. The reports point out the urgency, yet the figures of GHG emissions continue to increase. Faced with this, it is difficult to find a solution to deal with global warming. The question of whether NETs are a useful and likely way to mitigate global warming is not just a physical and technological debate. The debate is more philosophical: Are we really going to play the climate sorcerer's apprentice? Can we deny the fact that without NETs like BECCS, the 1.5 °C climate goals are hardly achievable? This is the dilemma that the experts involved had to face.

References

European Commission. (2018). *In-depth analysis in support of the Commission Communication COM (2018) 773A: Clean planet for all: A European long-term strategic vision for a prosperous, modern, competitive and climate neutral economy, Brussels.*

Fuss, S., Canadell, J. G., Peters, G. P., Tavoni, M., Andrew, R. M., Ciais, P., & Yamagata, Y. (2014). Betting on negative emissions. *Nature Climate Change, 4*(10), 850–853.

Gilli, Y. (2019). Solutionnisme technologique, mais quels avantages? *Bulletin des médecins suisses, 100*(10), 323–323.

Morozov, E. (2014). *Pour tout résoudre, cliquez ici: l'aberration du solutionnisme technologique*. Fyp.

Sustainable Operations for Airport Warehouse Cargo Management

Eylem Turhan, Ilkay Orhan, and Alper Dalkiran

Nomenclature

ACRP	Airport Cooperative Research Program
AWB	Airwaybill
ETV	Elevating Transfer Vehicles
KPI	Key Performance Indicator
LD	Lower Deck
MD	Main Deck
ULD	Unit Load Device
SLA	Service Level Agreement

1 Introduction

The sustainability concept is not suitable only for operational or construction companies, but it is also essential all over the world precisely. Connecting the airports through the airline bridges together has boosted negative environmental effects all over the world. Besides those environmental effects, there are operational,

E. Turhan
Department of Civil Aviation, Graduate School of Sciences, Eskişehir Technical University, Eskişehir, Türkiye
e-mail: eylemturhan@eskisehir.edu.tr

I. Orhan
Faculty of Aeronautics and Astronautics, Eskişehir Technical University, Eskişehir, Türkiye
e-mail: iorhan@eskisehir.edu.tr

A. Dalkiran (✉)
School of Aviation, Suleyman Demirel University, Keciborlu, Isparta, Türkiye
e-mail: alperdalkiran@sdu.edu.tr

153

social, and economic effects as well. The main pillars of sustainability for sustainable decisions can be listed as, caring for the environment and financially strong development plans. Sustainability advice will add value to warehouse operations (Dalkiran, 2018).

The ACRP (Airport Cooperative Research Program) study focuses on three sustainability areas: social, environmental, and economic airport practices. The results show that environmental sustainability is a key priority for airports, currently and in the future. The ACRP Airport Sustainability Practice report outlined sustainability obstacles from the most challenging to the least. In that order, these obstacles include funding, staffing, management, culture, and training (Asinjo, 2011).

The airport warehouse operations consist of receiving, storing, picking, and shipping cargoes, in suitably adapted places. For this purpose, and under organizational and technological conditions. Therefore, the airport warehouse process includes such sub-processes as receiving, storage, picking, and shipping. The airport cargo warehouse processes may take many different forms and include multiple sub-components. Functions and tasks of the logistics facility determine the selection and appropriate connection of this process. Each airport cargo warehouse process component is characterized by an appropriate sequence of actions that have to be performed to complete given goals and objectives (Klodawski et al., 2017).

Correct operation of warehouse facilities allows the realization of their logistic tasks at an appropriate and adequate customer quality level. Accordingly, it determines validity, cost-effectiveness, and the need for their functioning in supply chains. Therefore, attention in the literature is given to cases associated with the design of storage facilities as well as the modeling and organization of their warehouse processes (Baker & Canessa, 2009; Gu et al., 2010).

Analyzing airport cargo activities such as different shipments and special handling is essential because each shipment and special handling types require different working standards and service level agreements (SLA) parameters. It is important to meet SLAs with customers. Companies must be successful in fulfilling service-level agreements with users (customer perspective) (Rahman, 2013). Basic working standards must be measured, captured, and analyzed for defined activities to understand basic standards with measurements. Analyzing the impact of change in standards on SLA compliance and capacity utilization, actual working standards will be amended, and outputs will be analyzed post-implementation. According to those analyses, local standards can be set. Necessary actions affecting personnel, capacity, and customers must be taken based on the standard procedures to ensure standardization of daily critical operational decisions. For resource planning, existing manual planning systems should have re-evaluation. Handling companies should ensure that the manual system is used in regular practice.

Karkula (2014) analyzed the application of simulating a manually operated distribution warehouse characterized by complicated and dynamic processes. According to the author, simulation and models are needed to fulfill the challenges of the transportation and logistics problems of today and the future. One can say that during the analysis of the literature, it is possible to find that many of the suggested solutions concern specific issues and they often take into account one of the criteria of formulated tasks optimization (Karkula, 2014).

Fig. 1 Cargo operations
standardization – first-phase
scope
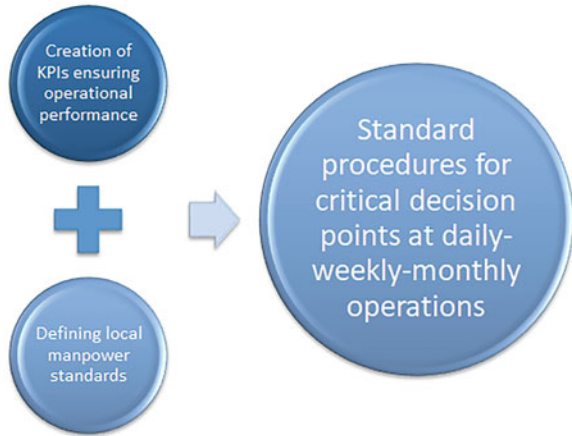
Rostering programs are based on systems and cover demand. If there is a need for rostering updates, absenteeism and communication between operational management and planners should be done. Rostering mistakes such as labor law, contractual requirements, and unequal workload distribution should be eliminated. Handling companies must find a real-time management system based on cargo operational needs. Implementation of the system must be complete for operations.

In this study, four airport cargo warehouse processes were examined. Buildup, breakdown, acceptance, and, delivery activities were focused on and measured during peak hours. These process steps are recorded manually. Cargo types, pieces, and tonnages were noted. Also, the types of equipment, agent, worker driver, and worker numbers used were measured. Their start and finish time stamps were recorded. The scope of these activities is summarized in Fig. 1.

A comparison table has been developed to compare measurements in order to determine the amount of human resources required to meet each criterion with various staffing arrangements. The current applied standard is defined, and suggestions will be created for improvement based on financial outcomes in the following studies. Also, the creation of KPIs ensuring operational performance will be completed. Manpower standards will be defined according to these measurement results and analyses. These measurements will help management to make legal and sustainable airport cargo operational decisions during daily, weekly, and monthly operations.

In Table 1, airport warehouse cargo acceptance and cargo delivery process are explained step by step. In the cargo acceptance process, the worker brings cargo to the edge of the truck, loading pieces on the euro pallet. The worker offloads from the truck with a hand lift, or the worker driver offloads from the truck with a forklift. The distinction between a worker and a worker driver is that the latter holds a handling equipment driver's license. After offloading process, an agent has to complete the weight, volume, and documentation check. For the cargo delivery process, the worker driver brings the cargo to the final delivery area. The security staff/handling

Table 1 Warehouse cargo acceptance and delivery steps

Process	Explanation of task	All process resources
Cargo acceptance	Bringing cargo to the edge of truck, loading pieces on euro pallet	A, W, WD, H, F
	Offloading from the truck with a forklift or handlift	A, W, WD, H, F
	Weight and volume check	A, W, WD, H, F
	Documentation check	A, W, WD, H, F
Cargo delivery	Bringing the cargo to the final delivery area	A, SA, W, WD, H, F
	Cargo clearance by security at the final delivery area	A, SA, W, WD, H, F
	Moving cargo to the edge of the truck	A, SA, W, WD, H, F
	Loading cargo to the trucks	A, SA, W, WD, H, F

A Agent, *W* Worker, *SA* Security Agent, *WD* Worker Driver, *H* Handlift, *F* Forklift

Table 2 Warehouse cargo buildup and breakdown steps

Process	Explanation of task	All process resources
Buildup	Bringing slave pallets to the area	WD, W, CA, S, H, F
	Shifting ULD/baggage cart to the buildup area	WD, W, CA S, H, F
	Moving euro pallet to the buildup area	WD, W, CA, S, H, F
	Pallet buildup by worker/supervisor	WD, W, CA, S, H, F
	Covering and netting by workers	WD, W, CA, S, H, F
Breakdown	Bringing slave pallets to the area	WD, W, CA, S, H, F
	Shifting ULD/baggage cart to the breakdown area	WD, W, CA, S, H, F
	Pallet breakdown by worker/supervisor	WD, W, CA, S, H, F
	Moving euro pallet to binning area	WD, W, CA, S, H, F

WD Driver, *W* Worker, *CA* Cargo Agent, *S* Supervisor, *H* Handlift, *F* Forklift

company's agent must ensure cargo clearance, pieces, tonnages, and documents at the final delivery area. The worker/worker driver should move the cargo to the edge of the truck with a hand lift or forklift.

In Table 2, the buildup and breakdown processes are explained. For buildup, the worker driver brings slave pallets to the area. After shifting the ULD/euro pallet/baggage cart to the buildup area, workers start the buildup. Covering and netting by workers is the last phase of the buildup process. Agent records all data during the buildup process. The breakdown is the opposite process of buildup. The worker driver brings slave pallets to the area and shifts the ULD/baggage cart to the breakdown area. Workers complete the pallet breakdown process, and the agent accepts the cargo to the cargo warehouse during the breakdown process.

2   Workforce Requirements for a Defined Process

Standard measurements will include all related status properties, such as pallet is on the station, the pallet is built up, covered with a net, and recorded in the system are measured. These measurements must be recorded as the same as in all subsidiaries. Records should have the below properties:

- Start time
- End time
- Cargo pieces and tonnage
- Cargo type
- Personnel count

Cargo terminologies such as main deck (MD), lower deck (LD), and unit load device (ULD) are used to define processes. Unit load devices (ULDs) are used to load passengers' checked baggage and air cargo for wide-body aircraft operations (Lu & Chen, 2012). The main deck is the highest deck running the full length of a vessel. The lower deck of an aircraft is usually used as cargo space. The various cargo sections are known as the hold and differ according to their position in the aircraft. The forward hold is located in the front section of the aircraft (in front of the wings) (Lurkin & Schyns, 2015). The term "Bulk" is used to define the loose type of loading, the cargoes load without unit load devices. Bulk cargo typically refers to cargo that is not containerized, such as pallets with stuff on them and a cargo net. Trucks are large, heavy road vehicles used for carrying goods, materials, or troops – a lorry. Forklifts are multi-functional and highly maneuverable trucks designed to transport and tow cargo and baggage at the hangar, warehouse, and airport. Handlift trucks are the solution to moving materials, boxes, and other items without strain. A handlift is designed to be used at industrial sites and in commercial applications, warehouses, and offices (Horberry et al., 2004).

Standards with different times and personnel relations should be measured. The below list can be used as an example. The minimum number of measurement requirements for each activity in different settings are listed below:

- 20 measurements for loose/euro pallet cargoes acceptance with different numbers of workers, agents, and types of equipment
- 20 measurements for loose/euro pallet cargoes delivery with different numbers of workers, agents, and types of equipment
- 20 measurements for MD/LD/loose/euro pallet buildup with different numbers of workers, agents, and types of equipment
- 20 measurements for MD/LD/loose/euro pallet breakdown with different numbers of workers, agents, and types of equipment

Measurements were recorded and analyzed for different cargoes, pieces, and tonnages. For cargo acceptance and delivery processes, trucks are separated into small trucks, medium trucks, and large trucks. For buildup and breakdown, the same division has been made for other types, such as MD, LD, loose, and ULD. It is

important to take at least 20 measurements. The number of metrics and scenarios are important to better understand how the presence of too many sub-processes in cargo acceptance, cargo delivery, buildup, and breakdown processes responds in different teams.

3 Relation of Continuous Measurement with Standardization and Performance

In the first phase, the scope of this study was set to reach manpower standards, shift performance, and efficiency of the team to the defined KPIs. Also, standardization of critical decisions with a predefined path. Following are some examples:

- MD pallet with 2 worker +1 forklift +1 Agent 30 min
- MD pallet with 3 worker +1 forklift +1 Agent 15 min
- MD pallet with 4 worker +1 forklift +1 Agent 10 min

The same measurement was made for other types such as MD, LD, bulk, ULD, small truck, and big truck. A minimum number of measurements for each activity was analyzed with different settings, for example, 10 measurements with 2 workers, 10 measurements with 3 workers, and 10 measurements with 4 workers for buildup or breakdown.

In the acceptance of cargo process, the average truck tonnage is 1.5 tons and the fastest truck process time is 30 min. In case of import, average weight of the euro pallet is 0.25 tons and the average euro pallet unit per delivery is 2.5 tons. The delivery gate process time per euro pallet is 2.7 min.

In case of export, the average MD/LD tonnage is 2 tons. The fastest MD/LD process time for buildup is 35 min with 4 workers and 1 worker driver. For the import side, the average MD/LD tonnage is 1.8 tons. The fastest breakdown MD/LD process time is 21 min.

4 Conclusion

All the results and analyses of warehouse processes' measurement support the warehouse management team's guide through their cost, social, and environmental targets. It is a matter of organizational arrangement and lost-profitability analysis to pursue those sustainability targets.

The acceptance, delivery, buildup, and breakdown processes were detailly examined in this airport cargo warehouse study. Pieces, tonnages, manpower, and equipment details were noted for each measurement. Manpower and equipment's start and finish times were measured. Measurements data were recorded during peak hours. According to these measurements, KPIs configurations are completed. Acceptance

activity starts with receiving the first pieces of AWB. After receiving the cargo, the agent measures and enters the volume and weight of the shipment, and the activity ends with the truck leaving the cargo warehouse dock. For each ton, 20 min is acceptable. For delivery orders lead time, the process starts when a customer requests the cargo at the delivery gate of the warehouse. When all pieces of the shipment are completed, the agent releases the last pieces of the shipment and confirms the delivery. 15 minutes is acceptable until 1 ton. If the shipment is more than 1 ton, 1 h for each ton is acceptable. According to 20 breakdown process measurements, 1 h and 1 worker are enough for 2.5 tons. In case of buildup productivity, the failure of the team to focus on a single flight in the operations department, the fact that the construction was started due to the entry of the loads/inspection or the paperwork, and the interruption due to operational reasons are the main reasons for the prolongation of the process. The buildup process was completed with two workers in 30 min for a container and this is acceptable.

Acceptance, delivery, buildup, and breakdown of airport cargo warehouse activities were the first phase. After the completion of this phase, another airport cargo warehouse activity can be analyzed, such as racking, de-racking, and ETV. These warehouse process measurement data will be simulated later on. These simulation studies will identify bottlenecks and determine and improve the efficiency of the airport warehouse processes. Another group of issues relating to the internal transportation of handling equipment is a problem associated with the scheduling of transportation tasks. The objective of the optimization is to minimize the total travel time of the forklift during the realization and receiving of all transport orders. Also, shift planning will be analyzed. It's aimed to minimize the overtime working hours of the personnel.

References

Asinjo, D. (2011). *Environmental management at sustainable airport models* (Research Papers. Paper 257).

Baker, P., & Canessa, M. (2009). Warehouse design: A structured approach. *European Journal of Operational Research, 193*(2), 425–436.

Dalkiran, A. (2018). Airport management: Sustainable projects to sustainable operations. *International Journal of Business Marketing and Management (IJBMM), 3*(11), 01–10. ISSN: 2456-4559.

Gu, J., Goetschalckx, M., & McGinnis, L. F. (2010). Research on warehouse design and performance evaluation: A comprehensive review. *European Journal of Operational Research, 203*(3), 539–549.

Horberry, T., Larsson, T. J., Johnston, I., & Lambert, J. (2004). Forklift safety, traffic engineering, and intelligent transport systems: A case study. *Applied Ergonomics, 35*(6), 575–581. https://doi.org/10.1016/j.apergo.2004.05.004

Karkula, M. (2014). Selected aspects of simulation modeling of internal transport processes performed at logistics facilities. *Archives of Transport, 30*(2), 43–56.

Kłodawsk, M., Jacyna, M., Lewczuk, K., & Wasiak, M. (2017). The issues of selection warehouse process strategies. In *10th international scientific conference transbaltica 2017: Transportation science and technology.*

Lu, H., & Chen, C. (2012). Safety stock estimation of unit load devices for international airline operations. *Journal of Marine Science and Technology, 20*(4), Article 11. https://doi.org/10.6119/JMST-011-0322-1

Lurkin, V., & Schyns, M. (2015). The airline container loading problem with pickup and delivery. *European Journal of Operational Research, 244*(3), 955–965. https://doi.org/10.1016/j.ejor.2015.02.027

Rahman, N. (2013). *Measuring performance for data warehouses – A balanced scorecard approach*. IJCIT, ISSN 2078-5828.

Outlines of Sustainable Air Transportation in ICAO Annex Documents: Roots of Sustainability

Rukiye Öztürk, Sara Kaya, and Alper Dalkıran

Nomenclature

AHP	Analytical Hierarchy Process
BWM	Best Worst Method
FAA	Federal Aviation Authority
FDM	Fuzzy Delphi Method
GRI	Global Report Initiative
ICAO	International Civil Aviation Organization
KPI	Key Performance Indicators
MABAC	Multi-attribute Border Approximation Area Comparison

1 Introduction

Sustainable aviation is a phenomenon that defines the long-term characteristics of the environment, social, and economic domains of a vision. Although Federal Aviation Authority (FAA) defines sustainable aviation with an additional "operational" domain, the literature understands this phenomenon in three domains, "social," "economical," and "environmental," both separately and together (FAA, 2022). Also, Fraport Group published a sustainability report based on Global Reporting Initiative (GRI) on Environment, Financial, and Personnel basis (Fraport, 2019).

However, there should be a better understanding of sustainable aviation metrics. Barros and Dieke (2008) have developed a two-stage semi-parametric model for

R. Öztürk · S. Kaya · A. Dalkıran (✉)
School of Aviation, Suleyman Demirel University, Keciborlu, Isparta, Türkiye
e-mail: alperdalkiran@sdu.edu.tr

airport economic efficiency. They have defined airports as an interest to contemporary economics due to their increasing strategic importance in the movement of people and goods in a globalized world. Due to airline deregulation and liberalization, the increased competition among airlines has created a much more competitive environment for airports. They analyzed the economic efficiency characteristics of 31 airports and found sustainability indexes such as the number of planes, the number of passengers, general cargo, handling receipts, aeronautical sales, commercial sales, labor costs, capital invested, and operational costs.

Brueckner and Abreu (2017) studied carbon emissions, an item of the environmental domain. They used annual data of airlines in North America between 1995 and 2015. They used the available ton-kilometers, and available seat-kilometers per aircraft rose in their study. They also and revealed the stage length rose by 100 miles, the load factor rose by 5%, aircraft vintage becomes younger, the fuel price rose, and optimal emissions during the flight.

Another study in the literature evaluated the environmental protection performance model (Chao et al., 2017), which used a Fuzzy Delphi Method (FDM), and dimensions, and indicators for assessing airport environmental protection performance were chosen. The first round of a questionnaire survey solicited expert opinions on the summarized indicators, followed by a second questionnaire designed to obtain the weights of the selected environmental rating indicators using the analytic hierarchy process (AHP) and examine the value functions of these indicators. All the environmental indicators have been grouped under green airport design, energy conservation and carbon reduction in airport operations, use of renewable resources, and airport environmental sustainability management.

Key performance indicators (KPIs) are vital to measuring sustainability. Eshtaiwi et al. have determined KPIs to assess airport success (2018). This study seeks to provide a collection of airport key performance indicators (KPIs) that may be used to monitor and assess the operation of Libyan airports. The technique analyzes the opinions of specialists with extensive experience in the airport business in Libya and high levels of knowledge. The results showed 25 KPIs under five domains: passenger service, airside area, financial perspective, safety and security, and environmental.

Contrarily, Indian airports have been examined by the integrated performance evaluation technique by Chakraborty et al. (2020). Using the best-worst method (BWM) and the multi-attribute border approximation area comparison (MABAC) method, the performance of 32 major Indian international airports was evaluated based on eight criteria: annual revenue, total passengers, aircraft movements, total freight, terminal area, number of routes, number of check-in counters, and distance from the city center.

This chapter looks at mediation to find an understandable way to categorize and group around the sustainability domains and indexes to assess annexes. The findings of the chapter were based on the basic methodology used to assess a group of aviation students.

2   Method

This research has planned to assess all subheadings of annex documents to examine according to the specified literature and evaluate all three main sustainability domains. The study comprised three main stages. First stage was the determination of sustainability metrics from the literature. Second stage was browsing of the annexes for possible relations and marking down on a mindmap diagram. Second stage was finalized after a discussion session to ensure the relation. The last stage, third stage, matched the findings with the related annex and sustainability indexes.

The research criteria constructed for the environment domian were obtained using the research created by Chao et al. (2017). There are 19 criteria to be considered in evaluating the sustainability performance and developing performance improvement plans according to the state of the aviation.

2.1   *Determination of Sustainability Metrics*

The competition caused by aviation liberalization influenced the formation of sustainable and efficient operations in which there is a relevant interest in the modern economy. Skillful aviation companies that find sustainable ways to operate provide guidance to improve aviation industries and society. Then, sustainability in terms of economics, altering the competition caused by the liberalization of airports and airlines, also ensures sustainable efficiency and interest in the modern economy.

It is seen that the utilization rate and the capacity of airports, which are increasing every day with the development of air transportation, do not meet each other according to the Asker and Battal (2017). For this reason, it has been observed that the effective and efficient use of airports will positively affect social, economic, and environmental sustainability. Airports are not the only source of aviation. Airlines are the other vital source of aviation. Tiwari et al. have proven the significance of low costs operations and simplicity as a strategy for a new company in the airline industry necessary to achieve ongoing sustainable profitability in an industry that is failing to turn a profit (2018).

This chapter examined aviation sustainability in three divisions: environmental, social, and economic domains, with the criteria below.

- Environmental domain

  - Waste management
  - Water management
  - Noise management
  - Energy management
  - Emissions and air quality
  - Biodiversity
  - Certifications

- Economic domain

  – Direct
  – Indirect
  – Development
  – Employment

- Social domain

  – Employee satisfaction
  – Customer satisfaction
  – Human rights
  – Safety and hazards
  – Shareholder relations
  – Ethical rules
  – Social accountability
  – Indirect social affects

2.2 Browsing the Annexes

A word-based scan was performed within the 19 annexes and appendix documents for the matching indexes grouped under three domains of sustainability. During this screening, the topic's content was examined by paying attention, and titles were taken. The headings specified in the annexes have been shared in the group to process them efficiently while scanning.

On the other hand, this study has focused to investigate the usefulness of these titles in terms of economic, social, and environmental domains was examined. As a result, the aim is achieved after the discussions are completed on these three domains. The results obtained from the mindmap after all headings and subheadings of annexes were browsed are shown in Fig. 1. The scheme thus created is called "the EYE." Thanks to this, a better understanding of the issue has been achieved.

After the annex subheading is placed under the appropriate sustainability category, a two-dimensional matrix system is generated.

Fig. 1 A mindmap graphic called the EYE of Annexes showing the relationship of sustainability indexes and the annex subheadings

3   Results

The latest versions of ICAO annexes and updates were examined until August 2022. The 29 documents examined containing 4,562 pages with their appendixes show that its contribution to sustainability-related development was found insufficient, considering environmental, economic, and social consequences. Furthermore, there is no direct relation to sustainability in the documents. However, there are indications of previously mentioned groups.

These documents were examined and compared with three domains of economic, social, and environmental sustainability. Sustainability indexes specified under these domains were compared regarding sustainable aviation. The most exciting result was found for the social domain, representing 69% of all connections. Of the results obtained, 28% matched with environmental and only 3% with the economic proportion, which are shown in Fig. 2.

According to the data obtained, the conclusion drawn is that there is an imbalance in the annexes. Imagine that this is a wheel to roll to carry the whole industry; it is pretty impossible to go forward due to the imbalance of the three domains of the sustainability wheel. The progress will not be accessible from a sustainability point of view because rims did not share equally.

3.1   Environmental Domain

Thus far, manufacturers, airlines, and airports have taken many sustainable actions for the environment. However, according to the results of the annexes, there is not much standardization related to the environment. The result were obtained when the

Fig. 2 Proportions of sustainability groups in annexes
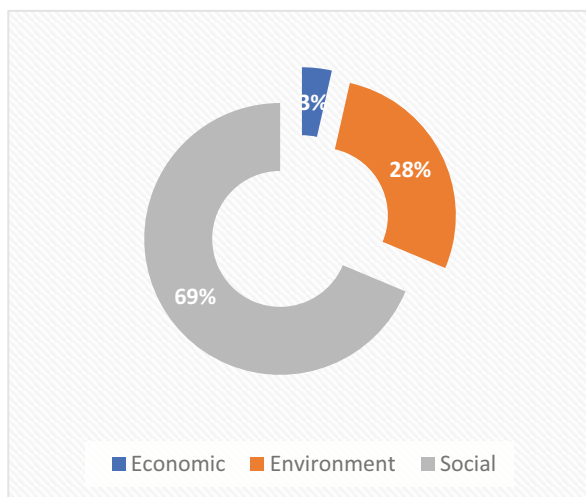
research shows the general characteristics of all appendixes, almost one-third of all indexes are confrontation of the environmental domain. This specified ratio should also consider the scarcity of data input. Table 1 shows the environmental finding of sustainability. According to this table, a total of 55 related indexes were found.

There are three crucial index groups noticed in Table 1. The first is "emissions and air quality," which is mentioned 24 times. "Certification" is mentioned ten times and "noise management" nine times. There are 22 sustainability indexes mentioned in Annex 16, and the contents of this annex are related with "aircraft noise". Headings of Annex 16 also cover "aircraft engine emissions." It is seen that these annexes, which tackle the two main sustainability problems of the aviation sector, have an impact on sustainable aviation.

3.2 Economical Domain

The economic aspect is vital in terms of continuing sustainability. Economic efficiency is often at the forefront for airlines and airports. The reason for this is the necessity to stay afloat. From this point of view, it should be understood that achieving economic sustainability is a breakthrough in terms of continuity in the sector and should not be sustainable if there is no economical plans present. In this context, the conclusion drawn from the table is that annexes are more focused on employment. In particular, failure to achieve standardization in terms of direct economic contributions may turn into a problem in terms of keeping the sector afloat.

It is known that these annexes were created from the ensuring standardization. However, it is seen that sustainability has not been mentioned from the economic point and no standardization has been achieved in this regard (Table 2).

The fact that there is little standardization in terms of cost structure shows that there is a high potential for long-term problems in the sector. As a result of the research conducted from this point of view, the necessity of introducing an economic standardization can be critical for aviation rules. ICAO determines direct economic contributions and, at the same time, the employers in the sector will know that they have economic contributions, thanks to this standardization.

3.3 Social Domain

In light of the studied documents, most of the entries were found from a social point of view. It is thought that this is because it has a lot to do with the content. Out of all annex documents, a content-appropriate title was determined with almost seven out of ten. In these indexes, 75 related safety and hazard topics have been found. As is known, "rules in aviation are written in blood." Due to this, serious measures have

Table 1 Findings in the environmental domain of sustainability

Environmental domain								
Annexes	Waste management	Water management	Noise management	Energy management	Emissions and air quality	Biodiversity	Certifications	Total
1				1	1			2
2				1			1	2
3					1			1
4		1						1
5								0
6			4				1	5
7								0
8							1	1
9		1				1		2
10					8			8
11					1			1
12					2			2
13					1			1
14		1		1	1		1	4
15			1	1				2
16	2	1	4	1	9		5	22
17								0
18								0
19							1	1
Total	2	4	9	5	24	1	10	55

Table 2 Findings in the economical domain of sustainability

Economic domain					
Annexes	Direct	Indirect	Development	Employment	Total
1			1	1	2
2		1	1		2
3					0
4				1	1
5					0
6					0
7		1			1
8	1				1
9					0
10					0
11					0
12					0
13					0
14					0
15					0
16					0
17					0
18					0
19					0
Total	1	2	2	2	7

been taken to close any security vulnerability. It is also pervasive for ICAO to standardize these measures.

Table 3 shows that shareholder relations is the second index with a count of 25. The third is the code of ethics with nine indexes. The main findings for this domain come from the sixth and tenth annexes – aircraft operation and aviation telecommunication, respectively. Since miscommunication between stakeholders in the aviation sector leads to significant accidents, ICAO focuses on standardization in this regard.

However, according to the table obtained, there is a serious standardization problem in the field of social responsibility too. It is foreseen that social sustainability studies in the sector can also pave the way if the society understands more on social standards and aviation industry. When we look at sustainability from a social point of view, innovation can be done by realizing the things that need to be improved faster in the sector. At the same time, awareness of important issues such as security can be achieved faster. It is assumed that this study is carried out in order to create an awareness to contribute to the air transportation sector. At the same time, in these rapidly advancing times, Industry 4.0 and Society 5.0 are blended with topics and offer the potential for the sector to become more sustainable.

Table 3 Findings in the social domain of sustainability

Social domain

Annexes	Employee satisfaction	Customer satisfaction	Human rights	Safety and hazards	Shareholder relations	Ethical rules	Social accountability	Indirect social affects	Total
1		1		4	1	3			9
2		1	1	5		1		1	9
3	1			2		1			4
4				1					1
5									0
6	1	1	1	18	1	3		5	30
7									0
8				2					2
9				2					2
10	2			9	8			1	20
11				7	7				14
12				1	1	1	1		4
13			1	2					3
14	1			5	1				7
15				7	2	4			13
16									0
17				7	1				8
18				1	2				3
19		1	1	2	1	2			7
Total	5	4	4	75	25	15	1	7	136

4   Conclusion

We have examined the the results of the annexes formed by ICAO standards. This research turns out the usefulness of the examined standards. All data indicate that the ICAO needs to achieve greater environmental and economic sustainability standardization. In particular, the results explained in seven topics in the field of economics, leaves a question mark in the heads about the sector's potential to survive in the long term.

The fact that the standard of this commercially made network is almost nonexistent calls into question the continuity of the sector. Organizations such as IATA protects airlines. However, it is known that the rule maker is ICAO. From an economic point of view, sustainability should be ensured and reflected in the documents.

These results show that looking at aviation from a sustainability framework will be very effective. Researchers can take the financial perspective on the economy. The environment, on the other hand, constitutes a category by itself. In this way, we can say that aviation of airport performance increase is directly connected to sustainability.

This study aims to contribute to the literature on sustainable aviation by analyzing the ICAO Annex documents. At the same time, it is necessary to bring sustainability to the sector attention for more reliable and integrated aviation. This research shows that the aviation sector needs to increase awareness of sustainable aviation and increase the number of studies.

References

Barros, C. P., & Dieke, P. U. C. (2008). Measuring the economic efficiency of airports: A Simar-Wilson methodology analysis. *Transportation Research Part E: Logistics and Transportation Review, 44*(6), 1039–1051. https://doi.org/10.1016/j.tre.2008.01.001

Battal, Ü., & Asker, V. (2017). Operational efficiency measurement at selected airports. *International Journal of Management Economics and Business, 13*(ICMEB17). https://doi.org/10.17130/ijmeb.2017icmeb1735613

Brueckner, J. K., & Abreu, C. (2017). Airline fuel usage and carbon emissions: Determining factors. *Journal of Air Transport Management, 62*, 10–17. https://doi.org/10.1016/j.jairtraman.2017.01.004

Chakraborty, S., Ghosh, S., Sarker, B., & Chakraborty, S. (2020). An integrated performance evaluation approach for the Indian international airports. *Journal of Air Transport Management, 88*(February), 101876. https://doi.org/10.1016/j.jairtraman.2020.101876

Chao, C. C., Lirn, T. C., & Lin, H. C. (2017). Indicators and evaluation model for analyzing environmental protection performance of airports. *Journal of Air Transport Management, 63*, 61–70. https://doi.org/10.1016/j.jairtraman.2017.05.007

Eshtaiwi, M., Badi, I., Abdulshahed, A., & Erkan, T. E. (2018). Determination of key performance indicators for measuring airport success: A case study in Libya. *Journal of Air Transport Management, 68*(March 2017), 28–34. https://doi.org/10.1016/j.jairtraman.2017.12.004

FAA. (2022). *Airport sustainability*. https://www.faa.gov/airports/environmental/sustainability/.
    Accessed 02 Aug 2022.
Fraport. (2019). *GRI report 2019*. https://www.fraport.com/content/dam/fraport-company/images/
    umwelt/en/gri-report-2019_final.pdf/_jcr_content/renditions/original.media_file.download_
    attachment.file/gri-report-2019_final.pdf. Accessed 02 Aug 2022.
Tiwari, R., Singh, M. K., & Mathur, S. K. (2018). Sustainability of low cost and simplicity in airline
    industry: A case of indigo. *International Journal of Management, Technology and Engineering,
    8*(12), 6034–6044.
United Nations. *The 17 Goals – Sustainable Development Goals, Department of Economic and
    Social Affairs Sustainable Development*. https://sdgs.un.org/

World Air Transportation Recovery After COVID-19 Restrictions

Alper Dalkıran

Nomenclature

ACI	Airport Council International
ASK	Available Seat Kilometer
COVID-19	Coronavirus Disease of 2019
IATA	International Air Transport Association
LF	Load Factor
MoM	Month-on-Month, Month-over-Month
PLF	Passenger Load Factor
RPK	Revenue per Kilometer
YtD	Year-to-Date
YoY	Year-on-Year, Year-over-Year, Year-to-Year

1 Introduction

The year 2022 was one of the most remarkable years in global aviation history. After fighting against the new Covid-19 pandemic for more than 2 years, many countries' epidemic prevention and control targets have achieved good outcomes. The domestic air transportation business has made a speedy recovery despite the epidemic. It will soon return to the level it was in 2019. At this time, it appears to be becoming better for international flight travel.

ICAO and IATA reports demonstrate that (ICAO, 2022; IATA, 2022a, b):

A. Dalkıran (✉)
School of Aviation, Suleyman Demirel University, Keciborlu, Isparta, Türkiye
e-mail: alperdalkiran@sdu.edu.tr

- While the global domestic market trended sideways before 2022, revenue passenger kilometers (RPKs) for international traffic were renewed to drive the recuperation of the worldwide aviation industry.
- Many significant international route locations outperformed 2019 levels in the same periods of 2022 monthly, while other carriers likely achieved RPK levels. Several of these sites were located in Africa (Anna, 2022).
- Asia Pacific airlines have seen significant international expansion for the past 4 months, achieving a recovery rate of 453.3% in the same era as year-on-year (YoY) measurements. This recovery rate significantly improved from the 103.5% seen in January 2022. This encouraging trend is anticipated to continue as the region will gradually reopen.
- The recovery of the global industry picked up speed, and global RPK reports presented a 64.1% improvement before the crisis. In May, domestic RPK reports pointed out that the improvement reached 76.7% of the previous peaks in 2019. The worldwide RPKs increased by 10.7% month-on-month (MoM) compared to April 2022.
- Inflation shows itself as the most considerable bottom lack for improvement. Low consumer confidence and demand and high jet fuel price have been unable to stop the upswing from continuing. The fact that comparisons over international and domestic bookings indicate that an increased desire to travel internationally continues to exist.

2   Reports

As the busiest travel period of the year approaches in the Northern Hemisphere's summer, the IATA has released passenger figures for May 2022 indicating that the resurgence in air travel is gaining momentum. Unless otherwise specified, we have reverted to comparing the volume of traffic YoY instead of comparing it to the period covered by 2019 thus far. The low traffic base in 2021 will result in some markets demonstrating good YoY growth, although their size is considerably smaller than in 2019.

As assessed by revenue passenger kilometers (RPKs), total traffic in May 2022 increased by 83.1% compared to May 2021. This increase was primarily related to the significant increase in overseas travel. Global traffic is 68.7% of what it was before the financial crisis. The amount of domestic travel increased by 0.2% in May 2022 compared to the previous month. Significant increases in some areas were offset by a 73.2% YoY fall in the Chinese domestic market due to COVID-19 restrictions. In May 2022, the volume of domestic traffic was 76.7% of what it was in May 2019. The amount of international traffic has increased by 325.8% since May 2021. The easing of travel restrictions across most of Asia is helping to restart the recovery of the international tourism industry. In May 2022, the international RPKs hit 64,1% of their May 2019 levels.

Table 1 Air transportation market detail (IATA, 2022a)

May 2022 (% YoY)	World share	RPK	ASK	PLF (%-PT)	PLF (Level)
Total market	100%	83.1%	52.8%	13.1%	79.1%
Africa	1.9%	124.9%	76.8%	14.9%	69.6%
Asia Pacific	27.5%	−4.7%	−8.2%	2.6%	69.6%
Europe	25.0%	258.8%	159.1%	22.4%	80.7%
Latin America	6.5%	99.3%	89.5%	4.0%	80.7%
Middle East	6.6%	279.6%	103.5%	35.4%	76.2%
North America	32.6%	56.3%	36.6%	10.8%	86.0%
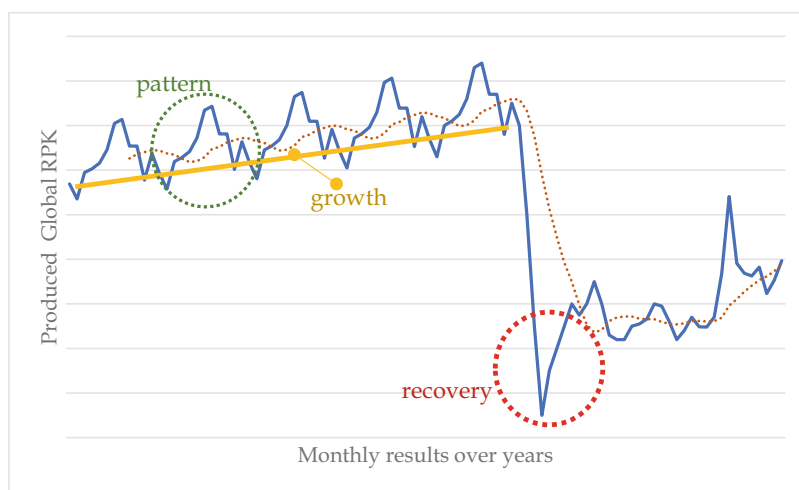
Fig. 1 Recovery period of RPKs all over the world. (Adapted from IATA, 2022b)

The travel industry is continuing to revive. Humans must travel. Moreover, they do so when governments eliminate COVID-19 prohibitions (ICAO, 2022). Numerous significant international route segments, such as those within Europe and those between the Middle East and North America, have already surpassed the 100 million passenger mark. The way forward is to eliminate all COVID-19 restrictions, with Australia being the most recent nation to do so this week. China's internal travel fell by a staggering 73,2% compared to the previous year, an enormous exception to the optimism surrounding this travel resurgence. The significantly delayed travel recovery related to China is evidence that this nation's prolonged implementation of a zero-COVID policy is incompatible with the norm in other parts of the world (Chen et al., 2022). Table 1 and Fig. 1 indicate the trends and the changes in regions and time. The aviation RPK values have indicated themselves by the patterns and YoY draws a regular increase. However, the recovery will represent some peaks to reach a new pattern in the following years of aviation (Oxley & Jain, 2015).

2.1 International Markets for Passengers

European carriers' traffic in May grew by 412.3% compared to 2021. The capacity increased by 221.3%, while the load factor (LF) climbed by 30.1–80.6%. Only regions directly touched by the crisis in Ukraine were impacted (Rutynskyi & Kushniruk, 2022).

Compared to May 2021, May traffic for Asia-Pacific airlines climbed 453,3%. This climb is significantly more extensive than the 295.3% YoY growth observed in April 2022 (Kim & Sohn, 2022). The capacity climbed by 118.8%, while the LF rose by 43.6–72.1%. Reductions in restrictions on most of the region's markets, except China, contribute to regional growth.

May airplane traffic in the Middle East surged 317.2% over 2021. The LF grew 37.1–76.6% this year compared to the previous month. The growing reopening of Asian markets is increasing Gulf hubs' trade volume.

North American carriers saw a 203.4% increase in traffic in May compared to the same month in 2021. The capacity grew by 101.1%, while the LF climbed by 27.1–80.3%. Tourism and a strong desire to travel continue to contribute to the global recovery, despite some route regions surpassing 2019 figures. The peak rises can be reviewed in Table 2.

May traffic for Latin American airlines climbed 180.5% compared to May 2021. In May, capacity expanded by 135.3%, while LF rose by 13.5 percentage points to 83.4%, the highest LF in the region for the twentieth consecutive month (Bhowmik & Eluru, 2022). Several routes, notably those between Central America and Europe and Europe and North America, surpass 2019 levels. Figure 2 demonstrates the trends in time and how the traffic capacity has improved in recent months. Europe and China need to consider how the markets react after global shocks.

2021 May RPKs for African airlines surged 134.9% compared to 2021 May. May 2022 capacity grew by 78.5%, but LF rose by 16.4–68.4%, the region's lowest.

Table 2 International RPK YoY change by regions (IATA, 2022b)

Sections	YoY change, April	YoY change, May
Industrial globally	330.6%	325.8%
Asia-Pacific	259.3%	453.3%
Europe	477.7%	412.3%
Middle East	258.3%	317.2%
North America	230.3%	203.4%
Latin America	262.8%	180.5%
Africa	120.4%	134.9%

China and Europe fall behind
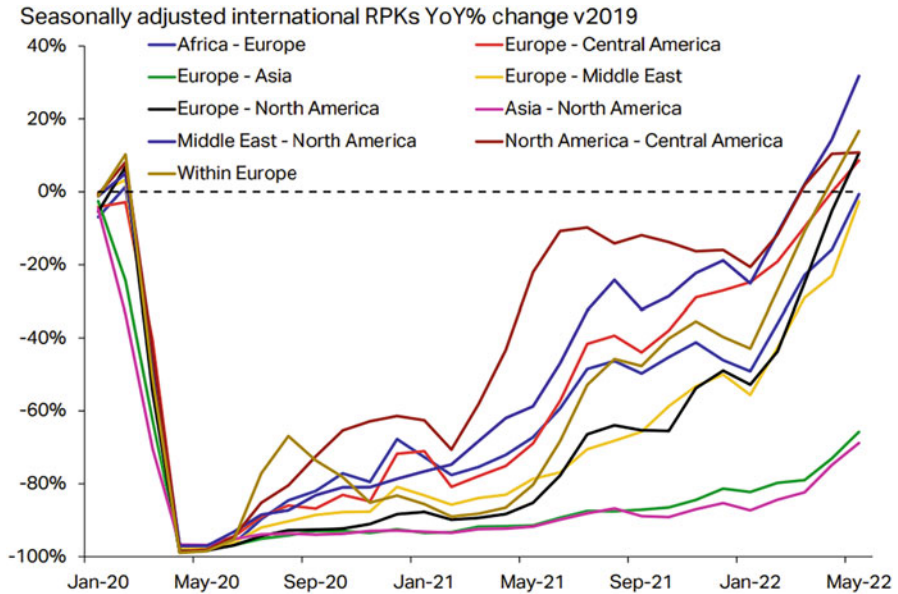
Fig. 2 International RPK's YoY change starting from Covid-19 pandemic. (IATA, 2022b)

2.2 Domestic Market for Passengers

India's domestic RPKs climbed by 405.7% YoY, much greater than the 78.6% in April. In May 2021, India experienced the most severe case of COVID-19 in its history. Domestic traffic in the United States increased by 26.1% in May compared to May 2021.

Passenger demand is catching up to 2019 levels, thanks to the healthy performance of the great majority of foreign and domestic markets compared to the previous year. In May 2022, total RPKs reached 68.7% of May 2019 levels, the most remarkable performance of the year relative to pre-COVID-19 travel levels.

China PR for domestic RPKs increased by 42.2% compared to the April 2022 (Zoubir & Tran, 2022). Even while the country's traffic numbers have recovered from the repeated shocks of tighter travel rules, they are still 71.5% lower than those before the outbreak.

The US domestic traffic improved by 3.1% MoM but is still below the RPK criteria for 2019. The number of RPKs sold in the United States has reduced by 4.7% compared to the same month in 2019 (compared to a loss of 1.6% in April). Although capacity has declined by 6.0% YoY, LFs across the nation have remained high at 88.7%.

This market may experience an increase in traffic congestion due to the high price of gasoline and the continuous labor shortage. In April, the rate of domestic RPK growth in the United States reached a peak of 48.1%; in May, it plummeted to 26.1%.

Table 3 Domestic air transportation market detail

May 2022 (% YoY)	World share	RPK	ASK	PLF (%-PT)	PLF (Level)
Domestic	62.3%	0.2%	−3.3%	2.9%	79.8%
Domestic Australia	0.8%	34.7%	23.1%	6.5%	75.6%
Domestic Brazil	1.9%	73.1%	89.6%	−7.1%	74.8%
Domestic China P.R	17.8%	−73.2%	−64.7%	−18.8%	59.1%
Domestic India	2.2%	405.7%	205.7%	32.4%	81.8%
Domestic Japan	1.1%	132.7%	70.7%	15.2%	56.9%
Domestic United States	25.6%	26.1%	15.6%	7.3%	88.7%

Adapted from IATA (2022a)

In May, volume levels in Brazil decreased from the previous month, resulting in a YoY increase of 73.1%. Traffic in India decreased by 0.3% compared to the April 2022 but increased by 405.7% compared to the previous year. As a result of loosened travel restrictions and increased consumer confidence, domestic RPK sales in Japan soared in May. Table 3 shows the domestic market in 2022 figures.

The volume of domestic traffic is currently 27.3% lower than it was prior to the epidemic and continues to recover. Even though the number of domestic RPKs in Australia decreased by 6.2% MoM, current levels are just 5.9% below 2019. China domestic market is undoubtedly the tailender in recovery activities by its nature of the most sensitive air passengers in the world. Table 4 compares the YoY vs. YtD figures, which support the recovery status for each market component.

2.3   China

China's international aircraft transportation has always had difficulty recovering, primarily due to the ongoing changes in the international pandemic situation, which are superimposed on other countries' varied epidemic prevention and control techniques. China's civil aircraft transportation industry has been subjected to extreme stress. Since the beginning of the new Covid-19 pandemic in February 2022, China's official data indicate that the country's civil air transportation business has accrued an overall loss of 31.25 billion USD. This figure is current as of February 2022. The subsequent aviation tragedy in Wuzhou that involved China Eastern Airlines made the situation much direr and ended the 4227-day-long streak of safe flight records for China Civil Aviation. Several significant obstacles, including the recurrence of epidemics in different parts of the country and the ongoing transformations in the international aviation industry, are currently hindering the expansion of China's aviation business.

China's civil aviation will facilitate up to 17 million take-offs and landings by 2025. In 2020, 9.05 million take-offs and landings were affected by the outbreak. In 2019, 11.66 million take-offs and landings were unaffected by the outbreak.

Table 4 Air passenger market in detail (YoY vs. YtD) – May 2022

	World share	Year to year			Year to date		
		RPK	ASK	PLF (%-pt)	RPK	ASK	PLF (%-pt)
Total market	**10**	**8.31**	**5.28**	**1.31**	**8.47**	**5.32**	**1.24**
Africa	0.19	12.49	7.68	1.49	7.8	4.66	1.18
Asia Pacific	2.75	−0.47	−0.82	0.26	−0.27	−0.33	0.04
Europe	2.5	25.88	15.91	2.24	24.19	15.47	1.88
Latin America	0.65	9.93	8.95	0.4	10.53	8.41	0.82
Middle East	0.66	27.96	10.35	3.54	21.32	8.67	2.79
North America	3.26	5.63	3.66	1.08	8.67	4.96	1.58
International	**3.77**	**32.58**	**15.21**	**3.2**	**27.6**	**13.08**	**2.72**
Africa	0.15	13.49	7.85	1.64	8.45	4.61	1.36
Asia Pacific	0.31	45.33	11.88	4.36	23.9	8	2.77
Europe	1.87	41.23	22.13	3.01	38.57	20.75	2.67
Latin America	0.21	18.05	13.53	1.35	21.03	14.18	1.76
Middle East	0.6	31.72	11.57	3.71	23.87	9.59	2.92
North America	0.62	20.34	10.11	2.71	20.85	9.26	2.73
Domestic	**6.23**	**0.02**	**−0.33**	**0.29**	**1.63**	**0.81**	**0.53**
Domestic Australia	0.08	3.47	2.31	0.65	3.46	2.65	0.43
Domestic Brazil	0.19	7.31	8.96	−0.71	6.46	6.04	0.2
Domestic China PR	1.78	−7.32	−6.47	−1.88	−4.9	−4.04	−1.05
Domestic India	0.22	40.57	20.57	3.24	4.55	2.19	1.29
Domestic Japan	0.11	13.27	7.07	1.52	7.16	5.19	0.58
Domestic United States	2.56	2.61	1.56	0.73	6	3.47	1.3

Adapted from IATA (2022b)

2.4 Europe

Following the March 2020 outbreak of the COVID pandemic, which caused interruptions in air travel, international travel was significantly disrupted for an extended period due to the restrictive and ever-changing travel laws that governments arbitrarily created (Tiknonov & Sazonov, 2022). Domestic services were easier to maintain in many European nations since travel restrictions impacted them less. These maintained services made them accessible to a broader audience.

After more than 2 years from the onset of the pandemic, the recovery rate of domestic capacity in Europe's major air transport markets varies substantially. Even though the outbreak began more than 2 years ago, this is the situation. The domestic air travel market recovery rate for the top 15 markets ranges from 50% in Germany to 117% in Italy. Germany has the fastest rate of economic recovery. Five countries have seen a rise in capacity, while three others have reached above 90%.
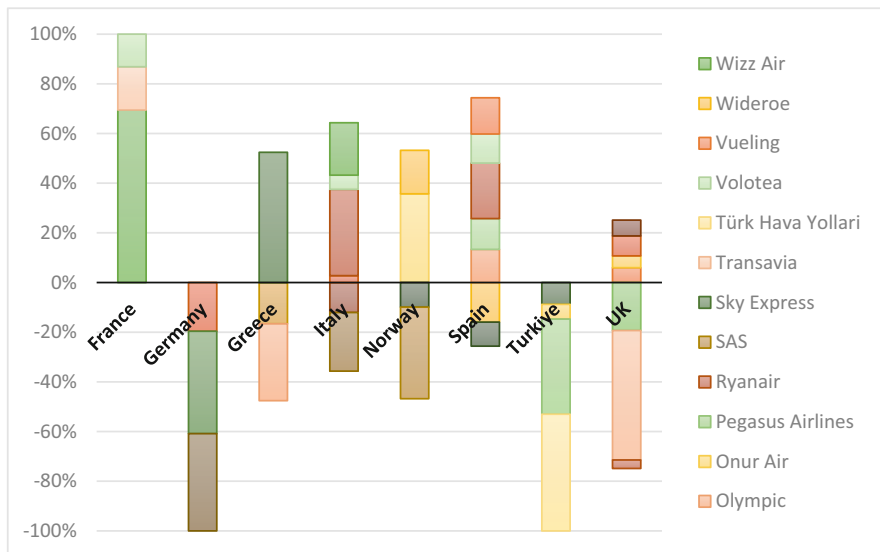
Fig. 3 The changes for European airlines for traffic recovery and available seat changes compared with the total change figures. (Airserviceone, 2022)

It is possible to determine which airlines have gained or lost passengers from Fig. 3. The comparable capacities between August 2019 and August 2022 have been distinguished as top country markets. Although the demise of the original Flybe was detrimental to the UK market's economy, there were no airline failures in the German market. It would appear that most Germans have altered their method of domestic travel due to the country's efficient high-speed train network and autobahns.

2.5   North America

The performance in North America significantly improved in the second quarter of 2021, following a lackluster performance in the first 3 months of the year. This advancement was made possible by a rapidly improving domestic market in the United States and an overall high immunization rate, which contributed to the area concluding 2018 at 65.1% of 2019 levels (Dube, 2022).

The fantastic success is anticipated to continue into 2022, allowing the region to beat all other regions and reach 89% of its 2019 level by the end of the year. North America is anticipated to be the first region to return to 2019 levels for an entire year as early as 2023.

3 Conclusion

Much uncertainty surrounds the aviation industry's resurgence, particularly in the medium to long term. Predicting how the recovery will unfold is still difficult and requires significant caution. In addition to the unpredictability surrounding vaccination, especially in emerging and developing nations, and the risk of an outbreak during the fall and winter seasons, we must now also consider the possibility of geopolitical conflict and related humanitarian crises, as well as a severe economic downturn and an imminent recession. These threats could hinder or prolong the healing procedure.

Despite the risks to the downside, the sector continues to be optimistic that a return to 2019 levels is possible within the next 2–3 years (OAG, 2022; Statista, 2022). According to the number of people who traveled at the beginning of summer, there is no doubt that many are eager to hit the road again. The elimination of travel restrictions will increase the demand for air travel and contribute to the revival of the business. This recovery is because "holiday deprivation" will be coupled with increased trust in air travel due to improved vaccination rates and safety measures. We anticipate a surge in demand for air travel in the second half of 2022, when most governments will abolish virtually all health precautions and travel restrictions to return to normalcy. This constraint removal will increase the number of individuals desiring to take flights. Table 5 provides a summary of the information presented as

Table 5 Air passenger market 2019 vs 2022 (IATA, 2022b)

	World share	RPK	ASK	PLF (%-pt)	PLF (Level)
Total market	100.0%	−31.3%	−2.89	−0.27	79.1%
Africa	1.9%	−29.2%	−3.11	0.19	69.6%
Asia Pacific	27.5%	−62.5%	−5.67	−1.08	69.6%
Europe	25.0%	−19.6%	−1.65	−0.3	80.7%
Latin America	6.5%	−15.7%	−1.3	−0.26	80.7%
Middle East	6.6%	−10.5%	−1.42	0.31	76.2%
North America	32.6%	−10.4%	−1.03	−0.02	86.0%
Domestic	62.3%	−23.3%	−1.92	−0.42	79.8%
Domestic Australia	0.8%	−5.9%	−0.52	−0.05	75.6%
Domestic Brazil	1.9%	−2.0%	0.7	−0.69	74.8%
Domestic China PR	17.8%	−71.5%	−5.95	−2.49	59.1%
Domestic India	2.2%	−12.8%	−0.4	−0.82	81.8%
Domestic Japan	1.1%	−27.8%	−0.72	−1.62	56.9%
Domestic United States	25.6%	−4.7%	−0.6	0.13	88.7%
International	37.7%	−35.9%	−3.43	−0.19	78.6%
Africa	1.5%	−33.2%	−3.44	0.12	68.4%
Asia Pacific	3.1%	−73.9%	−7.15	−0.66	72.1%
Europe	18.7%	−20.9%	−1.74	−0.35	80.6%
Latin America	2.1%	−30.2%	−2.96	−0.06	83.4%
Middle East	6.0%	−10.0%	−1.45	0.38	76.8%
North America	6.2%	−21.3%	−1.78	−0.35	80.3%
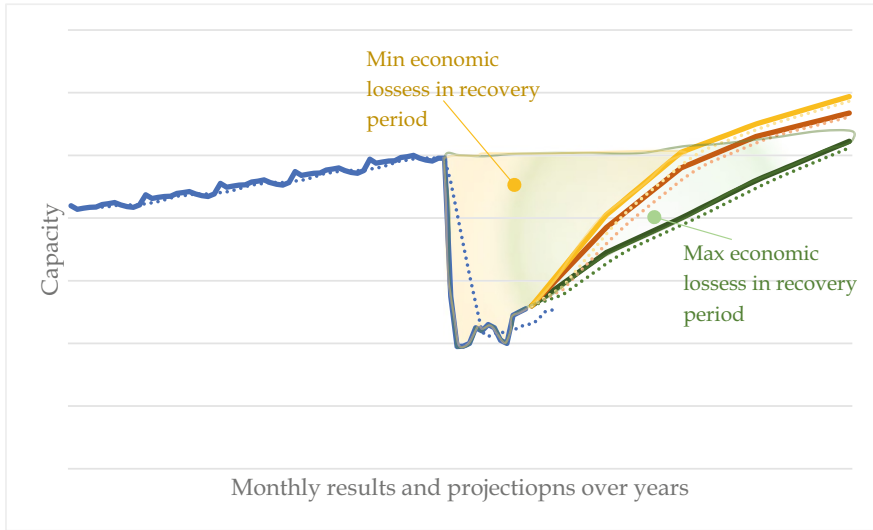
Fig. 4 Mid-term capacity projections. (Adapted from ACI, 2022)

recovery percentages. Vaccination distribution and acceptance will be effective in emerging and underdeveloped nations by 2022.

- The scenario accounts for the impact of Omicron in the first quarter of 2022.
- This forecast predicts that consumer confidence in travel return in 2022 will grow, inflation will be high but under control, and the likelihood of a recession will be low.
- It assumes a moderate improvement in the health of the aircraft fleet and a continued relaxation of travel restrictions in all regions of the world. It also shows that the supply-and-demand imbalance in the aviation industry does not meet industry-wide forecasts.
- As the globe becomes more accustomed to "living with COVID-19," subsequent epidemic and pandemic waves are expected to be both possible and manageable. These waves will not be localized and therefore have less effect on air travel bookings.

Recent projections indicate that the number of passengers traveling worldwide will likely surpass 2019 levels by the end of 2023, with a full-year return to 2019 levels in 2024. The overall rebound will be driven by domestic passenger traffic but will be hampered by Asia-Pacific and international travel (globally, domestic traffic accounted for 58% of total passenger traffic in 2019). Nevertheless, it is evident that, economic losses will affect the global economy; whether it is a minimum or maximum effect, it will stop investments globally (Fig. 4). This effect can trigger a global economic crisis.

Global domestic passenger traffic is expected to surpass 2019 levels by the end of the year 2023. The number of passengers will not reach 2019 levels until the second half of 2024. By 2025, the number of international passengers will have caught up to what it was in 2019.

Domestically significant markets are projected to recover to pre-COVID-19 levels between the middle and end of 2023. The anticipated traffic levels for 2019 will not be attained in international markets with high traffic until 2024 or 2025. Some country markets, especially emerging and developing countries, will not achieve 2019 passenger levels until 2025 or 2026, especially those dependent on international traffic. This is as a result of the uneven supply of vaccines, geopolitical turmoil, the resulting humanitarian crises, and the deteriorating economic outlook.

References

ACI. (2022). *The impact of COVID-19 on airports – And the path to recovery.* https://aci.aero/2022/06/28/the-impact-of-covid-19-on-airportsand-the-path-to-recovery/. Accessed 01 Aug 2022.

Air Service One. (2022). *European air traffic domestic capacity recovery rates vary from 50% in Germany to 117% in Italy.* https://airserviceone.com/european-air-traffic-domestic-capacity-recovery-rates-vary-from-50-in-germany-to-117-in-italy/. Accessed 01 Aug 2022.

Anna. (2022). *Weekly route constructions.* https://www.anna.aero/all-new-airline-routes/. Accessed 01 Aug 2022.

Bhowmik, T., & Eluru, N. (2022). An airport level framework for examining the impact of COVID-19 on airline demand. *Transportation Research. Part A, Policy and Practice, 159*, 169–181.

Chen, T., Fu, X., Hensher, D. A., Li, Z. C., & Sze, N. N. (2022). Air travel choice, online meeting and passenger heterogeneity – An international study on travellers' preference during a pandemic. *Transportation Research Part A: Policy and Practice, 165*, 439–453.

Dube, K. (2022). COVID-19 vaccine-induced recovery and the implications of vaccine apartheid on the global tourism industry. *Physics and Chemistry of the Earth, Parts A/B/C, 126*, 103140.

IATA. (2022a). *Strong international traffic propels continuing air travel recovery.* https://www.iata.org/en/pressroom/2022-releases/2022-07-07-02/. Accessed 01 Aug 2022.

IATA. (2022b). *Air passenger market analysis.* https://www.iata.org/en/iata-repository/publications/economic-reports/air-passenger-monthly-analysis%2D%2D-may-2022/. Accessed 01 Aug 2022.

ICAO. (2022). *Latest air traffic forecasts illustrate encouraging recovery and higher growth in global air travel.* https://www.icao.int/Newsroom/Pages/Latest-air-traffic-forecasts-illustrate-encouraging-recovery-and-higher-growth-in-global-air-travel.aspx. Accessed 01 Aug 2022.

International Civil Aviation Organization. (2022). *Effects of novel coronavirus (COVID-19) on civil aviation: Economic impact analysis (2020).* Air Transport Bureau, Montreal, Canada, from https://www.icao.int/sustainability/Documents/COVID-19/ICAO_Coronavirus_Econ_Impact.pdf. Accessed 06 July 2022.

Kim, M., & Sohn, J. (2022). Passenger, airline, and policy responses to the COVID-19 crisis: The case of South Korea. *Journal of Air Transport Management, 98*, 102144.

OAG. (2022). *Global total seats.* https://www.oag.com/coronavirus-airline-schedules-data Accessed 01 Aug 2022.

Oxley, D., & Jain, C. (2015). *Global air passenger markets: Riding out periods of turbulence.* IATA, The Travel & Tourism Competitiveness Report https://www.iata.org/en/iata-repository/

publications/economic-reports/global-air-passenger-markets-riding-out-periods-of-turbulence/. Accessed 01 Aug 2022.

Rutynskyi, M., & Kushniruk, H. (2022). European low-cost Airlines in Ukraine: Features of entry and consolidation in the national market. In *Challenges and opportunities for transportation services in the post-COVID-19 era* (pp. 104–139). IGI Global.

Statista. (2022). *Number of air passengers in China from 2010 to 2021*. https://www.statista.com/statistics/275907/number-of-air-passengers-in-china/. Accessed 01 Aug 2022.

Tikhonov, A., & Sazonov, A. (2022). Major trends in aviation industry during COVID-19. *Journal of Applied Engineering Science, 20*(4), 1093–1102.

Zoubir, Y. H., & Tran, E. (2022). China's health silk road in the Middle East and North Africa amidst COVID-19 and a Contested World Order. *Journal of Contemporary China, 31*(135), 335–350.

Index